



**UNITED
NATIONS**

EP

UNEP(DEPI)/MED WG.402/Inf.3



UNEP



**UNITED NATIONS
ENVIRONMENT PROGRAMME
MEDITERRANEAN ACTION PLAN**

20 October 2014
Original: English

Regional Training Workshop for Environmental Inspectorates

Athens, Greece, 25-27 November 2014

**Testing of a modeling system to assess the variations
Of EQSs with ELVs for nitrogen and mercury in
Gulf de Lion and Izmir Bay**

For environmental and economic reasons, this document is printed in a limited number. Delegates are kindly requested to bring their copies to meetings and not to request additional copies.

**Testing of a modeling system to
assess the variations of EQSs with
ELVs for nitrogen and mercury in
Gulf de Lion and Izmir Bay**

1201869-000

Title

Testing of a modeling system to assess the variations of EQSs with ELVs for nitrogen and mercury in Gulf de Lion and Izmir Bay

Client	Project	Reference	Pages
UNEP-MAP	1201869-000	1201869-000-ZKS-0016	67

Keywords

MEDPOL, Mediterranean, land based sources, ecosystem approach, EQS, ELV, nitrogen, mercury

Summary

This report discussed a methodology to provide a bridge between the ecosystem approach and the MEDPOL Land Based Sources Protocol, and tries to establish a relation between environmental quality standards (EQS) and emission limit values (ELV).

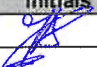

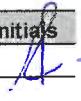
In this study we used two 3D modelling approaches. A "detailed 3D modelling" approach takes into account in detail the characteristics of the receiving water body. A "generalised Tier 3" method uses a simplified representation of the characteristics of the receiving water body, including sufficient site-specific information however, to allow application to the variety of coastal environments encountered in the Mediterranean.

Our case studies (Izmir Bay, Gulf of Lions) demonstrated that the generalized Tier 3 model provides results that are in the same range as the detailed 3D model, though not equal. We recommend the use of a safety factor of 2 to avoid the risk that the generalized Tier 3 model overestimates the ELV. This implies that the generalized Tier 3 model will lead to more conservative ELVs than the detailed 3D model. This is balanced by a much easier application than the detailed 3D model, and by a generic approach that can be applied to a large number of sites at low costs. Our case studies for nitrogen and mercury also demonstrate that it is vital to include the substance characteristics in the assessment.

In view of the large amount of hot spots around the Mediterranean and the diversity of these sites, in terms of their natural environment and the socio-economic conditions, we recommend that an easily applicable method will be made available to water managers and policy makers. The successful implementation of such a method probably requires a Guidance Document and a supporting software tool.

References

UNEP-MAP Contract RFP2 (23/10/2010)

Version	Date	Author	Initials	Review	Initials	Approval	Initials
	jan. 2012	Ir. J. van Gils		F. Kleissen Ph.D.		Ir. T. Schilperoort	
		C. Spiteri Ph.D.					
		M. Chatelain Ph.D.					
		Ir. T. van der Kaaij					

State
final

Contents

1 Introduction	1
1.1 Study Background	1
1.2 Study Objectives	3
1.3 Study Outline	3
1.4 Report Outline	4
2 Data collection	5
2.1 Izmir Bay	5
2.2 Gulf of Lions	6
2.3 Data availability and analysis from a Mediterranean wide perspective	9
2.4 Hot spots	11
2.5 ELVs and EQSs	11
2.5.1 Environmental Quality Standards (EQSs)	11
2.5.2 Emission Limit Values (ELVs)	12
2.6 Mercury in the marine aquatic environment	14
2.6.1 Mercury in the Mediterranean	15
2.7 Nitrogen in the marine environment	16
2.7.1 Nitrogen in the Mediterranean	17
3 Modelling strategy	19
3.1 Approach to assessing the variations of EQSs with ELVs	19
3.2 Spatial scales of analysis	21
3.3 Detailed 3D hydrodynamic modelling	22
3.4 Detailed 3D water quality modelling	23
3.5 The Screening Model for Coastal Pollution Control in the Mediterranean (1989)	25
3.5.1 Geometry	25
3.5.2 Currents	26
3.5.3 Water quality	27
3.6 Generalised Tier 3 model used in the present study	29
3.6.1 The modified SCREMO concept	29
3.6.2 Geometry of the study area	29
3.6.3 Currents in the study area	30
3.6.4 Water quality modelling	30
3.6.5 Overview of input for the Generalised Tier 3 model used in the present study	31
3.7 Near-field considerations	31
3.8 From individual simulations to an EQS-ELV dose-effect curve	32
4 Model set-up	35
4.1 Izmir Bay detailed 3D model	35
4.1.1 Model domain and bathymetry	35
4.1.2 Model forcing	36
4.1.3 Hydrodynamic model parameters	37
4.1.4 Water quality model parameters	37
4.2 Izmir Bay generalised Tier 3 model	38
4.3 Gulf of Lions detailed 3D model	39
4.3.1 Model domain and bathymetry	40
4.3.2 Model forcing	41

4.3.3	Hydrodynamic model parameters	42
4.3.4	Water quality model parameters	43
4.4	Gulf of Lions Generalised Tier 3 model	44
5	Modelling results	45
5.1	Izmir Bay detailed 3D model	45
5.2	Izmir Bay generalised Tier 3 model	47
5.3	Relation between ELVs and EQSs for Izmir Bay	48
5.4	Gulf of Lions detailed 3D model	52
5.5	Gulf of Lions generalised Tier 3 model	54
5.6	Relation between ELVs and EQSs for Gulf of Lions	55
6	Conclusions and recommendations	59
6.1	Conclusions	59
6.2	Recommendations	61
7	References	63
 Appendices		
A	Vertical velocity profiles	A-1

1 Introduction

1.1 Study Background

The present project is a part of the pollution component of the Mediterranean Action Plan, or the Mediterranean Pollution Monitoring and Research Programme (MEDPOL). This programme consists of:

- pollution control activities: a Land Based Sources (LBS) Protocol, leading to a Strategic Action Plan (SAP) defining targets, measures and deadlines, as well as legally binding specific regional plans and National Action Plans (NAP);
- pollution assessment by monitoring.

MEDPOL is introducing the ecosystem approach. The present project provides a bridge between the ecosystem approach and the MEDPOL LBS Protocol. As such, it tries to establish a relation between environmental quality standards (EQS) and emission limit values (ELV) following a combined, precautionary approach.

In this study, we use the concept of a mixing zone (Figure 1.1), as defined in the related EC Guidance Document (EC, 2010). A mixing zone (MZ) is an area around a discharge point where the concentration of a Contaminant of Concern (CoC) locally exceeds the EQS. As stated in the Guidance Document (EC, 2010), the dimensions of the MZ shall be restricted and proportionate, and their acceptability depends on, for example, the presence of protected or sensitive areas or drinking water intake points.

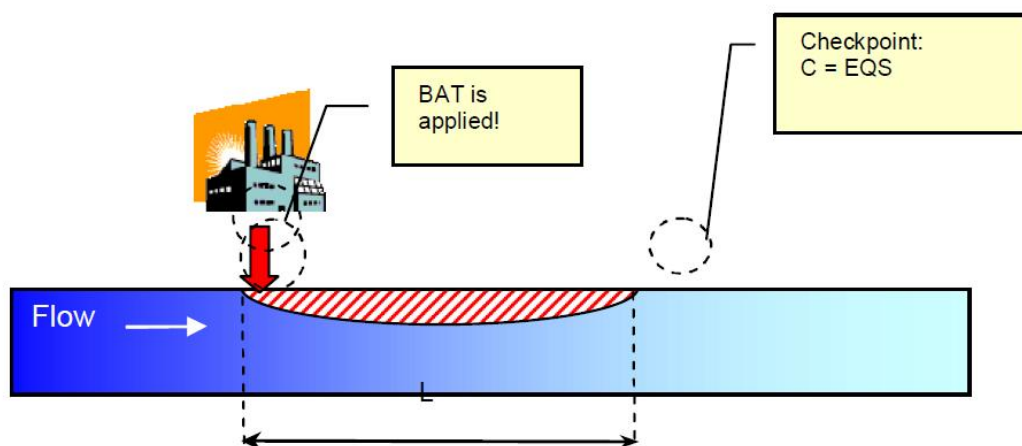


Figure 1.1 Illustration of a mixing zone in flowing waters, showing the “checkpoint” located at a distance “L” downstream of a pollution source where the EQS needs to be satisfied (Source: EC, 2010). BAT refers to “Best Available Technology”.

The EC Guidance Document (EC, 2010) advises a tiered approach (risk-based) to determine whether a MZ meets the accepted requirements:

- Tier 0: Contaminant of Concern present and effluent concentration > EQS? (if not then there is no MZ)
- Tier 1: Initial Screening (simple rules of thumb based on discharge data only, to eliminate insignificant discharges from further steps)
- Tier 2: Simple approximation (simple site-specific conservative approach)
- Tier 3: Detailed assessment (detailed site-specific approach)

If a certain Tier indicates that the discharge can be accepted, the assessment stops. If not, the assessment moves to the next level. In exceptional situations, a Tier 4 assessment (Investigative Study, comprising the characterisation of the actual impact of a discharge) may be carried out.

A tool that supports discharge tests for Tiers 0-1-2, in line with the EC Guidance Document (EC, 2010), is already available. The assessment at the Tier 2 level requires the specification of the dimension of the acceptable MZ as an input parameter. The size of the MZ is determined by the discharger and approved by the local regulators on a case-to-case basis.

For a given allowed ambient concentration, the related ELV can be derived if the relation between the effluent flow and concentration on one hand and the ambient concentration at the edge of the defined mixing zone on the other hand has been established. This relation depends on the characteristics of the discharge, on the characteristics of the substance of concern and on the characteristics of the receiving water body. In the receiving waters, the effluents will be mixed with ambient waters. In some water bodies, such as an open coastline with a strong current and/or strong tidal motion, sufficient hydrodynamic mixing dilutes the effluent resulting in a lower ambient concentration (rapid mixing). In others, such as semi-enclosed water body with small currents and tidal motion, the dilution capacity is limited (slow mixing). Thus, the characteristics of the water body determine the relation between the ELV and the EQS as illustrated in Figure 1.2.

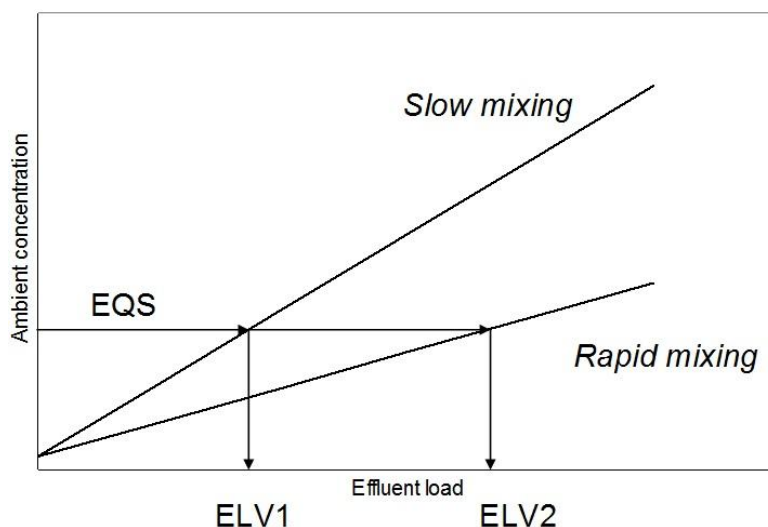


Figure 1.2 Relation between EQS and ELV for water bodies with different mixing characteristics.

The chemical characteristics of the substance under study also partly determine the relation between the ELV and the EQS. Firstly, if a substance is decaying or reacting, the concentration at the edge of the mixing zone will be lower than if the substance behaves conservatively. This difference depends on the time that substances remain within the mixing zone and on the decay/removal rate of the substance in question. Secondly, the substance properties may affect the partitioning of the substance (e.g. dissolved versus adsorbed), and in some cases the EQS applies to the dissolved fraction only. In such cases, the adsorbed fraction may effectively disappear from the water column due to settling of particles.

1.2 Study Objectives

Against the backgrounds discussed above, the objectives of the present study are:

- to carry out 3D water quality simulations which establish the relation between EQS and the ELV for two pilot locations (Gulf of Lions and Izmir Bay) for nitrogen and mercury (qualifying as a Tier 3 assessment);
- to run a number of loading scenarios through which “dose-effect” relationships are derived for each site;
- to provide, as much as possible, an approach that offers easy application, a generic/coherent/harmonized approach that can be readily applied to various other locations, and limited data requirements.

The third objective stems from the observation that the application of the proposed ELV/EQS tool will need to be extended to other pollutants of concern from land-based sources, such as phosphorus and cadmium, and to other hotspot demonstration sites, including Alexandria Bay, Tunis Bay, Barcelona Bay, Haifa Bay, the North Adriatic and the North Aegean.

A typical length scale for a mixing zone amounts to 500-1000 m (the EU Guidance (EC, 2010) mentions a maximum value of 1000 m). For this reason, the spatial scale of relevance in the presents study is limited so a distance of several mixing zone lengths, say < 5000 m.

1.3 Study Outline

The steps involved in the proposed approach are presented in Figure 1.3. Phase A of the study includes the collection of (i) site-specific data and (ii) substance specific data. This data is then used as input to Phase B.

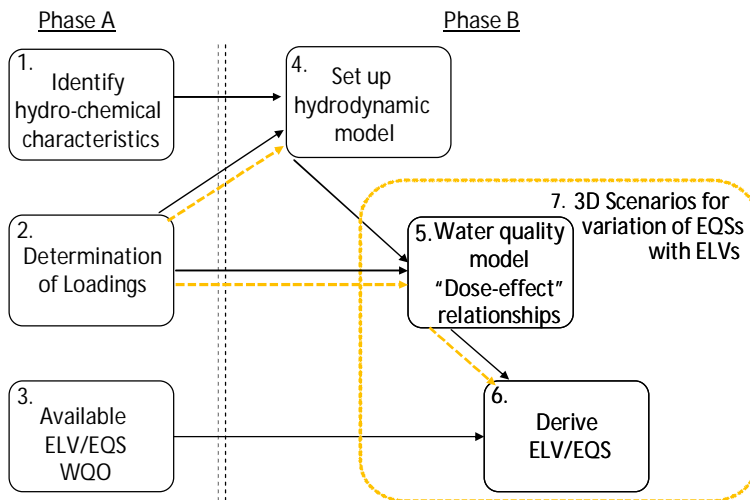


Figure 1.3 Schematic outline of study

In Phase B, the hydrodynamic/water quality models are set up based on the available data. In view of the objective to provide an easy applicable, generic, coherent and harmonized approach we follow two different ways of modelling: (1) a detailed modelling approach requiring a large amount of input data and a high level of skill, and (2) a generalised approach requiring limited data and limited skill.

For the second method, we rely on the existing SCREMO model, applied previously in a similar study on “Screening Model for Coastal Pollution Control in the Mediterranean” (Delft Hydraulics, 1989). With both models, 3D model simulations will be performed to establish dose-effect-relationships, providing the relation between the EQS and the ELV for a given site and a given substance.

1.4 Report Outline

The results from Phase A will be discussed in Chapter 2 of this report. The modelling methodology adopted during Phase B is discussed in Chapter 3. Chapter 4 discusses the set-up of the models, whereas Chapter 5 discusses the results from the modelling. Chapter 6 provides conclusions and recommendations.

2 Data collection

The location of the two selected pilot locations, Gulf of Lions and Izmir Bay, is shown in Figure 2.1.

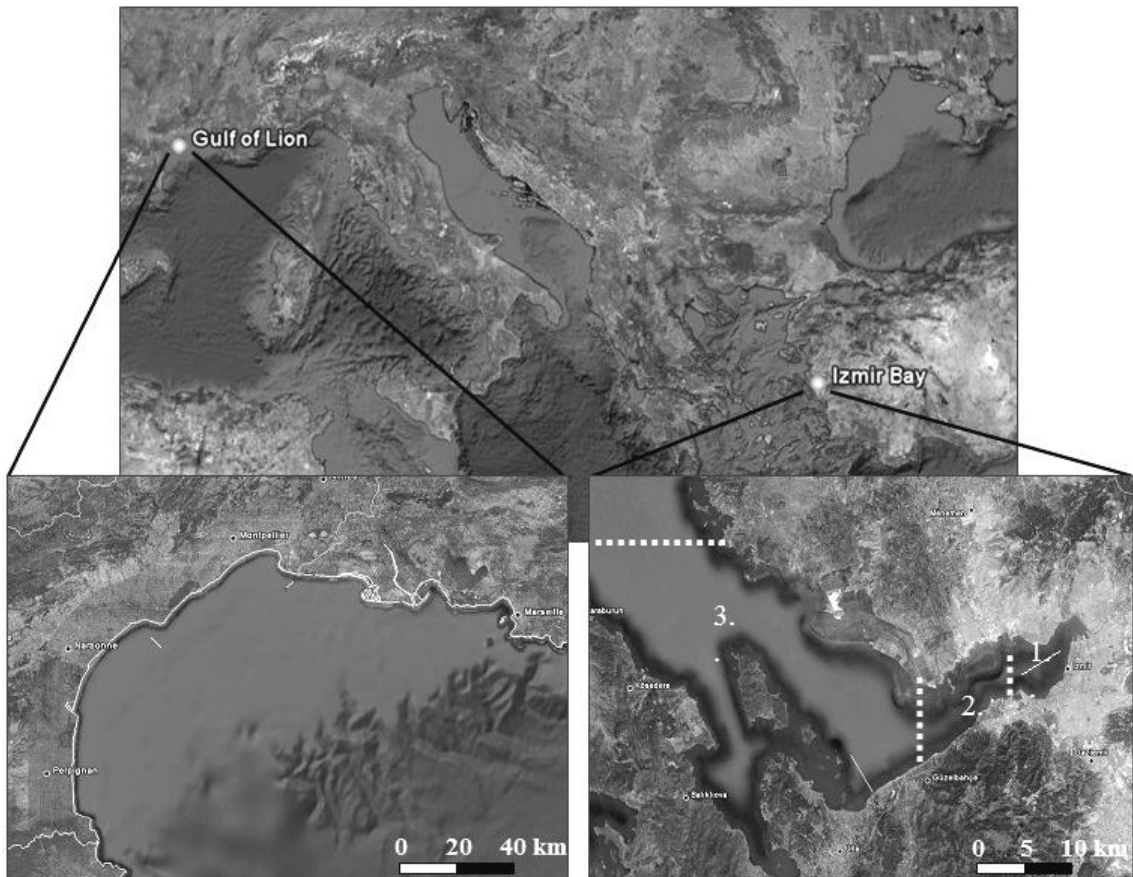


Figure 2.1 Google Earth image of the Mediterranean Sea showing the location of Gulf of Lions in Western Mediterranean and Izmir Bay in Eastern Mediterranean. The marked sections in Izmir Bay indicate the Inner Bay (1), Middle Bay (2) and Outer Bay (3).

2.1 Izmir Bay

Izmir Bay, located in Western Turkey, is one of the largest embayments in the eastern Aegean Sea. The bay can be divided into three sections (Inner, Middle and Outer; Figure 2.1) according to the physical characteristics of the different water masses. The water depth in the Inner Bay is generally less than 15 m (Figure 2.2). This part of the basin shows strong eutrophication and high counts of coliform bacteria. The Middle Bay (10 km long) is separated from the Inner Bay by a sill, the Yenikale Strait. The relatively unpolluted Outer Izmir Bay is about 45 km long and extends in a northwest-southeast direction. The Gediz River, which flows to the Outer Bay, is the biggest river in the Izmir Bay (Figure 2.3).

Tides are semidiurnal, ranging between 20 and 50 cm, and do not have a marked influence on the water circulation in the bay. The Izmir Bay region is under the influence of northerly winds all year around (Sayin, 2003). The movement of water masses is indicated schematically in Figure 2.3. The currents in the Inner Bay are very weak.

The water quality of Izmir Bay is highly impacted by the adjacent urban settlement, the city of Izmir that has a population exceeding 3 million inhabitants (2000 census). Izmir Bay, in particular the Inner Bay, is subject to effluents from the industrial developments (mainly iron, paper and pulp, textile, oil and soap industries, chlorine-alkali plants, paint and cement factories and beer industries), untreated wastewaters discharges, intensive harbour activities in the bay and agricultural activities in the surrounding areas. For more information, we refer to Biszel and Uslu (2000), Duman et al. (2004), Sayin (2003), Kontas et al. (2004), Kucuksezgin et al. (2006) and Kontas (2006).

2.2 Gulf of Lions

The Gulf of Lions (GoL), located in the north-western Mediterranean is characterized by a crescent-shape continental shelf between Cap Creus in Spain and Marseille in France (see Figure 2.4). Fresh water and sediment enter from eight rivers, in decreasing annual water flux order: Rhône, Herault, Aude, Orb, Têt, Tech, Vidourle and Agly (Bourrin and Durrieu de Madron, 2006). With a mean flow rate of around $1700 \text{ m}^3 \text{ s}^{-1}$ (Moutin et al., 1998), the Rhône River is the dominant (80%) source of terrigenous material in the GoL. Due to the oligotrophic nature of the Mediterranean Sea, the inputs of nutrients and chemical contaminants from the Rhône River can greatly modify the biological productivity, which is of major importance for fishery activity.

From a hydrodynamic point of view, the GoL can be considered a complex region, due to the simultaneous occurrence of several intense and highly variable phenomena. These processes include the strong general circulation along the continental slope, the formation of dense water both on the shelf and offshore, a seasonal variation of stratification and the extreme energies associated with meteorological conditions (see Figure 2.5). Tides and natural oscillations have small amplitudes, in the order of a few centimetres, and the associated currents are too weak to be measured on the shelf (Lamy et al., 1981). The most pronounced winds are the north-westerly (Tramontane) and northerly (Mistral) winds, with strengths up to 23 m s^{-1} .

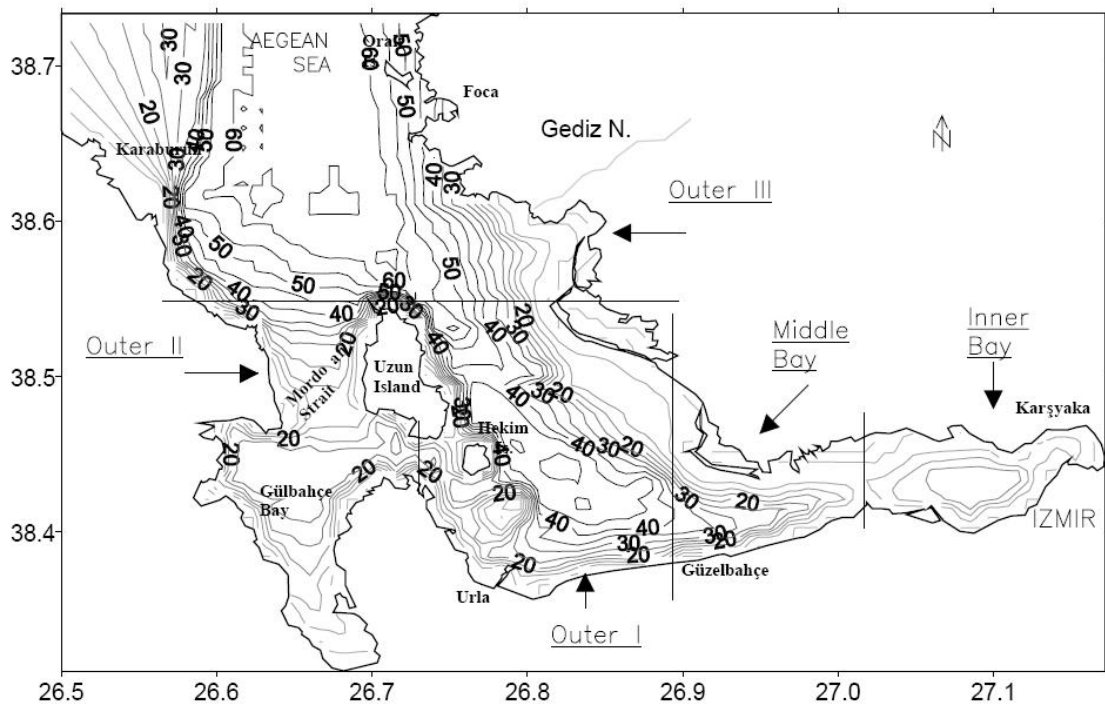


Figure 2.2 Izmir Bay area bathymetry, copied from Sayin (2003).

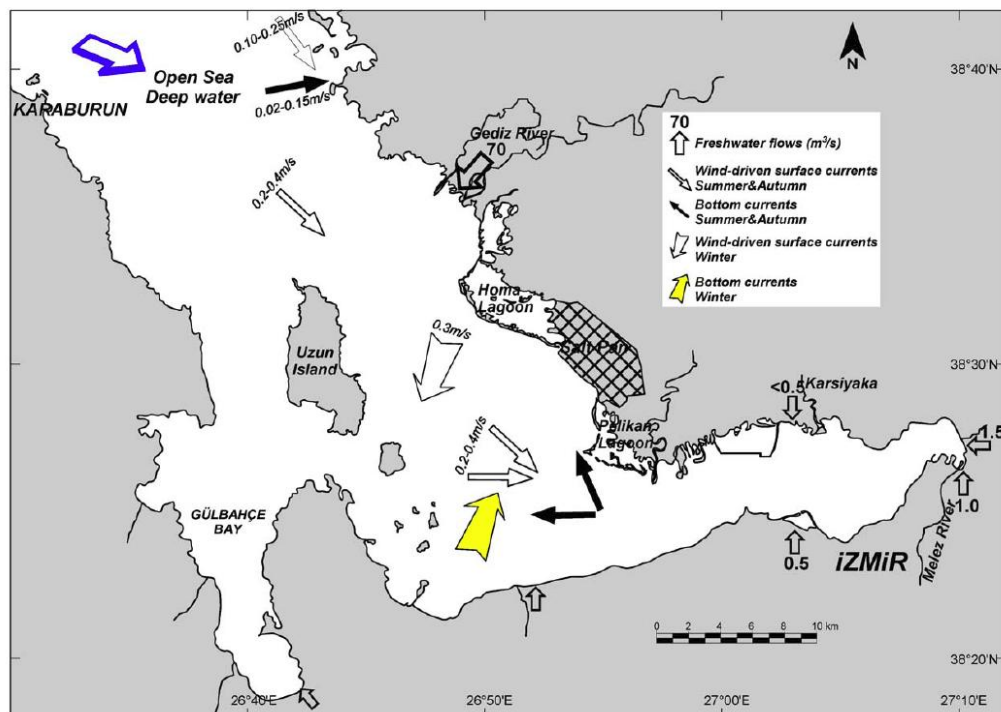


Figure 2.3 Map showing distribution of freshwater flows and wind-driven currents in Izmir Bay (copied from Duman et al., 2004).

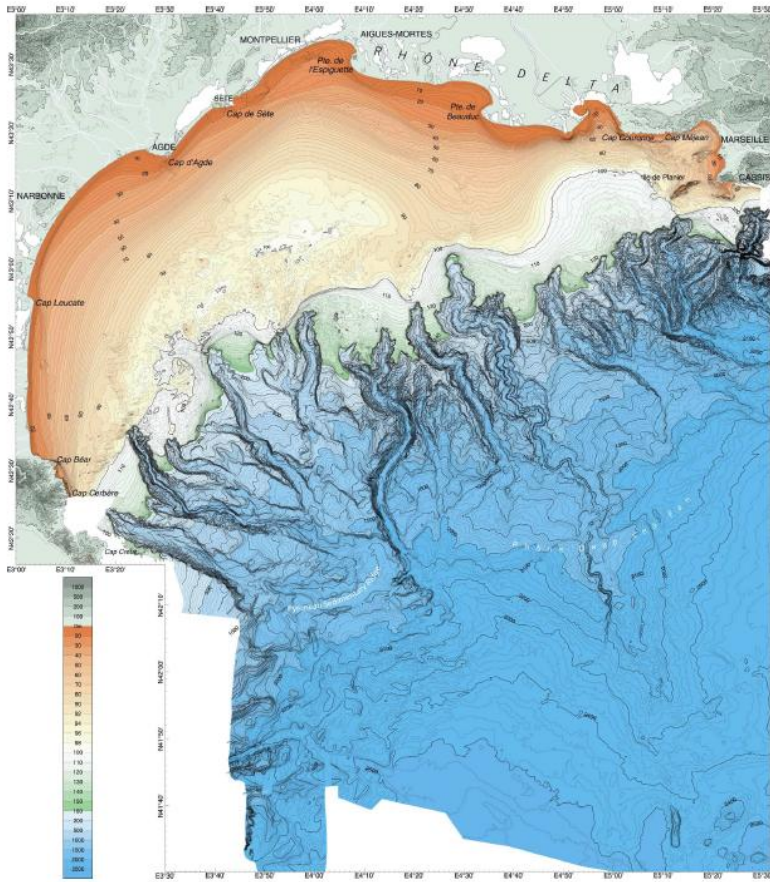


Fig. 1. Morpho-bathymetric map of the Gulf of Lions, displaying major topographic trends in this volume. Based on Berner et al. (2004). Bath data were extracted from sounding charts of the French Navy (Service Hydrographique de la Marine). Continental slope and river data are based on morpho-bathymetric surveys of Dronner.

Figure 2.4 Gulf of Lions bathymetry (Berne & Gorini, 2005).

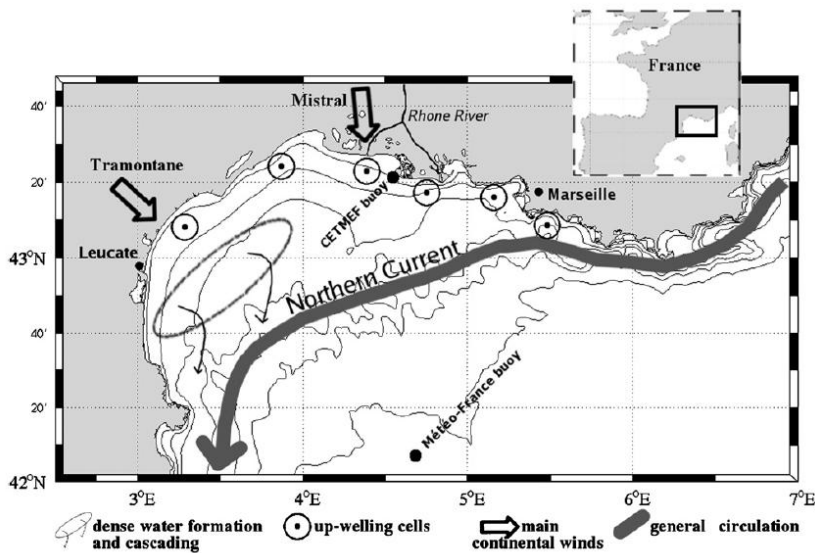


Figure 2.5 Main characteristics of the Gulf of Lions circulation (Dufois et al., 2008). The plot shows 20, 50, 90, 160, 500, 1000 and 2000m isobaths and the position of two buoys.

2.3 Data availability and analysis from a Mediterranean wide perspective

Several data sources provide information about the Mediterranean as a whole. As an example, bathymetry data are available from the ETOPO1 Global Relief Model (Amante and Eakins, 2009) at a 1 arc-minute resolution. The SRTM-30 gridded dataset by Scripps Institution of Oceanography at UCSD (SIO, 2011; Becker et al., 2009) is based on the Smith and Sandwell global grid (Sandwell and Smith, 2009) with other higher resolution grids added, resulting in a 30 arc-second global topography model. As an illustration, Figure 2.6 and Figure 2.7 provide the ETOPO1 bathymetry data at our two case study sites.

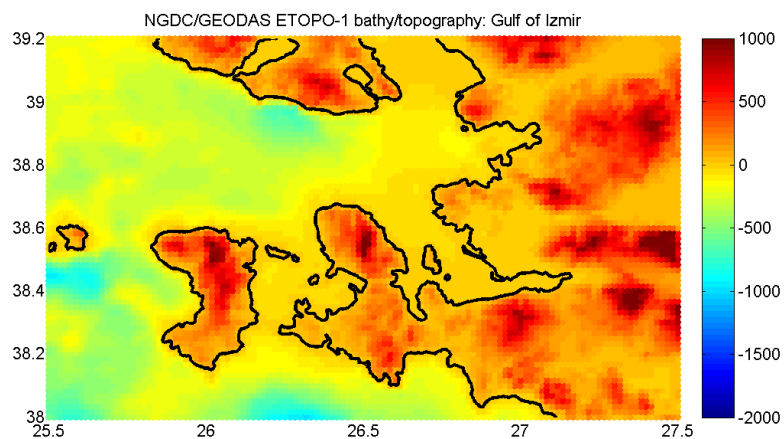


Figure 2.6 ETOPO1 bathymetry data for Izmir Bay

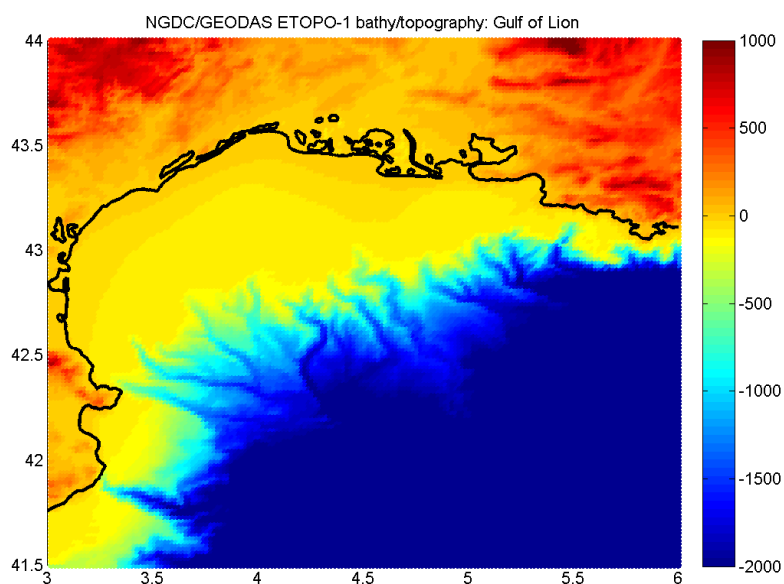
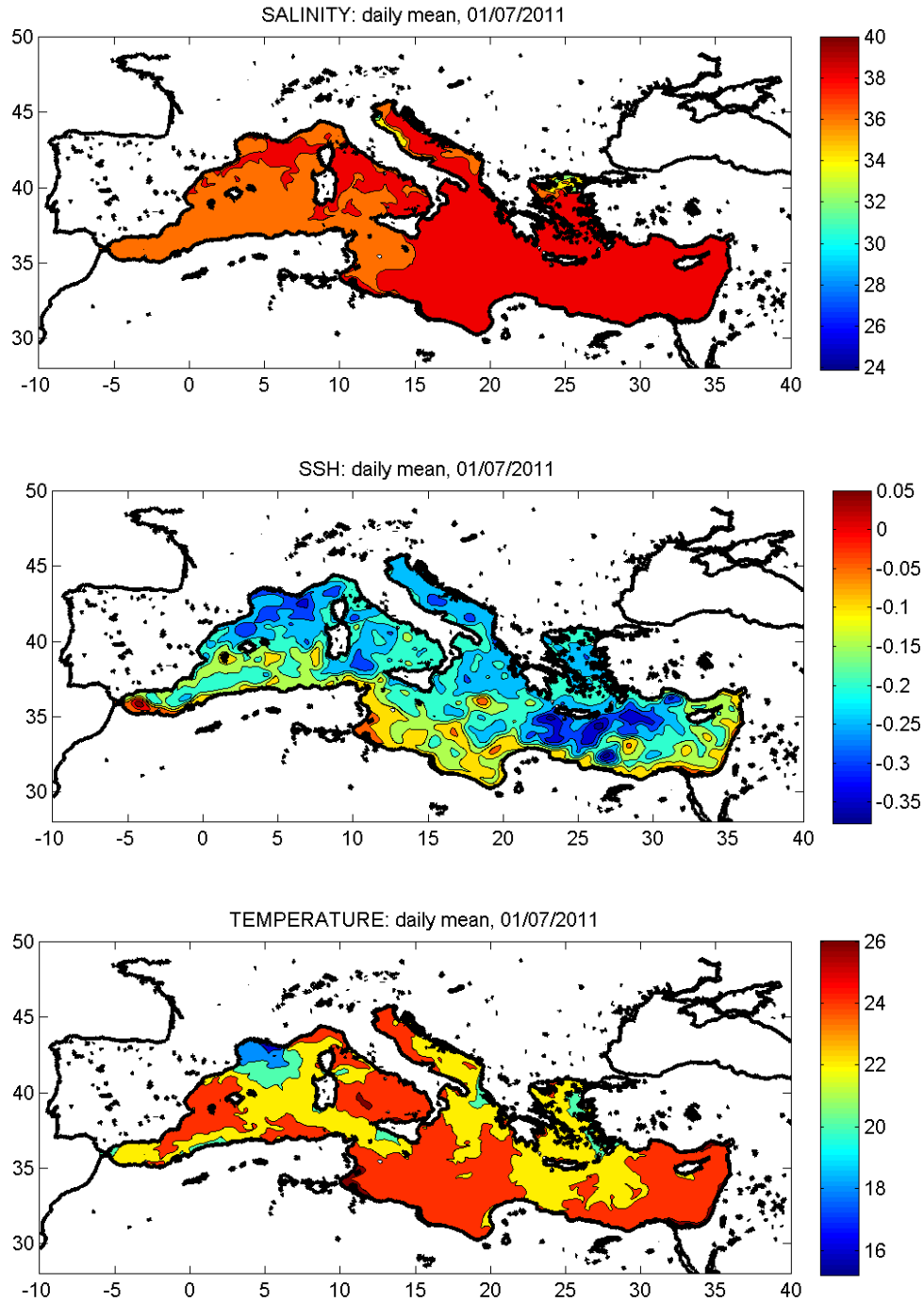


Figure 2.7 ETOPO1 bathymetry data for Gulf of Lions

On the scale of the Mediterranean as a whole, oceanographic data are available from the MyOcean initiative (www.myocean.eu). This data source provides records of daily means of the water level, currents, salinity and temperature. The horizontal resolution of the data is 1/16 of a degree (around 7 km at sea level along the equator or a meridian). The data are provided at 71 unevenly spaced vertical levels. Figure 2.8 shows examples for the Mediterranean as a whole.



Top: surface salinity in ppt, daily mean on 1 July 2011

Middle: sea surface elevation in m, daily mean on 1 July 2011

Bottom: surface temperature in ppt, daily mean on 1 July 2011

Figure 2.8 Oceanographic data for the Mediterranean, downloaded from MyOcean

Though of reduced importance, we note that tidal information can be obtained from various global databases, such as the TOPEX/Poseidon global tidal constituents database, the IHO tide database or the XTide tide database.

2.4 Hot spots

Figure 2.9 shows a map of the pollution hot spots around the Mediterranean. This picture illustrates that hot spots are indeed present in the study areas of the present project, the Gulf of Lions and Izmir Bay. The picture also illustrates that there are many more hot spots around the Mediterranean.

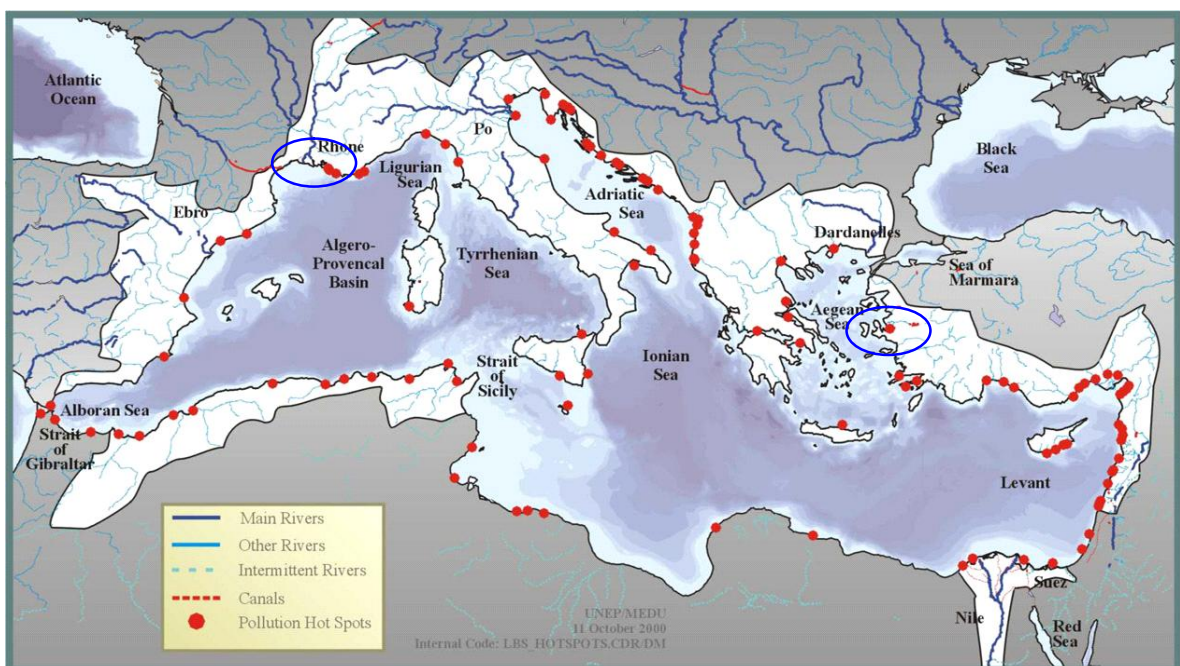


Figure 2.9 Main rivers and pollution hot spots around the Mediterranean. Ellipses indicate the hot spots in the study areas of the present project, Gulf of Lions and Izmir Bay.

2.5 ELVs and EQSs

2.5.1 Environmental Quality Standards (EQSs)

Since the 1970s up to 2000, water policy in Europe was set at a national level, leading to a multitude of ELVs and EQSs across Europe. Since 2000, overall water policy is shaped at the European level, with details set at the level of countries and/or river basins. The Water Framework Directive (WFD) 2000/60/EC of 23 October 2000 calls for “good ecological status” of all European water bodies and establishes a framework for community action in the field of water policy. Its daughter Directive 2008/105/EC of 16 December 2008, formulates environmental quality standards in the field of water policy. It encompasses the pre-existing Directives 82/176/EEC on Mercury discharges by industry, 83/513/EEC on Cadmium discharges, 84/156/EEC on Mercury discharges by industry, 84/491/EEC on HCH discharges and 86/280/EEC on discharges of dangerous substances (defined in Dir. 76/464).

For mercury, Directive 2008/105/EC formulates EQSs at a European level. These read:

- the maximum allowable concentration of mercury and its compounds in so-called “other surface waters” (as opposed to “inland surface waters”) equals 0.07 µg/l (MAC-EQS);
- the annually averaged concentration of mercury and its compounds in other surface waters should not exceed 0.05 µg/l (AA-EQS);
- these EQSs apply to the dissolved concentration: the dissolved phase of a water sample obtained by filtration through a 0.45 µm filter or any equivalent pre-treatment (EC, 2008).

The WFD does not formulate EQSs for nitrogen at a European level. If member states conclude that the concentrations of nitrogen should be regulated to ensure Good Ecological Status, nitrogen can be nominated a basin specific problem substance, and assigned an EQS at the basin or sub-basin scale.

We note that the EU Guidance Document (EC, 2010) asks for explicit consideration of separate “MAC-EQS” and “AA-EQS” mixing zones, in particular if a MAC-EQS is defined. This implies that the acceptable area of exceedence of the AA-EQS (protecting against chronic effects) may be different than the acceptable area of exceedence of the MAC-EQS (protecting against acute effects). In some European countries, the MAC-EQS MZ is substantially smaller than the AA-EQS MZ (e.g. MAC-EQS MZ is 2.5% of the AA-EQS MZ).

Though it is obvious that only a smaller number of the Mediterranean riparian countries are EU member states and thus legally committed to the WFD, we will use the WFD EQS for the present project, for demonstration purposes only.

2.5.2 Emission Limit Values (ELVs)

An emission limit value sets a limit to an individual discharge. The MAP Land Based Sources (LBS) Protocol defines an ELV as “the maximum allowable concentration measured as a “composite” sample, of a pollutant in an effluent discharged to the environment”. In the remainder of this report, we will denote such an ELV as a “c-ELV” where the letter “c” indicates that the ELV is expressed as an effluent concentration. Alternatively, we will use “m-ELV” (mass per time) to indicate the maximum allowable discharged mass of a substance of concern to the environment. The relation between the c-ELV and the m-ELV is as follows:

$$\text{m-ELV} = \text{c-ELV} * Q_e$$

where Q_e represents the effluent flow expressed as a volume flux (volume per time).

The MAP LBS Protocol includes the obligation to phase out the inputs of certain (Annex I) chemicals by national and regional action plans. Furthermore, it contains the provision to regulate point sources e.g. by ELVs, Best Available Techniques (BAT) and Best Environmental Practices (BEP). The Strategic Action Programme provides targets for emission reduction, various guidelines at a regional level and inventories and other actions at a national level. The Programme plans to formulate and adopt, as appropriate, environmental quality criteria and standards for point source discharges and emissions of heavy metals (mercury, cadmium and lead). Specific c-ELVs have been adopted for releases into the sea of mercury (0.050 mg/l), cadmium (0.2 mg/l), zinc (1.0 mg/l) and copper (0.5 mg/l).

In 2009, a series of Decisions has been adopted by the 16th Meeting of the Contracting Parties. Regional ELVs for BOD₅ have been set within Decision IG.19/7 adopting the "Regional Plan on the reduction of BOD₅ from urban waste water in the framework of the implementation of Article 15 of the LBS Protocol". Since this Decision refers to domestic waste water, and since domestic waste water is a source of nitrogen for the coastal waters, this Decision is relevant for nitrogen as well. For some substances, a zero emission policy is adopted, for example by Decision IG.19/8 on the "Regional Plan on the elimination of Aldrin, Chlordane, Dieldrin, Endrin, Heptachlor, Mirex and Toxaphene in the framework of the implementation of Article 15 of the LBS Protocol" and by Decision IG.19/9 on the "Regional Plan on the phasing out of DDT in the framework of the implementation of Article 15 of the LBS Protocol". It is noted that Decision IG.19/10 on "Sound management of chemicals" urges the Contracting Parties to agree to start preparing Regional Plans/Programmes pursuant to Article 15 of the LBS Protocol, on various chemicals, including Mercury.

2.6 Mercury in the marine aquatic environment

Hg exists as various species: gaseous elemental (Hg^0), divalent (Hg^{2+}), methylated ($(\text{CH}_3)\text{Hg}$ or MeHg), in dissolved and particulate forms. The main transformations between these forms are methylation/demethylation and reduction/oxidation through photochemically- and biologically-mediated processes (see Figure 2.10 copied from Monperrus et al., 2007).

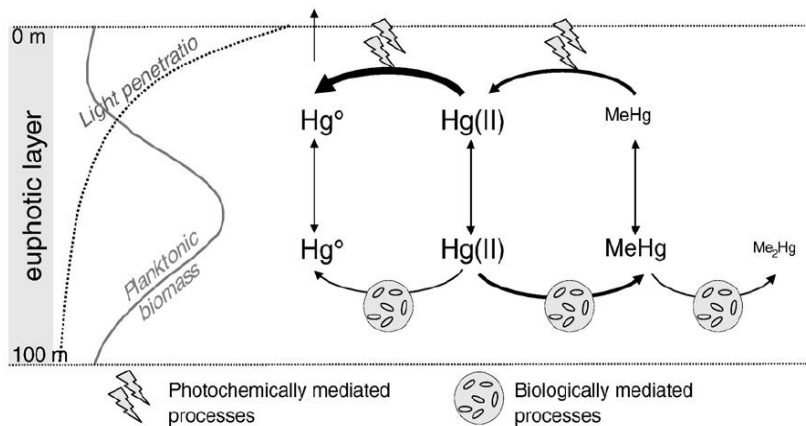


Figure 2.10 Schematic representation of the major processes for Hg transformations in the euphotic marine layer.

Rivers are the most important source of Hg contamination from land, with most of the Hg transported in the particulate form. The partition coefficient (K_d in l/kg), which equals the concentration in the solid phase (C_s in mg/kg) divided by the concentration in the water phase (C_w in mg/l), is a function of salinity, thus varying along the freshwater-seawater interface (see Figure 2.11 copied from Cossa & Martin, 1991).

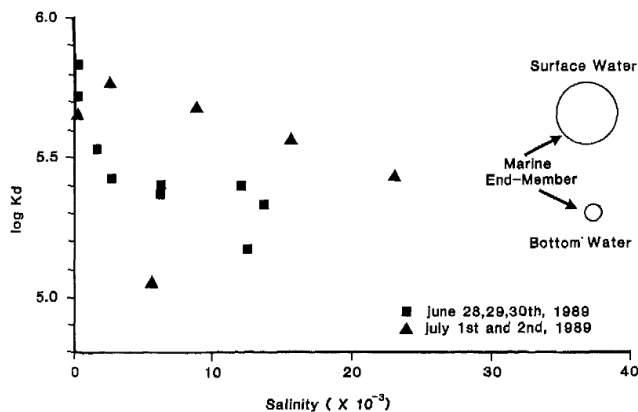


Figure 2.11 Logarithm of partition coefficient between particulate and dissolved mercury (K_d , l/kg) as a function of salinity in the Rhône delta.

Based on the information reported for the Rhône delta, for coastal waters with a salinity exceeding 35 ppt, the logarithm of K_d for surface water is 5.60-5.64 (see Table 2.1, copied from Cossa & Martin, 1991).

Table 2.1 Mercury partitioning field data from the Rhône delta.

Date (day/month/year)	Hour (GMT)	Salinity (10^{-3})	Suspended matter (mg l^{-1})	Particulate mercury ($\mu\text{g g}^{-1}$)	Dissolved mercury (pM)	$\log K_d$
Rhône plume						
03/7/89	9:10	35.32	2.5	0.69	7.9	5.64
03/7/89	9:25	37.37	1.8	0.60	6.9	5.64
04/7/89	11:20	38.80	–	–	8.5	–
04/7/89 ^a	9:30	38.70	0.5	0.71	9.0	5.60
04/7/89 ^b	8:30	–	1.7	0.58	15.0	5.28

Note that 1pM= 0.2 ng/l. Note that K_d is given in l/kg.

2.6.1 Mercury in the Mediterranean

Mercury distribution and cycling in the Mediterranean Sea has been the subject of research and controversy for the past 40 years. Since the early 1970s, various studies showed that Hg concentrations were higher in pelagic fish from the Mediterranean than in the same species from the Atlantic. In particular, Hg in fish tissues occurs mainly as the bioaccumulative and toxic methylated species, methylmercury (MeHg). Concerns about Hg are based on its effects both on ecosystems and human health. The principal pathway for human exposure is the consumption of contaminated fish.

Taking into account the low concentrations of chlorophyll-a in the surface layers of the Mediterranean Sea, particularly in the summer, photochemical processes play an important role in reduction and demethylation. On the other hand, the high bacteria-mediated methylation potential is attributed to the high water temperatures of the Mediterranean Sea.

Rivers are the most important source of Hg contamination from land, with most of the Hg transported in the particulate form. Mercury, particularly in its elementary form, can be transported long distances through air and water, making atmospheric deposition one of the most important sources. However, on the basin scale, Hg evasion from the sea back to the atmosphere exceeds deposition, implying that the Mediterranean is a net source of total Hg for the atmosphere and the connecting seas.

The Mediterranean Basin is rich in Hg from natural and anthropogenic sources, both of which have been attributed as possible sources of the so-called "Mediterranean Hg anomaly". Natural sources include the occurrence of a large number of natural deposits of cinnabar along the coast of many riparian countries such as Italy (Mount Amiata), Algeria (Medjjerda), Spain (Almaden) etc. and volcanoes. Other sources include anthropogenic activities in hotspot areas such as mines. For example, the Idrija mercury mine situated 50 km west of Ljubljana, Slovenia is the second largest Hg mine in the world. It has been in operation continually for 500 years until 1988, when a decision was adopted on its definite shutdown. The tailings and contaminated soils in the Idrija region are continuously eroded and serve as a legacy source of Hg for the Idrija- Soča- Gulf of Trieste watershed. The data collected to-date shows that even years after closure of the mine, Hg concentrations in river sediments and water are still very high and do not show the expected decrease of Hg in the Gulf of Trieste.

(Main sources: Cossa and Conquary, 2005; Monperrus et al., 2007; Rajar et al., 2007; Žagar et al., 2007)

2.7 Nitrogen in the marine environment

In marine waters, nitrogen (N) inputs in a water body come from two distinct sources: the new production, supported by newly available nitrogen and the regenerated production, supported by recycled nitrogen (Dugdale and Goering, 1967).

The new production consists of riverine inputs and atmospheric deposition, supplemented locally by domestic and industrial point sources. Nitrogen in rivers exists in various dissolved, particulate, organic and inorganic forms. Particulate organic nitrogen (PON) is the dominant N form, even if dissolved inorganic nitrogen (DIN) becomes increasingly important due to a growing anthropogenic contribution (Seitzinger et al., 2005). Note that rocks do not contain N-bearing minerals, although some DIN can be absorbed on particles.

The pollutants that contribute to nitrogen atmospheric deposition derive mainly from nitrogen oxides (NO_x) and ammonia (NH_3) emissions. In the atmosphere NO_x is transformed to a range of secondary pollutants (including nitric acid (HNO_3), nitrates (NO_3^-) and organic compounds, such as peroxyacetyl nitrate (PAN), while NH_3 is transformed to ammonium (NH_4^+). Both the primary and secondary pollutants may be removed by wet deposition (scavenging of gases and aerosols by precipitation) and by dry deposition (direct turbulent deposition of gases and aerosols). Wet deposition, predominantly rain and snow, carries nitrate (NO_3^-) and ammonium (NH_4^+). Dry deposition involves complex interactions between airborne nitrogen compounds and water.

Domestic point sources carry their nitrogen loads in various forms, depending on the degree of treatment. Untreated wastewater or primarily treated waste waters contain mostly PON and ammonium, while higher degrees of treatment will result in a higher share of oxidised nitrogen (nitrites and nitrates). For industrial point sources, the nitrogen speciation will depend on the process type and the treatment applied.

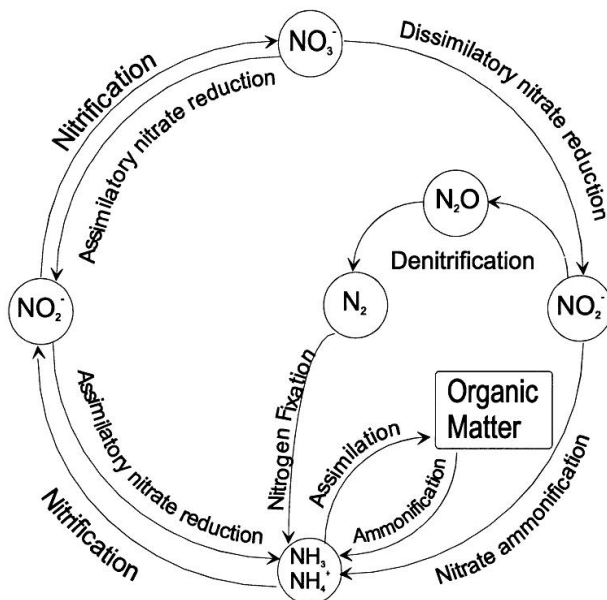


Figure 2.12 The nitrogen cycling showing the chemical forms and key processes involved in the biogeochemical cycling of nitrogen (after Caumette et al., 1996; Herbert 1999).

The regenerated N production results from the biogeochemical transformation of organic nitrogen (both dissolved and particulate) into inorganic nitrogen. Note that N recycling mainly occurs in the water column in deep waters, while sedimentary N cycling is predominant in shallow coastal waters and is called early diagenesis (Bernier, 1980).

The major transformations recognized so far in the nitrogen cycle are microbially catalyzed (Figure 2.12) and include the release of NH_4^+ during the degradation of organic matter, the oxidation of NH_4^+ to NO_2^- (nitrite) and NO_3^- by aerobic nitrifying bacteria (nitrification), and the bacterial denitrification of NO_2^- and NO_3^- to N_2 under anoxic conditions (Herbert, 1999). Denitrification is a drain for readily available N from the ecosystem and plays a role in nutrient limitation of primary production (e.g. Devol, 1991; Seitzinger and Giblin, 1996). It mainly occurs in the sediment, resulting in a N_2 flux at the sediment-water interface, but is also likely to occur in anoxic water layers.

2.7.1 Nitrogen in the Mediterranean

In the semi-enclosed Mediterranean Sea, nitrogen sources are of prime importance, considering the oligotrophic status of the system and the nitrogen and/or phosphorus limitation of primary production (Diaz et al., 2001; Ludwig et al., 2009). Nitrogen budgets in the western and eastern basins depend on the water flows and nitrogen concentrations across the straits of Gibraltar and Sicily, together with atmospheric, terrestrial and recycled influxes. The eastern part is ultra-oligotrophic: its average phytoplankton productivity of $60\text{--}80 \text{ gC m}^{-2} \text{ y}^{-1}$ is approximately half of that measured in other oligotrophic areas of the world's oceans such as the Sargasso Sea (Béthoux 1989; Krom et al., 2003). The main reason for the very low productivity is the unusual anti-estuarine circulation in the basin in which nutrient depleted surface water flows in through the straits of Sicily, while more saline Levantine intermediate water flows out at intermediate depths (200–500 m) carrying with it dissolved nutrients, including nitrate and phosphate.

Nitrate shows relative moderate area specific fluxes in the Mediterranean, indicating that nitrogen pollution is not a major problem in the Mediterranean rivers (Table 2.2, Ludwig et al., 2009). Nitrate fluxes in the Rhône, Po and Ebro rivers increased steadily from the beginning of the 1970s up to the 1990s, before they remained approximately constant, or even decreased during recent years. Nitrogen terrestrial inputs are usually dominated by diffuse sources, in particular agriculture, which is characterized in southern Europe by less intensive cultivation practices. Greater nitrates fluxes were reported in the North-Western part of the Mediterranean, where agricultural land is more densely developed. However, the fluxes remained low compared to what is commonly reported for the large European rivers further to the north, such as the Seine and Rhine rivers (Billen and Garnier, 2007).

The sediment is the second major source of DIN, as inorganic nitrogen is released from the seafloor by biodiffusion and advective processes on continental shelves. For instance, in the Gulf of Lions, biodiffusive sedimentary DIN contribution was estimated equivalent to around 20-30% of the Rhône River inputs (Denis et al., 2001).

Finally, dry atmospheric deposition of nitrogen and dinitrogen (N_2) in the Mediterranean is a non-negligible pathway for nitrogen to the photic zone of the open sea, where there is little riverine input (e.g. Benitez-Nelson, 2000). The dry deposition is not only a significant source of nutrients to surface waters at the yearly scale (Herut et al., 2002), but it is also likely to contribute noticeably to new production during the dry oligotrophic season.

Table 2.2 Averaged nitrate and phosphorus levels in Mediterranean and Black Sea rivers during recent years (after Ludwig et al. 2009).

River	Basin	Country	av. N-NO ₃		av. P-PO ₄		Q (mm)	F-NO ₃ (kg N km ² yr ⁻¹)	F-PO ₄ (kg P km ² yr ⁻¹)
			(mg l ⁻¹)	Period	(mg l ⁻¹)	Period			
Acheloois	ION	Greece	0.29	01-02	0.010	01	1023	292	10
Aliakmon	AEG	Greece	1.02	01-02	0.125	01-02	123	125	15s
Arno	NWE	Italy	2.39	01-05	0.149	01-05	255	609	38
Aude	NWE	France	1.51	00-05	0.107	00-05	290	437	31
Axios	AEG	Greece	1.94	00-02	0.540	00	198	384	107
Danube	BLS	Rumania	2.33	00-02	0.095	00-02	257	599	24
Ebro	NWE	Spain	2.39	00-05	0.065	00-03	110	263	7
Evros	AEG	Greece/Turkey	1.16	02	1.470	02	124	144	182
Herault	NWE	France	0.58	00, 06	0.023	00, 06	590	340	13
Isonzo	ADR	Italy	1.54	01-05	0.007	01-05	1830	2818	14
Jucar	NWE	Spain	4.01	00-05	0.080	05	58	233	5
Kamjia	BLS	Bulgaria	5.31	00-05	0.146	00-05	113	600	16
Llobregat	NWE	Spain	2.19	01-04			95	208	
Mijares	NWE	Spain	1.07	00-05			79	85	
Neretva	ADR	Croatia	0.66	03-05	0.007	03-05	1169	767	8
Nestos	AEG	Greece	1.58	00-04	0.088	00-04	179	283	16
Piave	ADR	Italy	1.33	00-05	0.020	03-05	780	1039	15
Pinios	AEG	Greece	2.09	00-02	0.703	00-02	69	144	49
Po	ADR	Italy	1.91	01-05	0.082	01-05	683	1302	56
Rhone	NWE	France	1.44	00-05	0.050	00-05	564	812	28
Strymon	AEG	Greece	1.39	00-04	0.222	00-04	157	218	35
Tagliamento	ADR	Italy	1.23	01-05	0.031	01-05	750	924	23
Tevere	TYR	Italy	2.10	03-04			446	937	
Turia	NWE	Spain	3.22	00-05	0.235	05	42	135	10
Vjose	ADR	Albania	1.04	01-05	0.018	01-05	917	951	16

Average concentrations were taken from EEA (2007), except data for the Danube (TNMN, 2002) and the Aude and Herault rivers (Ludwig et al. (2003)). Long-term average runoff values from Ludwig et al. (2003) were used for flux calculations (F-NO₃ and F-PO₄).

3 Modelling strategy

3.1 Approach to assessing the variations of EQSs with ELVs

In this section we present the approach to assess the relation between the Emission Limit Value (m-ELV, expressed as g/s) of a point source of pollution and the Environmental Quality Standard (EQS, expressed as g/m³) applicable to the receiving waters. We note that other units, like kg/day or tons/year for the m-ELV or µg/L or ng/L for the EQS may also be used. The use of such units does not affect the approach, but may require the use of scale factors.

The m-ELV is expressed as a mass flux (in g/s). With a given effluent discharge flow expressed as a volume flux (Q_e in m³/s), the m-ELV can be translated to a maximum allowable effluent concentration (c-ELV in g/m³) as follows:

$$c\text{-ELV} = m\text{-ELV} / Q_e$$

A mixing zone (MZ) is an area around the discharge point where the concentration of a Contaminant of Concern (CoC) may exceed the EQS. Figure 1.1 illustrates the concept of a mixing zone in flowing waters. The figure demonstrates that the EQS needs to be satisfied at a checkpoint located some distance L (the maximum allowable length of the MZ) downstream of a pollution source. If no mixing zone would be allowed, the relation between the c-ELV and the EQS would be simple: the concentration in the effluent should not exceed the EQS, or $c\text{-ELV} \leq \text{EQS}$.

When a mixing zone is defined, the ELV will depend on the maximum allowable size of the mixing zone. The larger the mixing zone, the more space will be available for mixing of effluents and ambient water, and the lower the concentration at the edge of the mixing zone will be, because of a given discharge. Inversely, with a given accepted concentration at the edge of the mixing zone, the emission needed to exceed that value will be larger if the mixing zone is larger.

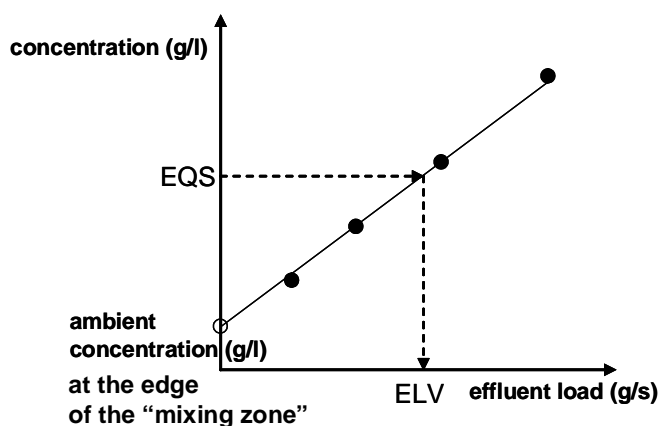


Figure 3.1 Schematic representation of the relation between the EQS and the m-ELV.

The relation between the m-ELV and the EQS for a given MZ is shown in Figure 3.1. This figure shows how with increasing effluent load (horizontal axis), the ambient concentration at the edge of the defined mixing zone increases (vertical axis). Note that with an effluent load of zero, the concentration still has a value above zero. This is the background concentration represented by the open circle. Figure 3.1 illustrates that for a given allowed ambient concentration (the EQS), the related m-ELV can be derived if the relation between the effluent load and the ambient concentration at the edge of the defined mixing zone has been established.

There is a tool, called “Discharge Test”, to support an assessment of the relation between the ELV and the EQS according to the Tiers 0-1-2, as discussed in Section 1.1¹. In its Tier 2 approach for coastal waters, this Discharge Test establishes the relation between the ELV and the EQS, taking into account:

- the discharge characteristics (location, effluent volume, effluent concentration, effluent density, effluent pipe diameter, vertical position);
- the receiving water characteristics; for a coastal discharge the only option is a straight coastline, where the user defines the water depth, the vertical density distribution and the long shore currents.

This Discharge Test allows easy application and offers a generic, coherent and harmonized approach that can be readily applied to various other locations, with limited data requirements. However, the method does not account for the substance properties, nor does it account for other coastal environments than those having a straight coastline or for the variability of the coastal environment.

In this study, we provide a “detailed 3D modelling” approach to establish the relation between the effluent load and the ambient concentration at the edge of the defined mixing zone, taking into account in detail the characteristics of the receiving water body and the substance characteristics. Such an approach however, requires a high level of skill from its user, is very site specific and requires detailed input data. The effort required for the detailed 3D modelling approach is so large that the application to all hot spots (see Figure 2.9) would be very costly, and would not lead to coherent and harmonised results.

In a 1989 study titled *Screening Model for Coastal Pollution Control in the Mediterranean* (Delft Hydraulics, 1989) an intermediate “generalised Tier 3” method is proposed, which combines the strong points from the Tier 2 and detailed 3D modelling approaches. It allows for easy application and offers a generic, coherent and harmonized approach, but at the same time, it includes more site-specific information that allows application to the variety of coastal environments encountered in the Mediterranean.

In this report, we describe simultaneous applications of the detailed 3D modelling and generalised Tier 3 methods. The objective of these simultaneous applications is to explore the possibilities to have credible and site-specific results from the generalised Tier 3 method, which can much easier be applied to a large amount of sites than the detailed 3D modelling approach. In the next Sections, we present the detailed 3D modelling and generalised Tier 3 modelling methods. We note that these are generic descriptions; the implementation to our

1. Discharge test, in support of Tier 1 and Tier 2 of the Technical Guidelines for the identification of mixing zones pursuant to Art. 4(4) of the Directive 2008/105/EC, <http://dgs-as2.geodelft.nl/eitoets/>

study sites will be discussed in Chapter 4. Before discussing these modelling approaches, we first provide some considerations regarding the spatial scale of the analysis, in relation to the mixing zones for the MAC-EQS and the AA-EQS (as defined in Section 2.5.1).

3.2 Spatial scales of analysis

The “near field” is defined as the area close to a waste water outlet where the momentum of the (buoyant) waste water jet, causing entrainment of ambient water into the jet, is the dominant transport mechanism. During the following “far field” stage, the fate of the discharge is determined by transport with the ambient currents and, for some substances, decay or removal processes. During the near field stage, the jet may move in a vertical direction and will undergo dilution. The final elevation and dilution at the end of the near field are determined by the elevation, geometry and opening diameter of the discharge pipe(s), the density of the discharged fluid and the ambient flows and ambient water density and vertical density gradients.

As discussed in Section 2.5.1, the spatial scale of the mixing zone for an evaluation of the AA-EQS typically extends to 500-1000 m. At such spatial scales, the concentration patterns resulting from the discharges under study are determined mostly by the far field stage. This holds especially for relatively small discharges without advanced discharge structures like multi-port diffusers, in a situation with relatively small background currents and small tidal motion. For this reason, both the detailed 3D modelling and generalised Tier 3 modelling methods focus on the far field stage of the pollutant transport, taking into account however, the relevant near-field aspects.

As discussed in Section 2.5.1, the spatial scale of the mixing zone for an evaluation of the MAC-EQS may be much smaller. In some countries, mixing zones of 10-25 m are used to evaluate the MAC-EQS. At these small spatial scales, the concentration patterns resulting from the discharges under study are determined mostly by the near field stage, and both the detailed 3D modelling and generalised Tier 3 modelling methods lose their relevance. At such occasions, a dedicated near-field model is more appropriate. For this reason, the Discharge Test tool mentioned above includes an approach to account for the near field stage in a rather accurate fashion, as long as there are no complex (multi-port) diffusers.

We note that software exists to calculate the near field transport of a marine discharge (e.g. CORMIX, <http://www.cormix.info/>). The direct integration of near field and far field transport phenomena within one calculation procedure is still in a development stage.

Since it is not up to the authors to decide whether or not a MAC-EQS mixing zone should be smaller than a AA-EQS mixing zone, we provide two alternative approaches:

- 1 As a part of the application of the detailed 3D modelling and generalised Tier 3 modelling methods, we will provide an approach to deal with the MAC-EQS mixing zone in the case that it is of the same order as the AA-EQS mixing zone.
- 2 As a part of the discussion of the results, we will provide an approach to deal with the MAC-EQS mixing zone in the case that it is much smaller than the AA-EQS mixing zone.

3.3 Detailed 3D hydrodynamic modelling

The currents and water levels in the coastal waters are modelled using the 3D hydrodynamic modelling system Delft3D-FLOW (Lesser et al., 2004). This system solves the unsteady hydrostatic shallow-water equations in three dimensions. The system of equations consists of the horizontal momentum equations, the continuity equation, the transport equation, and a k-ε turbulence closure model. The vertical momentum equation is reduced to the hydrostatic pressure relation as vertical accelerations are assumed to be small compared to gravitational acceleration and are not taken into account. The model equations are solved on a spherical curvilinear grid in the horizontal (Kernkamp et al 2005), while applying sigma layering in the vertical. Based on the governing equations, the model is suitable for predicting the flow in shallow seas, coastal areas, estuaries, lagoons, rivers, and lakes, taking into account relevant physical processes due to e.g. barotropic tide, river discharges and baroclinic density currents.

In Cartesian co-ordinates, the three-dimensional hydrostatic shallow water equations for horizontal velocities u , v and water level variation ζ , with σ -co-ordinates in the vertical, are described by:

$$\begin{aligned} \frac{\partial u}{\partial t} + u \frac{\partial u}{\partial x} + v \frac{\partial u}{\partial y} + \frac{\omega}{d+\zeta} \frac{\partial u}{\partial \sigma} - fv &= -\frac{1}{\rho} P_u + F_u + \frac{1}{(d+\zeta)^2} \frac{\partial}{\partial \sigma} \left(\nu_v \frac{\partial u}{\partial \sigma} \right) \\ \frac{\partial v}{\partial t} + u \frac{\partial v}{\partial x} + v \frac{\partial v}{\partial y} + \frac{\omega}{d+\zeta} \frac{\partial v}{\partial \sigma} + fu &= -\frac{1}{\rho} P_v + F_v + \frac{1}{(d+\zeta)^2} \frac{\partial}{\partial \sigma} \left(\nu_v \frac{\partial v}{\partial \sigma} \right) \\ \frac{\partial \omega}{\partial \sigma} &= -\frac{\partial \zeta}{\partial t} - \frac{\partial [(d+\zeta)u]}{\partial x} - \frac{\partial [(d+\zeta)v]}{\partial y} + H(q_{in} - q_{out}) + P - E \end{aligned}$$

with d denoting water depth below reference datum, $H = d + \zeta$ the total water depth, f the Coriolis parameter, P_u , P_v , F_u , F_v , q_{in} , q_{out} the components of the pressure gradients, horizontal viscosity and lateral mass exchanges, P and E representing precipitation and evaporation, and ν_v the vertical eddy viscosity. The horizontal viscosity is based on the so-called Boussinesq eddy viscosity concept, in which the Reynolds-stresses are parameterized by the product of an eddy-viscosity with the spatial gradient of the mean quantities. The vertical velocities ω in the σ -co-ordinate system are computed from the continuity equation:

$$\frac{\partial \zeta}{\partial t} + \frac{\partial [(d+\zeta)U]}{\partial x} + \frac{\partial [(d+\zeta)V]}{\partial y} = Q$$

by integrating in the vertical from the sea bed to a level σ ($-1 \leq \sigma \leq 0$). Here, U and V denote the depth-integrated velocity components, respectively. The (comparatively small) vertical velocity w in the x-y-z Cartesian co-ordinate system can be expressed in the horizontal velocities, water depth, water level and vertical σ -velocities ω according to:

$$w = \omega + u \int_{\sigma}^0 \frac{\partial H}{\partial x} + \frac{\partial \zeta}{\partial x} + v \int_{\sigma}^0 \frac{\partial H}{\partial y} + \frac{\partial \zeta}{\partial y} + \int_{\sigma}^0 \frac{\partial H}{\partial t} + \frac{\partial \zeta}{\partial t}$$

where ω is the vertical velocity relative to the moving σ -plane.

This may be interpreted as the velocity associated with up- or downwelling motions. In the continuity equation, Q represents the flow contributions per unit area due to the discharge or withdrawal of water, precipitation P and evaporation E :

$$Q = H \int_{-1}^0 (q_{in} - q_{out}) d\sigma + P - E$$

The shear-stress at the bed is specified by a quadratic friction law:

$$\vec{\tau}_b = \frac{\rho_0 g \vec{U} |\vec{U}|}{C_{2D}^2}$$

with the 2D-Chézy coefficient C_{2D} prescribed by the Manning's formula, which is based on the total water depth and a user-defined Manning's coefficient. Optionally, the model can solve the transport equations for heat and salinity, and feed back the result to the pressure gradient and vertical eddy viscosity.

The governing equations for the 3D hydrodynamic model described above are discretized applying a finite difference method on an Arakawa C type grid, implying that water levels and velocity components are defined on the grid cell centres and cell faces respectively. For the time integration, the Alternating Direction Implicit (ADI) method is used to solve the continuity and horizontal momentum equations. For details we refer to Twigt et al. (2009) and references therein.

3.4 Detailed 3D water quality modelling

The water quality in the coastal waters is modelled using the 3D water quality modelling system Delft3D-WAQ. The 3D water quality model is based on the advection-diffusion equation (Crank, 1975; Thomann & Mueller, 1987; Chapra, 1997). In three spatial dimensions this equation reads:

$$\frac{\partial C}{\partial t} = -U_x \frac{\partial C}{\partial x} + \frac{\partial}{\partial x} \left(D_x \frac{\partial C}{\partial x} \right) - U_y \frac{\partial C}{\partial y} + \frac{\partial}{\partial y} \left(D_y \frac{\partial C}{\partial y} \right) - U_z \frac{\partial C}{\partial z} + \frac{\partial}{\partial z} \left(D_z \frac{\partial C}{\partial z} \right) + S$$

where C represents the concentration in g m^{-3} , U_x, U_y, U_z represent the water flow velocity in m s^{-1} , D_x, D_y, D_z represent the dispersion coefficient in $\text{m}^2 \text{s}^{-1}$, and S a source term in $\text{g m}^{-3} \text{s}^{-1}$. The advection (U_x, U_y, U_z) and diffusion (D_x, D_y, D_z) terms represent the transport of substances because of the movement of the transporting medium (water). The values U_x, U_y, U_z and D_z are derived directly from the hydrodynamic model. D_x and D_y are input to the model. All quantities are a function of space and time (x, y, z, t). This equation can be applied for one substance, or for a collection of substances.

The source term S in the equation represents the specified load(s) of the modelled substance(s) entering the water system, as well as various physical and biochemical processes affecting the modelled substance(s). For substances that are present in particulate forms, these processes include the transport of substances to and from aquatic sediments, driven by particle fluxes.

In this study, three substances (pollutants) are simulated: (1) a conservative (non-decaying) substance; (2) total nitrogen; and (3) total mercury. The word “total” refers to the sum of all relevant species of nitrogen and mercury respectively, as discussed in Chapter 2. The pollutants are carried away from the discharge point by the currents calculated by the hydrodynamic model. There is a sink term included in the equation that represents decay and removal processes for nitrogen and mercury respectively.

For total nitrogen (N), a removal term expressed as a first order decay rate k_N in d^{-1} is introduced:

$$S = -k_N \times N$$

As argued in Chapter 2, only the denitrification process is responsible for the removal of nitrogen from the water column. According to an EPA review, typical values of k_N are in the range of $0.02 - 0.10 d^{-1}$, and act on the nitrates fraction of total nitrogen only. These values are given for a water temperature of $20^\circ C$ (EPA, 1985). Based on this information, we selected a decay rate of $k_N = 0.03 d^{-1}$ for the present simulations.

For mercury (Hg), the model accounts for the net sedimentation of the fraction of Hg in the suspended solids phase. The partitioning of Hg between the solids and water phase is modelled by the conventional water to sediment partition coefficient (K_d , Thomann & Mueller, 1987). The removal term is calculated from two parameters related to the particles in the water: the particle concentration SS (in $g m^{-3}$) and the particle settling velocity V_s (in $m s^{-1}$). For a given partition coefficient K_d (in m^3/g), the fraction of Hg attached to particles f_p can be calculated as follows:

$$f_p = \frac{K_d \cdot SS}{1 + K_d \cdot SS}$$

The flux F of Hg settling with the particles in $g m^{-2} s^{-1}$ can now be calculated as follows:

$$F = SS \times V_s \times \frac{f_p \times Hg}{SS} = f_p \times Hg \times V_s$$

This can be converted to an equivalent first order decay rate k_{Hg} (d^{-1}):

$$k_{Hg} = -\frac{f_p \times V_s}{H}$$

where H represents the total water depth. Therefore, the decay rate for mercury k_{Hg} depends on the partition coefficient K_d , which we consider a substance property ($K_d = 0.437 m^3/g$, see Chapter 2), and on the environmental parameters suspended solids (SS), water depth (H) and the particle settling velocity (V_s). The water depth follows from the model bathymetry, the environmental parameters SS and V_s are user input.

Note that the dissolved fraction is computed from the total concentration as follows:

$$f_d = \frac{1}{1 + K_d \cdot SS} = 1 - f_p$$

The advection-diffusion equation described above is discretized and solved numerically by a finite volume technique, as provided by the general purpose water quality modelling programme DELWAQ (Postma & Hervouet, 2006), which is embedded in Delft3D. It concerns the Flux Correct Transport (FCT) Method, based on the 2nd order Lax-Wendroff method (Lax & Wendroff, 1960), while the typical oscillations are suppressed by a method from Boris and Book (1973).

3.5 The Screening Model for Coastal Pollution Control in the Mediterranean (1989)

The original "Screening Model for Coastal Pollution Control in the Mediterranean" (SCREMO, Delft Hydraulics, 1989) allows the assessment of up to five coastal discharges in a relatively small spatial domain (typically 5x2 km or smaller). For each of the discharges, the location, flow, the concentration and the near field dilution factor need to be specified. The resulting concentrations are calculated by a 3D water quality model that is forced by the estimated currents in the study area.

3.5.1 Geometry

SCREMO uses a strong simplification of the marine environment, consisting of a rectangular section of the marine waters along a straight coastline (see Figure 3.2). The bottom slope is uniform and optionally can be separated in two sections (Figure 3.3). In the case of a strong stratification, only the buoyant surface layer is modelled; the denser bottom layer is considered irrelevant for evaluating the effects of the discharge.

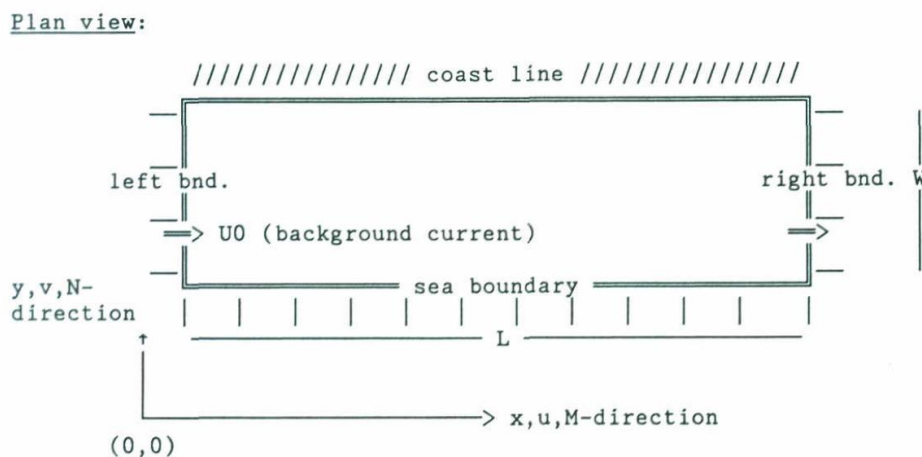


Figure 3.2 Plan view of a SCREMO model

Cross section (see appendix A)

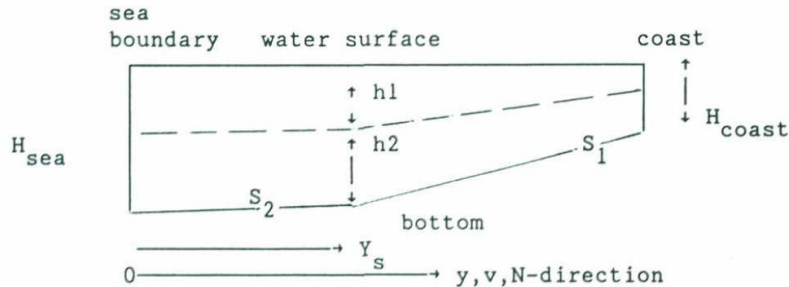


Figure 3.3 Cross section of a SCREMO model

3.5.2 Currents

SCREMO uses simplified steady-state current patterns: it assumes that wind-driven vertical circulation is the dominant mechanism affecting the distribution of the discharged pollutants. This wind-induced circulation causes a current in the direction of the wind near the water surface, assumed equal to 3% of the wind speed, and a reverse current further down. The left side of Figure 3.4 shows an example of such a wind induced overall vertical velocity profile (see also Appendix A).

In addition, a background current can be defined (see “U0” in Figure 3.2). This current can be a part of a larger scale, wind-induced horizontal circulation. This leads to a velocity profile as shown on the right side of Figure 3.4 (see also Appendix A). Going from the sea boundary towards the coast line, the magnitude of the background current diminishes due to the decreasing water depth that causes an increasing effect of the bottom friction. This is expressed by a simplified energy loss approximation:

$$U(y) = \left(\frac{H(y)}{H_{sea\ boundary}} \right)^{2/3} \cdot U_{sea\ boundary}$$

As a final step in the calculation of the currents, the vertical currents are calculated by applying a water balance equation, which ensures that the water level remains constant.

Other mechanisms are neglected; density differences and short waves are assumed irrelevant at small spatial scales (< 5 km) and the tide is considered too small to have a significant effect. We note that the currents generated by the water volume of the discharge are neglected as well.

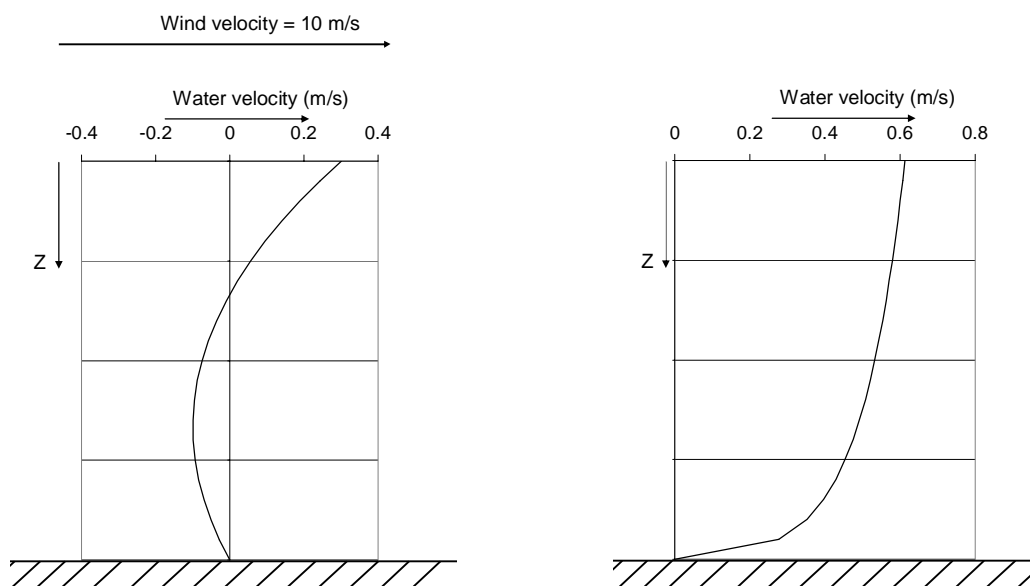


Figure 3.4 Examples of a wind-induced vertical velocity profile (left) and a velocity profile associated to the background current (right).

3.5.3 Water quality

SCREMO performs 3D Delft3D-WAQ simulations of the water quality (see Section 3.4) on a 20x10 cells horizontal grid. SCREMO offers the following selection of substances: a conservative substance, faecal coliforms, Biochemical Oxygen Demand (BOD) and Dissolved Oxygen (DO). The relevant processes are implemented, dependent on the water temperature, the solar radiation, etc. SCREMO also takes into account the background concentration of the modelled pollutants. Individual SCREMO simulations hold for one set of conditions, independent of time (“steady state”). Figure 3.5 shows a typical result of a single SCREMO simulation.

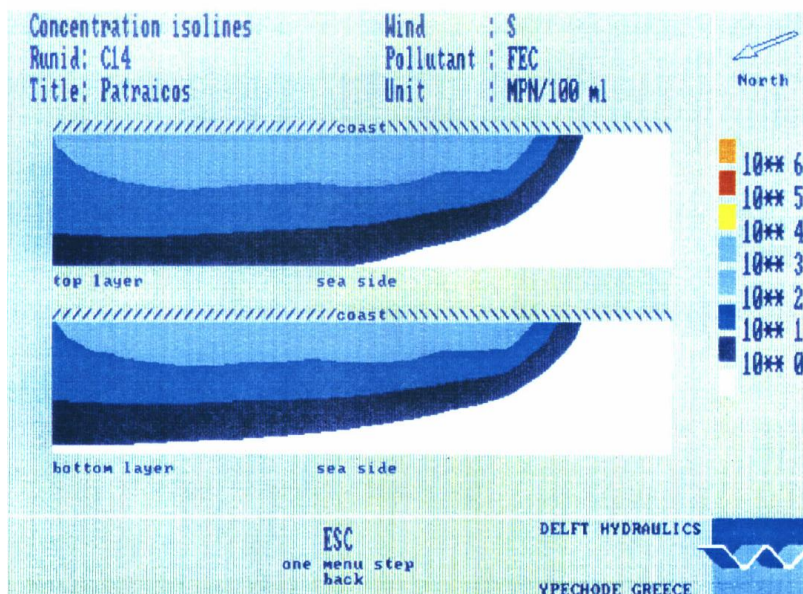


Figure 3.5 Typical result of a single SCREMO simulation (plan view)

The variable character of the conditions, in particular of the wind forcing, is taken into account: 9 simulations are made for 9 different wind directions with different probabilities of occurrence to compile a picture of the variability of the pollutant distribution. Figure 3.6 shows these results for one single location. The composite result is an aggregation of the results from the 9 individual simulations, where every result is attributed the probability of occurrence of its input conditions. Thus, a spatially varying “expected” concentration can be calculated, as well as the probability that a certain standard will be violated (see Figure 3.7).

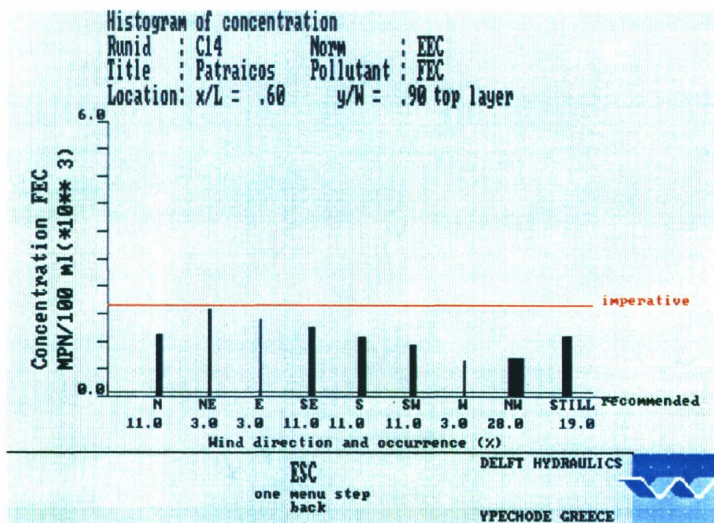


Figure 3.6 Simulated concentration (bar height) and probability (bar width) for a composite of 9 SCREMO simulations for different wind conditions at a single location.

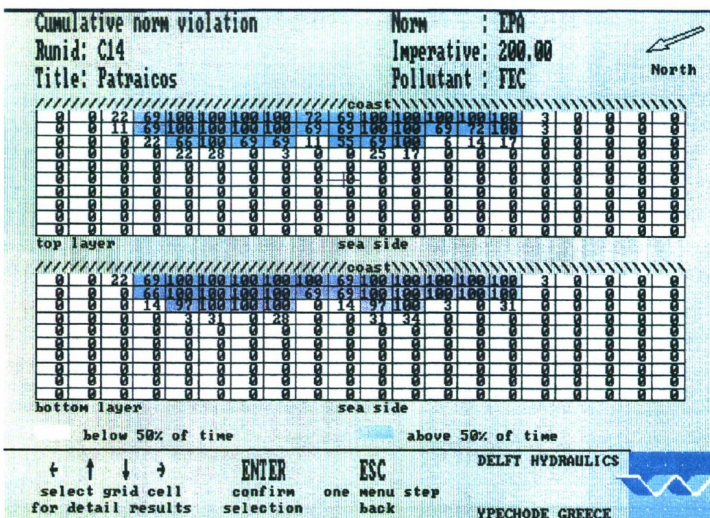


Figure 3.7 Simulated risk of standard violation (% of time) for a composite of 9 SCREMO simulations for different.

For a full description of the SCREMO approach, we refer to the original report (Delft Hydraulics, 1989).

3.6 Generalised Tier 3 model used in the present study

3.6.1 The modified SCREMO concept

The concept of SCREMO offers interesting perspectives to obtain site-specific and substance-specific results in an easily applicable way. There are reasons however, to reconsider some assumptions and simplifications used by SCREMO, in order to enhance the acceptability. First, today's computers have a much higher capacity than those from the 1980s. Therefore, we increased the model resolution to obtain a more detailed spatial pattern. Other relevant updates and modifications have been developed during the present study based on the applications to the Gulf of Lions and Izmir Bay. They will be discussed below.

3.6.2 Geometry of the study area

We found that the assumption of a straight coastline and a rectangular coastal area with open boundaries at three sides (as shown in Figure 3.2) could not always be used. Figure 3.8 shows the Izmir Bay area, with some 5000m x 2000m boxes representing a typical study area around a (hypothetical) pollution source. In this case, the geometry adopted by the original SCREMO (Case I in Figure 3.9) would be acceptable in some cases (A, B) but not always (C). To represent case C properly, an approximated geometry consisting of a water body enclosed along three sides has been added to the SCREMO concept (Case II in Figure 3.9).

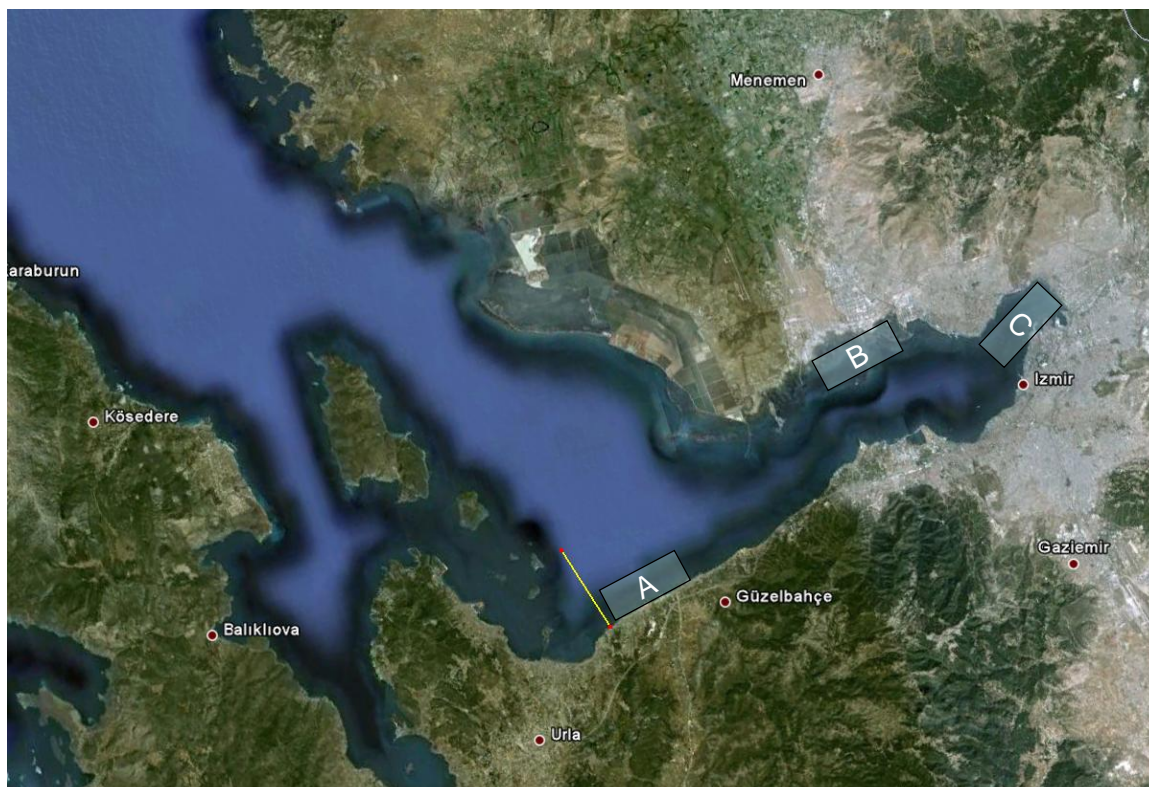


Figure 3.8 Izmir Bay, with several boxes (A, B and C) showing 5000x2000 m areas

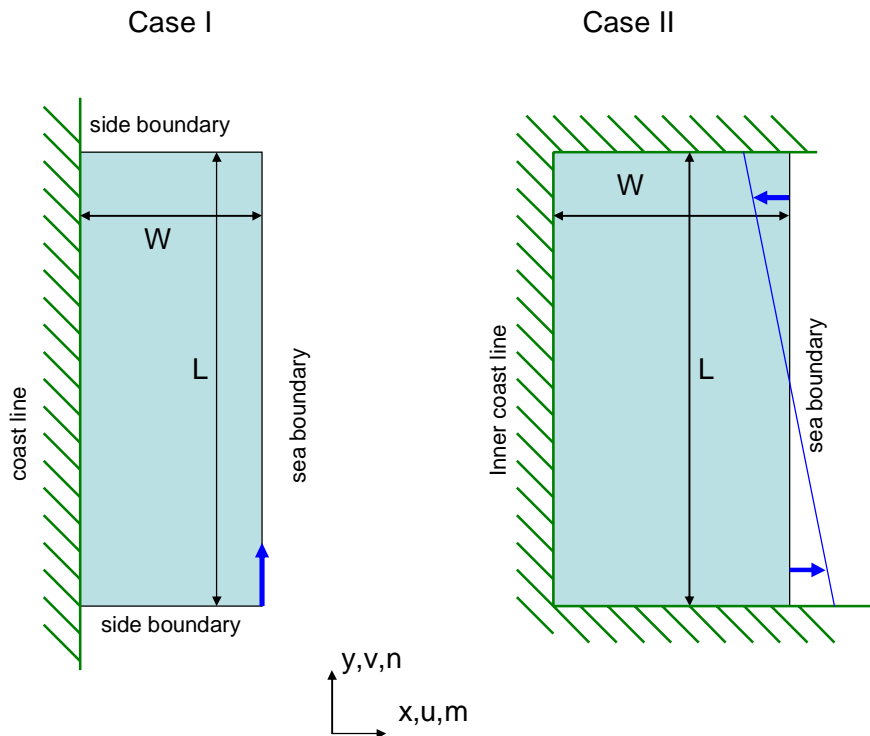


Figure 3.9 Approximate geometries adopted in the modified SCREMO concept.

3.6.3 Currents in the study area

In the modified SCREMO concept, we adapted the definition of the currents in the study area. This was necessary for Case II especially (Figure 3.9). For Case II, it is not possible to implement a background current as in Case I (blue arrow in Figure 3.9, left side): in stead, we implemented a horizontal circulation pattern (blue arrows in Figure 3.9, right side). Along the open sea boundary, the currents are defined as indicated by the blue line in Figure 3.9. The integral along the open sea boundary is zero: there is just as much water flowing in on one side as there is flowing out on the other side. Going from the sea boundary towards the inner coastline, the magnitude of the circulation currents perpendicular to the inner coastline diminishes due to the decreasing water depth that causes an increasing effect of the bottom friction. This is expressed by a simplified energy loss approximation (see Section 3.5.2). The changes in the currents perpendicular to the inner coastline are balanced by currents parallel to the inner coastline. All currents are represented by vertical profiles like the one shown on the right side of Figure 3.3. As in Case I, a wind-induced vertical circulation pattern is added like the one shown on the left side of Figure 3.3.

As a final step in the calculation of the currents, the vertical currents are calculated by applying a water balance equation, which ensures that the water level remains constant.

3.6.4 Water quality modelling

In the Generalised Tier 3 model, we use exactly the same water quality model formulations as discussed in Section 3.4. The horizontal and vertical dispersion coefficients are input to the model.

Near field effects are treated just as in the SCREMO model. We specify the discharge at the position it has at the end of the near field, and we estimate the horizontal and vertical position according to the instructions in the SCREMO documentation.

We carry out an explicit check on the concentrations calculated at the edge of the mixing zone: these cannot be larger than those calculated from the near field dilution alone. Since the grid of the generalised Tier 3 model is much finer than the SCREMO grid, the mixing of the discharge in the discharge point grid cell is much smaller. This may result in an underestimation of dilution near the discharge point.

Finally, we apply the correction of the simulated concentrations to account for the fact that the water volume of the discharge is neglected, just as in SCREMO.

3.6.5 Overview of input for the Generalised Tier 3 model used in the present study

An overview of all input used for one single simulation of the Generalised Tier 3 model used in the present study is presented in Table 3.1. Contrary to the original screening model, the number of single simulations is no longer fixed, and there is no restriction to varying the input parameters between the individual simulations.

3.7 Near-field considerations

In both the detailed 3D modelling and the generalised Tier 3 modelling approaches, elements of the near field need to be considered. This is done as discussed in the SCREMO documentation.

The horizontal position of the discharge should be specified taking into account the horizontal plume movement during the near field phase: the documentation provides rules of thumb to estimate this distance. The SCREMO documentation recommends for practical situations, while most discharges are expected to be fresh, to specify the discharge at the water surface regardless of the physical position of the discharge point. Exceptions to this rule of thumb are discharges from a strongly mixing diffuser at a large depth in water with a vertical density gradient, and discharges of water with equal or only slightly lower density than the receiving water.

The dilution of the discharge at the end of the near field zone is also of importance, because it determines the volume of water affected by the discharge at the end of the near field zone. This may be accounted for by specifying the discharge not in a single cell of the far field model, but mixed over a cluster of cells.

We note that our approach is to some extent arbitrary. Also other ways to deal with the near field could have been selected.

Table 3.1 Overview of input data for a single simulation of the Generalised Tier 3 model.

Input item	Symbol	Comments
Description		
Length (m)	L	See Figure 3.9.
Width (m)	W	See Figure 3.9.
Direction of grid (°)		Angle of Y-axis with respect to North (see Figure 3.9), measured in a clockwise direction
Water depth along inner coast line (m)		
Water depth along sea boundary (m)	H	15
Nr of grid cells (-)		Along L, along W, vertical
Direction of wind (°)		Measured relative to north, so north = 0°, east = 90°, south = 180°, west = 270°
Wind speed at 10 m (m/s)		
Circulation in (m/s)		For Case I: the background current along the open sea boundary (positive as indicated in Figure 3.9), for Case II the maximum circulation current at the open sea boundary (positive if circulation is counter-clockwise)
Frequency of occurrence (%)		The sum of all single simulations should equal 100%
Position of discharge (x,y,z) (m)		Position of the discharge at the end of the near field stage
Discharge flow rate (m ³ /s)	Q _e	
Near field dilution factor	S	
Suspended solids (mg/l)	SS	This quantity is used to calculate the particulate fraction of substances that show partitioning
Settling velocity of particles (m/d)	V _s	This quantity is used to calculate the effective removal rate of substances that show partitioning due to the settling of particles
Representative water depth (m)		This quantity is used to calculate the effective removal rate of substances that show partitioning due to the settling of particles
Horizontal dispersion (m ² /s)	D _x , D _y	
Vertical dispersion (m ² /s)	D _z	

3.8 From individual simulations to an EQS-ELV dose-effect curve

As discussed in Section 2.5.1, EQSs can be defined for maximum concentrations and for mean concentrations. For the detailed 3D model, the simulated concentrations are statistically processed and converted to a spatially variable maximum and mean concentration. This is a standard functionality of Delft3D-WAQ.

For the generalised Tier 3 model, a number of different water quality simulations is carried out, each of them representing a situation with a given probability of occurrence. The overall statistical properties of the results from the generalised model are determined based on the

results from the individual simulations. The maximum concentration at a given location equals the maximum concentration at that location obtained during any of the individual simulations. The mean concentration at a given location is calculated as the weighted average of the concentrations at that location obtained during all individual simulations, with their respective frequency of occurrence as the weight factor.

The next step is to derive the maximum and mean concentrations at the edge of the mixing zone, as a function of the mixing zone dimension. In this case, we consider the mixing zone to be circular, with the discharge point at the centre of the circle. This is done for a conservative tracer, for nitrogen and for mercury. In the mercury case, the results are converted to reflect the dissolved fraction only.

As a final step in the evaluation of the results, the relation between the m-ELV and the EQS is established. So far, all water quality simulations have been conducted with a discharge of the simulated pollutants of 1 g/s. In view of the fact that the water quality processes formulations used are linear, we use this property of linearity to obtain solutions for an arbitrary discharge rate by scaling the solution for a discharge rate of 1 g/s with the real discharge rate.

If necessary, a background concentration can be added to the solution. In this way, linear relations between the emission and the ambient concentrations are obtained, as shown by Figure 3.1. The relation between an m-ELV and an EQS can be obtained, for a given mixing zone from this dose-effect-relation.

4 Model set-up

4.1 Izmir Bay detailed 3D model

The Izmir Bay detailed model has been set up in a way that allows the simulation of wind-induced currents, causing both vertical and horizontal circulation patterns. The pollution hot spot in this case is the shallow Inner Izmir Bay, with depths not exceeding 15 m (Sayin, 2003). The Inner Bay is too shallow to be affected by stratification, with a pycnocline at 20-35 m (Sayin, 2003).

4.1.1 Model domain and bathymetry

Figure 2.1 shows the main features of Izmir Bay. The detailed model covers the Inner and Middle parts of the Bay, and has an open boundary at the location where the Outer bay starts. Figure 4.1 shows the model grid and bathymetry. The bathymetry was derived from the SRTM-30 dataset discussed in Chapter 2.

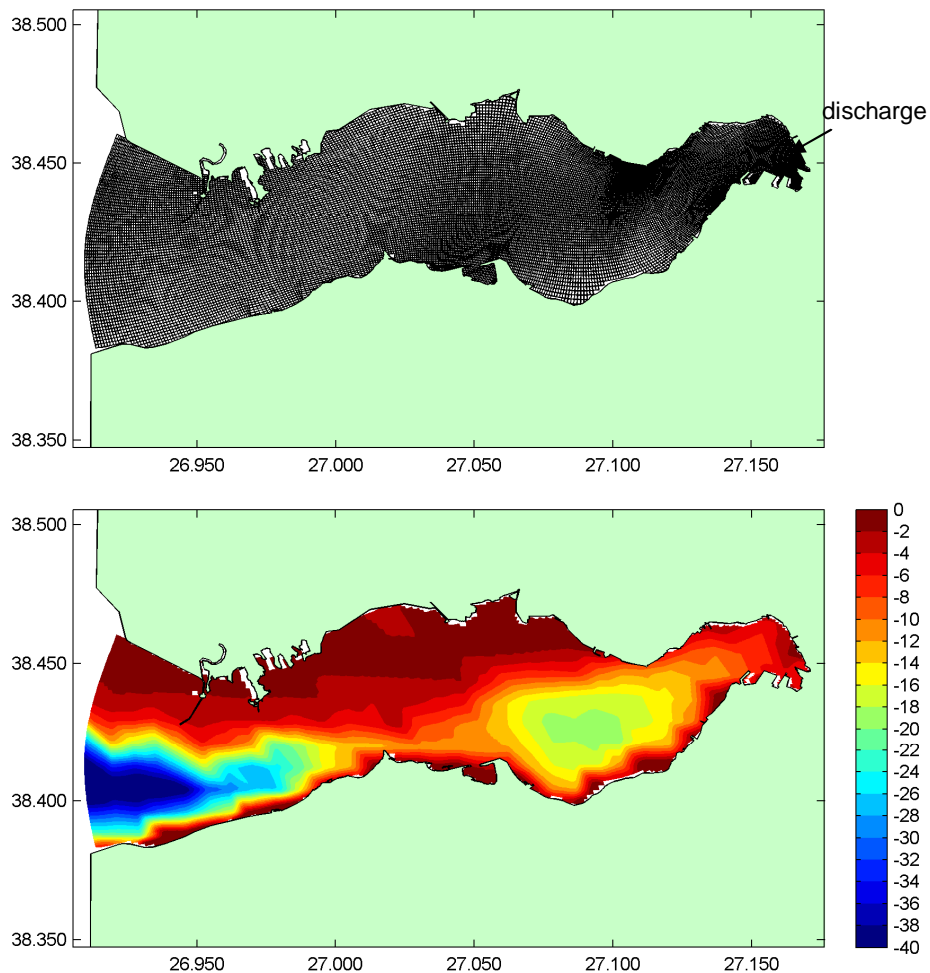


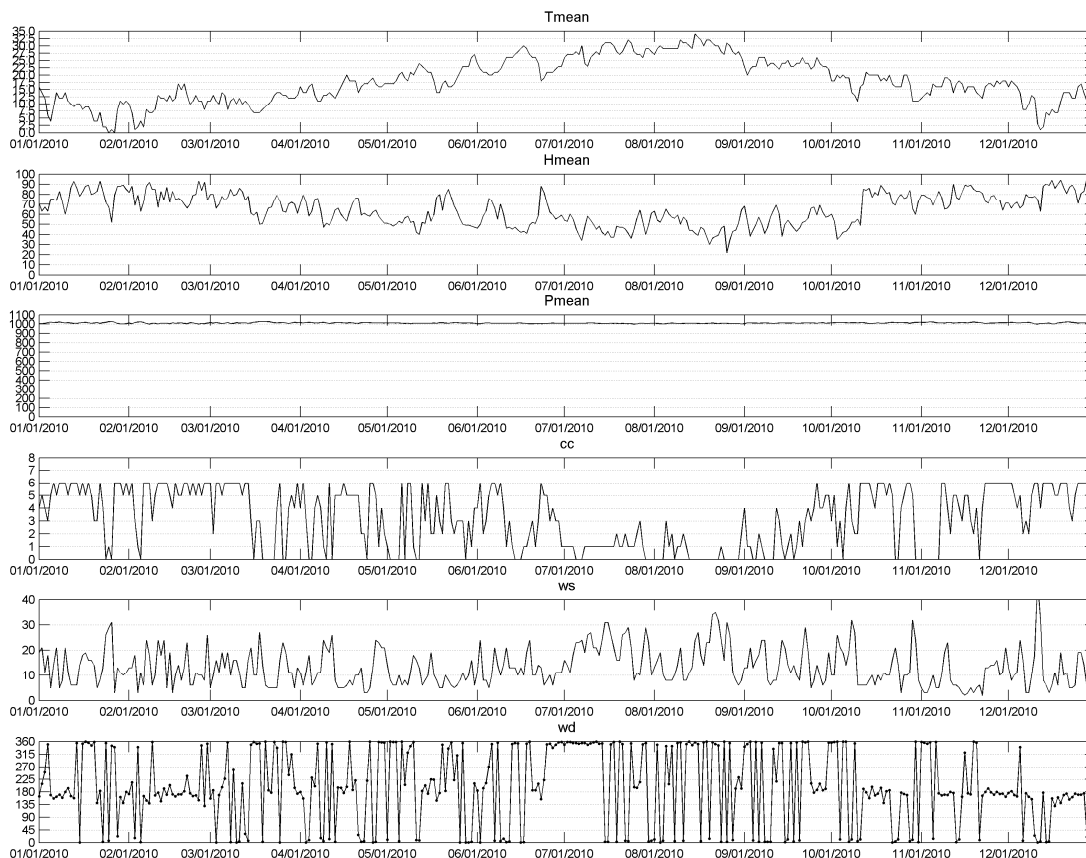
Figure 4.1 Grid (top) and bathymetry (bottom) of the detailed 3D model for Inner Izmir Bay.

In the vertical direction, six layers of equal thickness are used to represent vertical velocity gradients. The (hypothetical) pollution discharge is in the Inner Bay (see Figure 4.1). In view of the very shallow nature of the area, the presence of density gradients has been neglected (salinity and temperature have not been simulated). Similarly, the small fresh water discharges in the Inner Bay have been neglected.

4.1.2 Model forcing

At the open boundary, the tidal movement is prescribed by means of a series of tidal components derived from Alpar et al. (1997). The water level signal imposed at the open boundary shows small tidal water level variations; the amplitude is typically less than 20 cm. There is a spring-neap cycle, with the neap tide amplitude well below 10 cm.

Meteorological information with a daily resolution for the station Izmir has been derived from an open domain internet source at www.wunderground.com. Figure 4.2 shows these data for the year 2010. The bottom graph of Figure 4.2 shows alternate north (around 0/360 degrees) and south (around 180 degrees) winds. Apparently, 2010 is an atypical year. Sayin (2003) claims that north winds are dominant in the area.



Tmean = average temperature (°C); Hmean = average humidity (%); Pmean = average air pressure (mbar); cc = cloud cover (okta); ws = wind speed (m/s); wd = wind direction (degr. rel. to N)

Figure 4.2 Meteorological conditions used for the Izmir Bay simulations

For reasons of computational efficiency, the volume of the discharge has been neglected. The model was initialised with zero water level and zero velocity, and a period of 5 days was allowed to adapt to the forcing and loose the influence of the initial conditions.

By this way of forcing, the model is suited to assess the impact of wind driven currents, generated by the local geometry and bathymetry.

4.1.3 Hydrodynamic model parameters

The bed roughness is specified by a Manning coefficient of $0.026 \text{ s m}^{-1/3}$. The horizontal eddy viscosity is defined by a constant and homogeneous value of $1 \text{ m}^2 \text{ s}^{-1}$. The vertical eddy viscosity is calculated by a k- ϵ -turbulence model. The equations are solved with a time step of 30 seconds.

4.1.4 Water quality model parameters

We consider a discharge with a flow rate varying between $0.05\text{-}0.5 \text{ m}^3/\text{s}$ from a pipe with a diameter of 0.5 m, consisting of fresh water. For an ambient water temperature in the range of $12\text{-}26^\circ\text{C}$ and an ambient salinity of 39 ppt (Sayin, 2003), the relative density difference between the discharge and the ambient water is 0.03. If the discharge would be a surface discharge, the estimated extent of the near field would be between 4.4 and 44 m, while the initial dilution would be between 1.3 and 8.5 (calculated according to Appendix B of Delft Hydraulics, 1989). If the discharge would be a sub-surface discharge, near the bottom in 5 m deep water, the estimated extent of the near field would be smaller than 10 m, while the initial dilution would be between 5 and 10 (estimated according to Appendix B of Delft Hydraulics, 1989). For the present simulations, we select a discharge rate of $0.25 \text{ m}^3/\text{s}$, a near field of 25 m and an initial dilution of 5.

The horizontal dispersion coefficient is $1 \text{ m}^2/\text{s}$, which is a suitable value for 3D dynamic water quality simulations with a fine grid. The vertical dispersion coefficient is calculated by the hydrodynamic model and copied to the water quality model.

The concentration of suspended solids is derived from Bizsel and Uslu (2000, average value of 22 mg/l for Inner Bay station 2). This value of SS causes 90% of mercury to be in the particulate phase (calculated according to equations in section 3.4). Based on a settling velocity of 1 m/d (expert judgement) and a representative depth near the discharge of 5 m, the effective removal rate of mercury is 0.18 d^{-1} (calculated according to equations in section 3.4).

4.2 Izmir Bay generalised Tier 3 model

For Izmir Bay, we selected four single simulations with variable wind conditions. The statistics of the wind conditions have been derived from the input to the detailed 3D model. Table 4.1 provides an overview of the input data to the generalised Tier 3 model.

Table 4.1 Input data for Izmir Bay calculations

Input item	Simul. 1	Simul. 2	Simul. 3	Simul. 4
Description	Medium North winds	Weak North winds	Medium South winds	Weak South winds
Length (m)	2000	2000	2000	2000
Width (m)	5000	5000	5000	5000
Direction of grid (°)	150	150	150	150
Water depth along inner coast line (m)	3	3	3	3
Water depth along sea boundary (m)	15	15	15	15
Nr of grid cells (-)	40 x 100 x 6	40 x 100 x 6	40 x 100 x 6	40 x 100 x 6
Direction of wind (°)	0	0	180	180
Wind speed at 10 m (m/s)	4.49	1.67	4.65	1.74
Circulation in (m/s)	-0.05	-0.02	0.02	0.05
Frequency of occurrence (%)	40.0%	6.7%	26.7%	26.7%
Position of discharge (x,y,z) (m)	Surface	Surface	Surface	Surface
Discharge flow rate (m ³ /s)	0.25	0.25	0.25	0.25
Near field dilution factor	5	5	5	5
Suspended solids (mg/l)	22	22	22	22
Settling velocity of particles (m/d)	1	1	1	1
Representative water depth (m)	5	5	5	5
Horizontal dispersion (m ² /s)	0.1	0.1	0.1	0.1
Vertical dispersion (m ² /s)	0.001	0.001	0.001	0.001

The strength of the horizontal circulation has been selected by expert judgement, based on the results from the detailed 3D model.

The grid size is 50x50 meters. This implies that the horizontal extent of the near field (see Section 4.1.4) is smaller than a grid cell, and the discharge does not need to be shifted in the grid of the generalised 3D model to represent near field effects.

The simulation results are sensitive to the horizontal dispersion coefficient. The higher it is, the lower the simulated environmental concentrations will be. In a simplified method, we prefer to take a conservative approach. Therefore, we selected a relatively low value of 0.1 m³/s. The vertical dispersion coefficient equals 10⁻³ m²/s. This is a value suitable for well-mixed conditions.

4.3 Gulf of Lions detailed 3D model

The pollution hot spots in the Gulf of Lions are all located near Marseille (Figure 2.9). Therefore, the detailed hydrodynamic model focuses on the bay of Marseille. This bay consists of an eastern and a western part, separated by the “Ile de Frioul”. The passage between the Ile de Frioul and the shore has a depth of approximately 20 m. Both the eastern and the western bay have a maximum depth of 70 m at their entrance. Near the shore and near the entrance of the harbour of Marseille the water depth is approximately 10 – 20 m (see Figure 4.5 and Figure 4.6).

The MyOcean project (www.myocean.eu) provides information on the hydrodynamic behaviour of the marine waters near Marseille. These data provide limited spatial detail on the scale of the Marseille bay: the bay is covered by only 2 grid cells. The MyOcean data indicate a relatively stagnant waters with small flow velocities (see Figure 4.3).

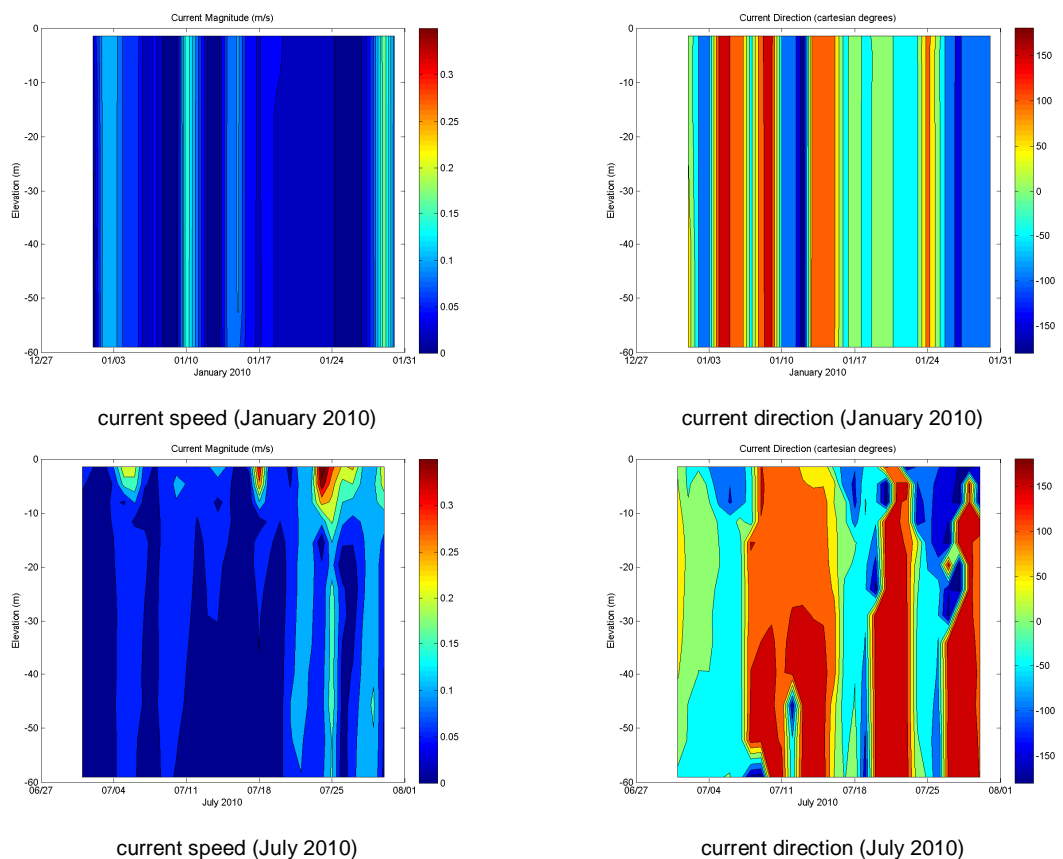


Figure 4.3 Plots of the vertical distribution of the currents during January 2010 and July 2010 respectively, at a station 15 km south of Ile de Frioul (derived from MyOcean).

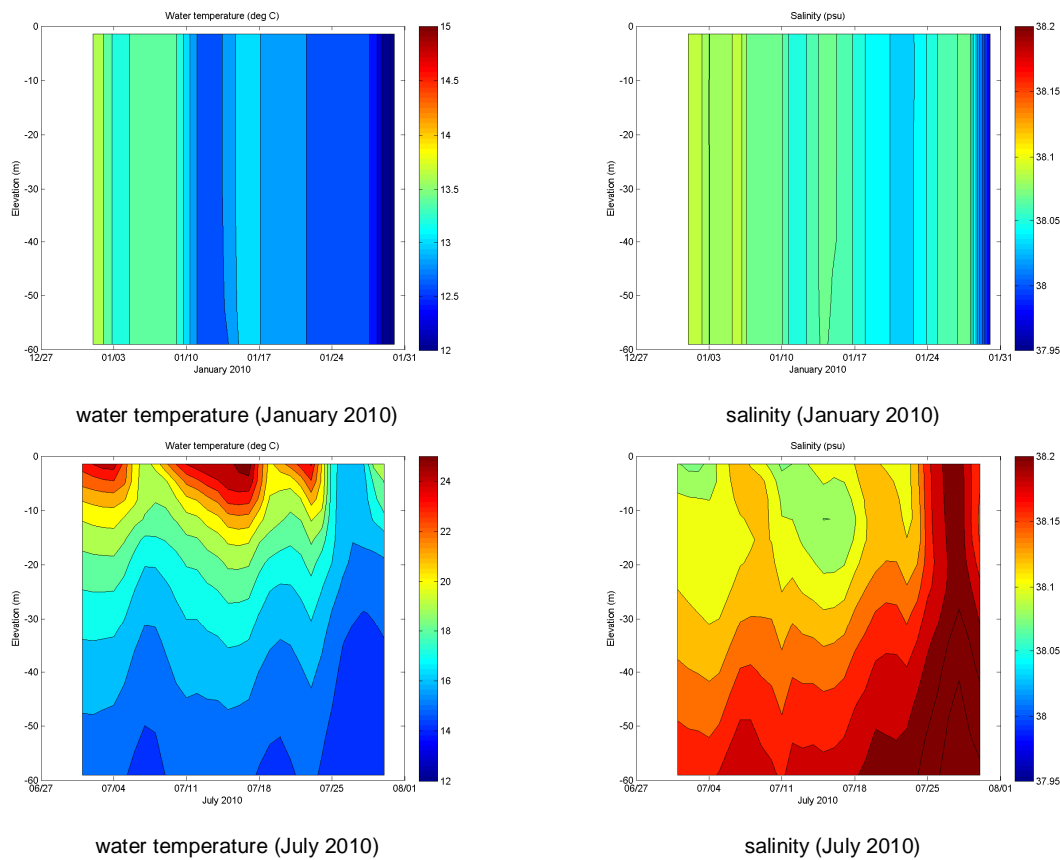


Figure 4.4 Plots of the vertical distribution of the water temperature and salinity during January 2010 and July 2010 respectively, at a station 15 km south of Ile de Frioul (derived from MyOcean).

The MyOcean data also indicate that during winter the marine waters near Marseille are well mixed. The salinity is approximately 38 psu, indicating that the fresh water Rhone discharge is not affecting the area. The water temperature during winter is approximately 13°C over the entire water depth. During summer, the MyOcean data suggest a vertical temperature gradient (25°C at the surface, decreasing to 15°C in deep water) which is periodically disappearing due to vertical mixing episodes coinciding with strong northerly winds (Figure 4.4). Again, the salinity is around 38 psu, with very small vertical differences.

Velocity measurements in the centre of the eastern bay confirm the stagnant character of the Marseille bay (Vousdoukas et al., 2011). These measurements reveal maximum flow velocities near the bed not exceeding 0.1 m/s.

4.3.1 Model domain and bathymetry

Figure 4.5 and Figure 4.6 show the model grid and the bathymetry of the Marseille bay hydrodynamic model. The model covers both the eastern and western bay. In the vicinity of the harbour, the grid cell size is approximately 50 m. Bathymetry data have been extracted from the (numerical) high-resolution bathymetric map published by Ifremer (Berné et al., 2004). There are two open boundaries, the eastern bay boundary and the western bay boundary. In the vertical direction, six layers of equal thickness are used to represent vertical velocity gradients. The (hypothetical) pollution discharge is located approximately 100 m offshore from the Marseille Harbour breakwater.

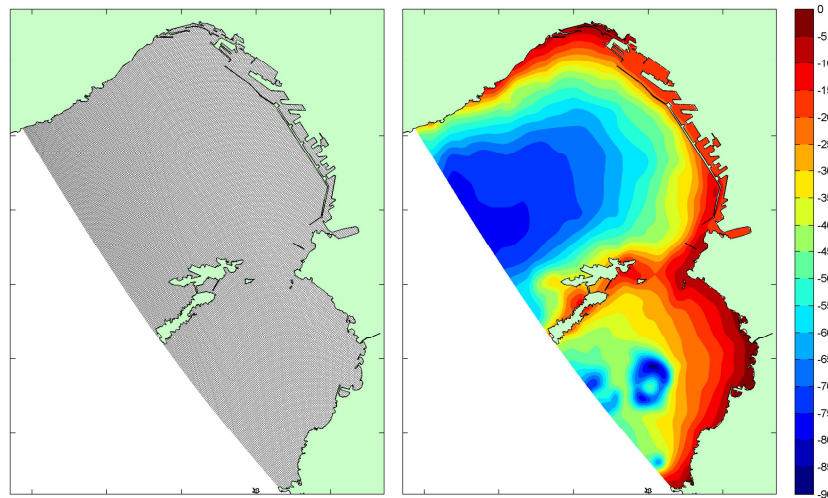


Figure 4.5 Grid layout and bathymetry of the detailed Marseille Bay model (overall)

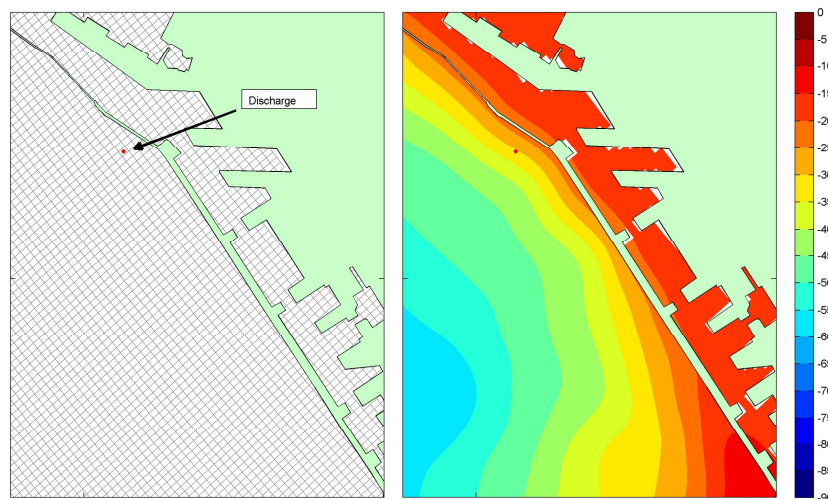


Figure 4.6 Grid layout and bathymetry of the detailed Marseille Bay model (detail)

4.3.2 Model forcing

Meteorological information with a daily resolution for Marseille has been derived from an open domain internet source at www.underground.com. Figure 4.7 shows this data for the year 2010. Two predominant wind directions appear to occur: N to NW wind directions resulting from the Mistral and S to SW wind directions. This is consistent with wind roses for Frioul (on the Ile de Frioul) and Port-de-Bouc (northwest of Marseille) presented by Pairaud et al. (2011). During the winter months the N to NW winds appear to occur more frequent than during the summer months. The average wind velocity is about 5 m/s. The maximum wind velocity is approximately 15 m/s.

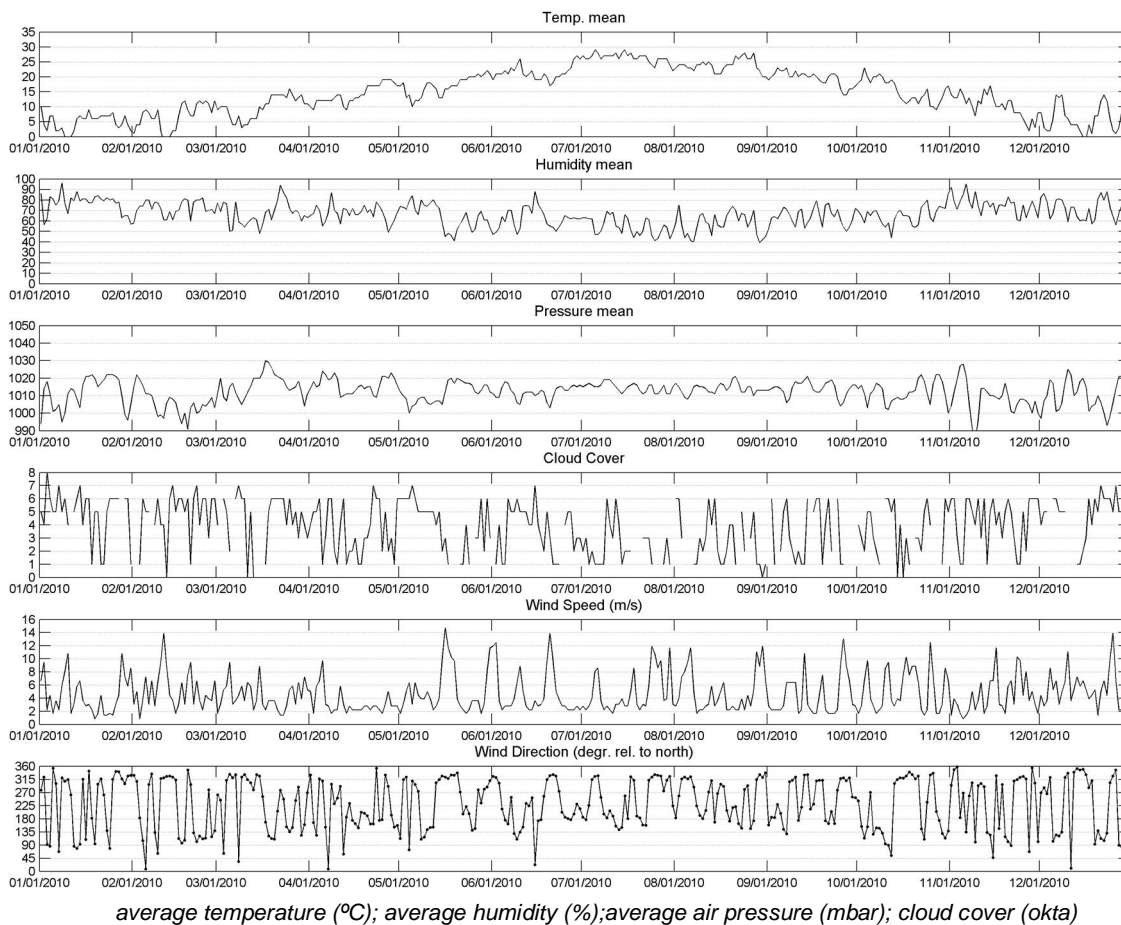


Figure 4.7 Meteorological conditions used for the Gulf of Lions simulations

A uniform (in space and time) water level equal to Mean Sea Level is applied as a boundary condition. The small tidal motion is neglected (see Section 2.2). This implies that the computed velocity patterns within the bay are generated by wind in combination with the local geometry and bathymetry.

For reasons of computational efficiency, the volume of the discharge has been neglected. The model was initialised with zero water level and zero velocity, and a period of 5 days was allowed to adapt to the forcing and loose the influence of the initial conditions.

By this way of forcing, the model is suited to assess the impact of wind driven currents, generated by the local geometry and bathymetry.

4.3.3 Hydrodynamic model parameters

The bed roughness is specified by a Manning coefficient of $0.026 \text{ s m}^{-1/3}$. The horizontal viscosity equals and $1 \text{ m}^2/\text{s}$. Locally, near the open boundaries of the model, a value of $50 \text{ m}^2/\text{s}$ is used to avoid undesirable model behaviour near the boundaries. The vertical eddy viscosity is calculated by a k- ϵ turbulence model. The equations are solved with a time step of 30 seconds.

4.3.4 Water quality model parameters

We consider the same discharge as in the Izmir Bay case: a flow rate varying between 0.05-0.5 m³/s from a pipe with a diameter of 0.5 m, consisting of fresh water. For an ambient water temperature of 13-25°C and an ambient salinity of 38 ppt (Pairaud et al., 2011), the relative density difference between the discharge and the ambient water is 0.03. If the discharge would be a surface discharge, the estimated extent of the near field would be between 4.4 and 44 m, while the initial dilution would be between 1.3 and 8.5 (calculated according to Appendix B of Delft Hydraulics, 1989). If the discharge would be a sub-surface discharge, near the bottom in 25 m deep water, the estimated extent of the near field would be smaller than 15 m, while the initial dilution would be between 30 and 80 (estimated according to Appendix B of Delft Hydraulics, 1989). For the present simulations, we select a discharge rate of 0.25 m³/s, a near field of 25 m and an initial dilution of 50.

The horizontal dispersion coefficient is 1 m²/s, which is a suitable value for 3D dynamic water quality simulations with a fine grid. The vertical dispersion coefficient is calculated by the hydrodynamic model and copied to the water quality model.

Information about the concentration of suspended solids is lacking. Adopting an estimated value of 20 mg/L, 90% of mercury to be in the particulate phase. Based on a settling velocity of 1 m/d (expert judgement) and a representative depth near the discharge of 25 m, the effective removal rate of mercury is 0.036 d⁻¹.

4.4 Gulf of Lions Generalised Tier 3 model

For the Gulf of Lions, we selected four single simulations with variable wind conditions. The statistics of the wind conditions have been derived from the input to the detailed 3D model. Table 4.2 provides an overview of the input data to the generalised Tier 3 model.

The strength of the horizontal circulation has been selected by expert judgement, based on the results from the detailed 3D model.

The grid size is 50x50 meters. This implies that the horizontal extent of the near field (see 4.3.4) is smaller than a grid cell, and the discharge does not need to be shifted in the grid of the generalised 3D model to represent near field effects.

For reasons explained in Section 4.2, the horizontal dispersion coefficient equals $0.1 \text{ m}^3/\text{s}$. The vertical dispersion coefficient equals $10^{-3} \text{ m}^2/\text{s}$. This is a value suitable for well-mixed conditions.

Table 4.2 Input data for Gulf of Lions calculations

Input item	Simul. 1	Simul. 2	Simul. 3	Simul. 4
Description	Medium Northwest winds	Weak Northwest winds	Medium Southeast winds	Weak Southeast winds
Length (m)	5000	5000	5000	5000
Width (m)	2000	2000	2000	2000
Direction of grid (°)	145	145	145	145
Water depth along inner coast line (m)	20	20	20	20
Water depth along sea boundary (m)	60	60	60	60
Nr of grid cells (-)	100 x 40 x 6	100 x 40 x 6	100 x 40 x 6	100 x 40 x 6
Direction of wind (°)	320	280	90	110
Wind speed at 10 m (m/s)	5.83	1.67	5.19	2.01
Circulation in (m/s)	0.05	0.02	-0.02	-0.01
Frequency of occurrence (%)	40.0%	13.3%	20.0%	26.7%
Position of discharge (x,y,z) (m)	Surface	Surface	Surface	Surface
Discharge flow rate (m^3/s)	0.25	0.25	0.25	0.25
Near field dilution factor	50	50	50	50
Suspended solids (mg/l)	20	20	20	20
Settling velocity of particles (m/d)	1	1	1	1
Representative water depth (m)	25	25	25	25
Horizontal dispersion (m^2/s)	0.1	0.1	0.1	0.1
Vertical dispersion (m^2/s)	0.001	0.001	0.001	0.001

5 Modelling results

5.1 Izmir Bay detailed 3D model

A water quality simulation has been carried out with the Izmir Bay detailed 3D model for a period of 30 days. The discharge of all 3 simulated pollutants, a conservative tracer, total nitrogen and total mercury, equals 1 g/s.

Figure 5.1 shows snap shots from the simulation results for the conservative tracer. These results show that the transport patterns of the released tracer are to a large extent determined by local circulation patterns. These circulations cause most of the released material to move towards the outer bay along the north coast if the wind is from a southern direction and along the south coast if the wind is from a northern direction. The circulation patterns are clearly the result of the variable wind in combination with the coastline and bathymetry.

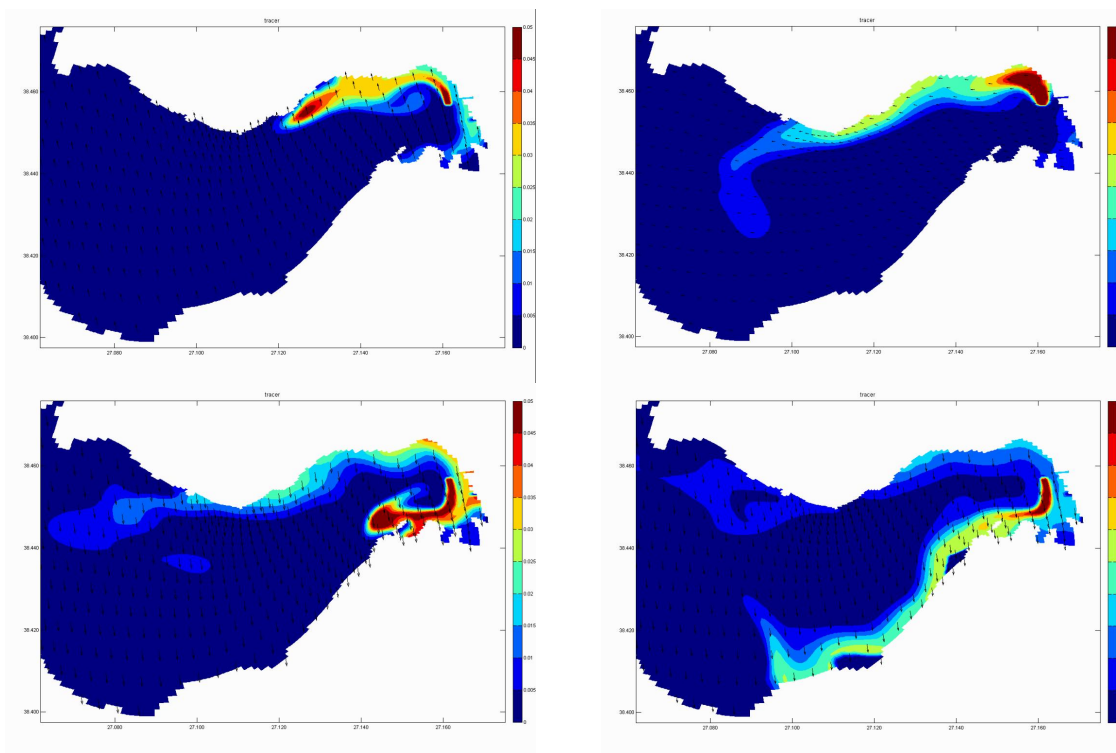


Figure 5.1 Snap shots from the Izmir Bay simulation. Colours represent the concentrations of a conservative tracer released in the inner part of the Bay. The arrows represent the wind direction.

The temporal changes of the transport patterns are best observed from the Izmir Bay animation provided with this report. The statistical properties of this time behaviour are best expressed by the mean concentration and the maximum concentration observed at any grid point. Figure 5.2 shows the maximum and mean concentrations for a conservative tracer. Figure 5.3 shows the mean and maximum concentrations for total nitrogen and dissolved mercury. For these substances, the concentrations are lower than for the conservative tracer, due to the removal and partitioning processes in the simulations.

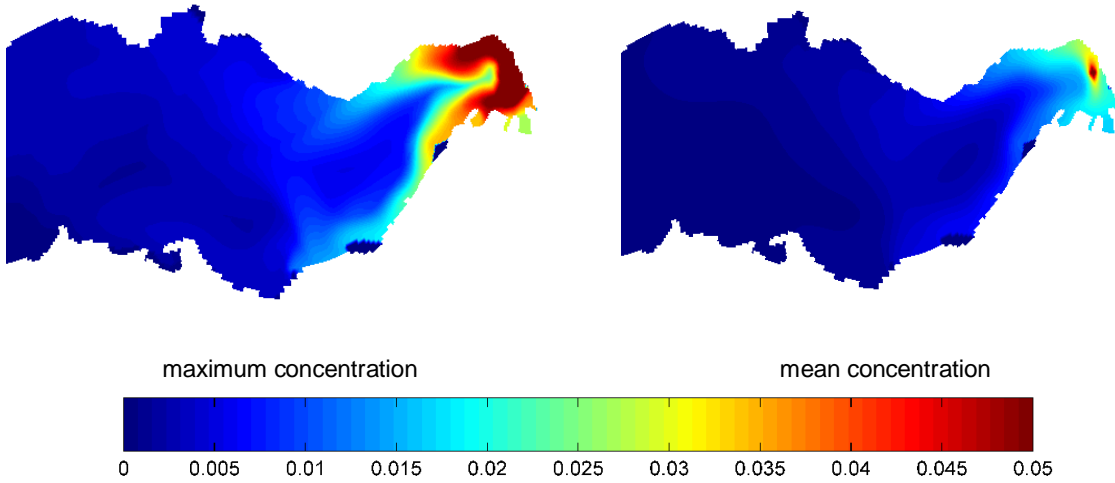


Figure 5.2 Maximum (left) and mean (right) simulated concentrations of a conservative substance released in Inner Izmir Bay at a rate of 1 g/s (detailed model).

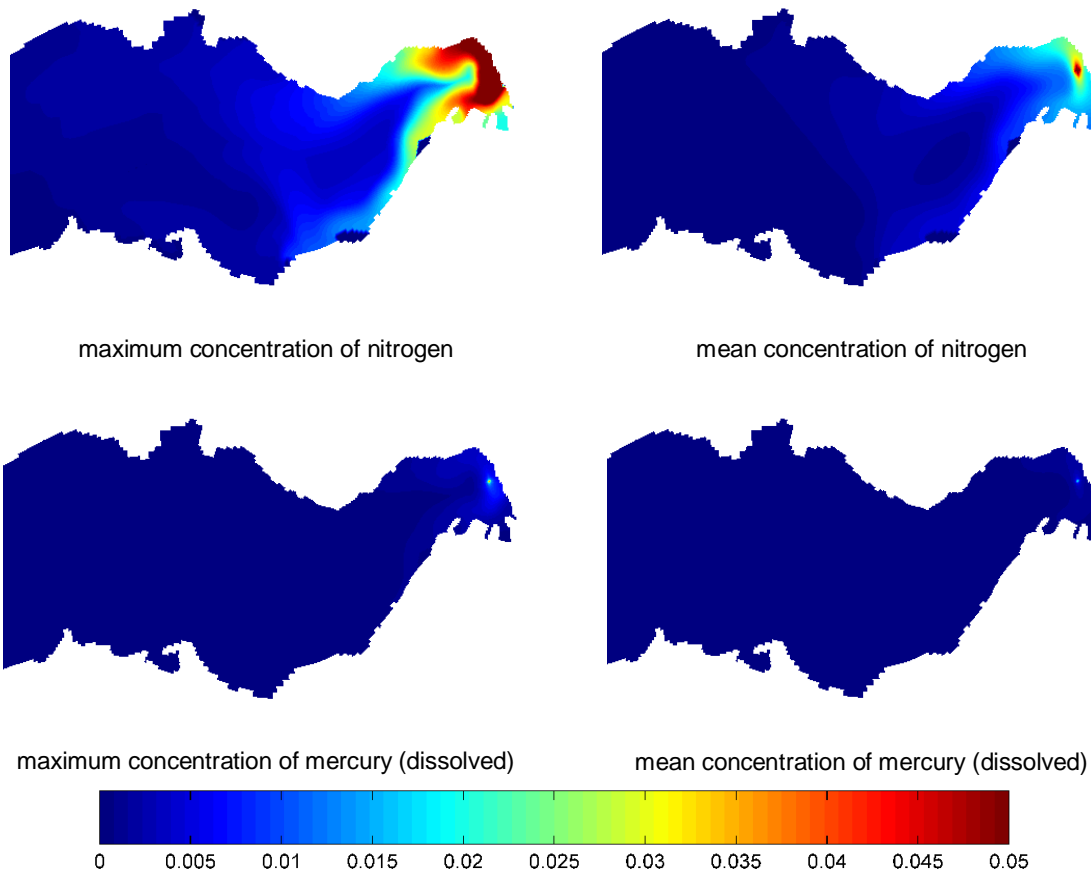


Figure 5.3 Maximum and mean simulated concentrations of total nitrogen and dissolved mercury, released in Inner Izmir Bay at a rate of 1 g/s (detailed model).

5.2 Izmir Bay generalised Tier 3 model

Four water quality simulations have been carried out with the Izmir Bay generalised Tier 3 model, each of them coinciding with one particular set of environmental conditions, in particular the wind direction and strength. The input data for the simulations are summarised in Table 4.1.

Figure 5.4 shows the overall statistical properties of the results from the generalised model for a conservative tracer. Figure 5.5 shows these results for nitrogen and dissolved mercury. Again, the concentrations of these substances are lower than the conservative tracer, due to the removal and partitioning processes considered in the simulations.

We note that the colour scales used are the same as in Figure 5.2 and Figure 5.3, to allow easy comparison with the detailed model results. Though the generalised model lacks detail both in the geometry and in the details of the concentration patterns, the concentrations obtained from both models are very comparable. This will be further elaborated below for the relationships between the ELVs and the EQSs from both models.

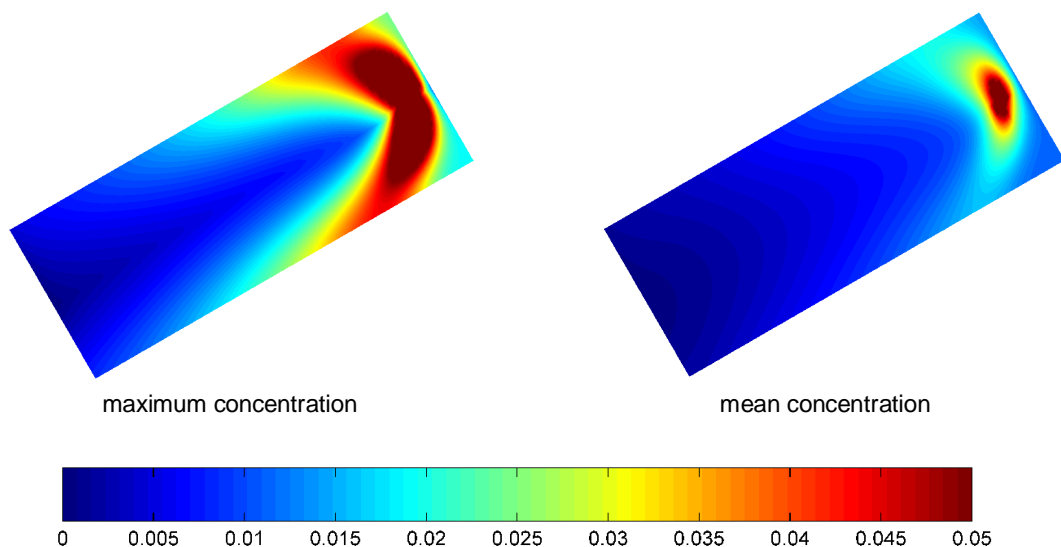


Figure 5.4 Maximum (left) and mean (right) simulated concentrations of a conservative substance released in Inner Izmir Bay at a rate of 1 g/s (generalised model).

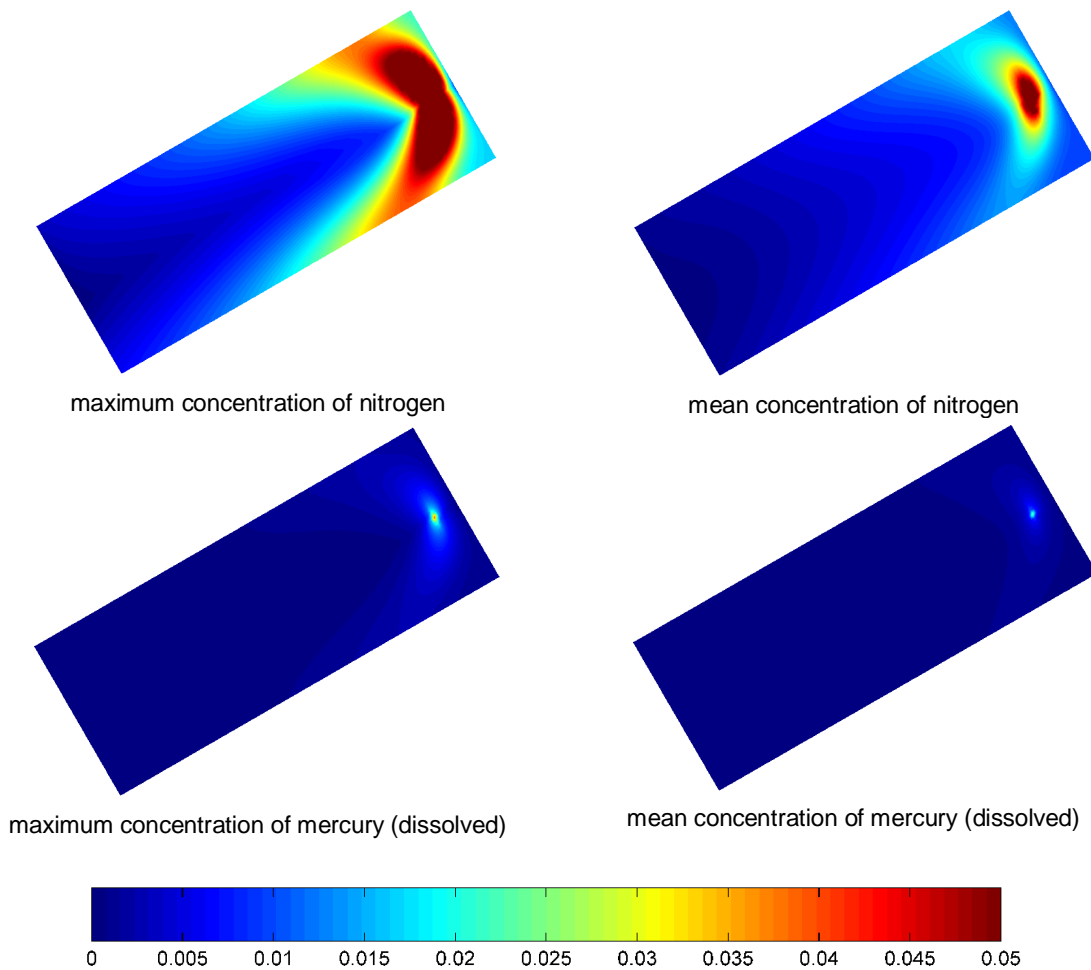


Figure 5.5 Maximum and mean simulated concentrations of total nitrogen and dissolved mercury, released in Inner Izmir Bay at a rate of 1 g/s (generalised model).

5.3 Relation between ELVs and EQSs for Izmir Bay

Based on the results from the detailed 3D model and the generalised Tier 3 model, we derive the concentrations of the simulated pollutants at the edge of the mixing zone, as a function of the mixing zone dimension. In this case, we consider the mixing zone to be circular, with the discharge point at the centre of the circle. Table 5.1 shows the results.

These results are affected by processes specific for nitrogen and mercury. The differences between both model approaches are best illustrated by similar results for a conservative tracer. These are shown graphically in Figure 5.6. This figure illustrates that the results from both modelling approaches are comparable but not equal. In this case, the generalised model calculates higher concentrations than the detailed model for small mixing zones, while for larger mixing zones the detailed model calculates higher concentrations.

Table 5.1 Simulated concentrations at the edge of the mixing zone (Izmir Bay, all discharges are 1 g/s)

mixing zone radius (m)	detailed model				generalized Tier 3 model			
	Nitrogen (total)	Nitrogen (total)	Mercury (dissolved)	Mercury (dissolved)	Nitrogen (total)	Nitrogen (total)	Mercury (dissolved)	Mercury (dissolved)
	max	mean	max	mean	max	mean	max	mean
100	0.1349	0.0481	0.01133	0.00387	0.1933	0.0860	0.01703	0.00746
200	0.1148	0.0372	0.00937	0.00283	0.1314	0.0559	0.01107	0.00464
300	0.1041	0.0330	0.00832	0.00241	0.1021	0.0426	0.00825	0.00341
400	0.0983	0.0300	0.00776	0.00212	0.0845	0.0339	0.00659	0.00261
500	0.0913	0.0285	0.00709	0.00196	0.0727	0.0283	0.00546	0.00209
600	0.0822	0.0272	0.00625	0.00182	0.0625	0.0243	0.00457	0.00171
700	0.0722	0.0264	0.00533	0.00173	0.0554	0.0213	0.00390	0.00145
800	0.0650	0.0254	0.00468	0.00164	0.0498	0.0194	0.00340	0.00127
900	0.0576	0.0243	0.00403	0.00152	0.0456	0.0184	0.00301	0.00117
1000	0.0538	0.0241	0.00367	0.00149	0.0425	0.0177	0.00277	0.00111
1100	0.0510	0.0232	0.00336	0.00140	0.0407	0.0173	0.00261	0.00106
1200	0.0489	0.0198	0.00317	0.00115	0.0399	0.0164	0.00251	0.00097
1300	0.0479	0.0188	0.00307	0.00107	0.0394	0.0155	0.00245	0.00089
1400	0.0463	0.0178	0.00291	0.00099	0.0384	0.0144	0.00232	0.00083
1500	0.0423	0.0171	0.00255	0.00092	0.0365	0.0134	0.00213	0.00076
1600	0.0394	0.0165	0.00231	0.00087	0.0350	0.0126	0.00200	0.00072
1700	0.0380	0.0160	0.00218	0.00082	0.0325	0.0117	0.00179	0.00065
1800	0.0364	0.0153	0.00206	0.00076	0.0308	0.0110	0.00166	0.00061
1900	0.0348	0.0149	0.00199	0.00072	0.0292	0.0104	0.00153	0.00057
2000	0.0333	0.0146	0.00193	0.00070	0.0269	0.0098	0.00136	0.00052

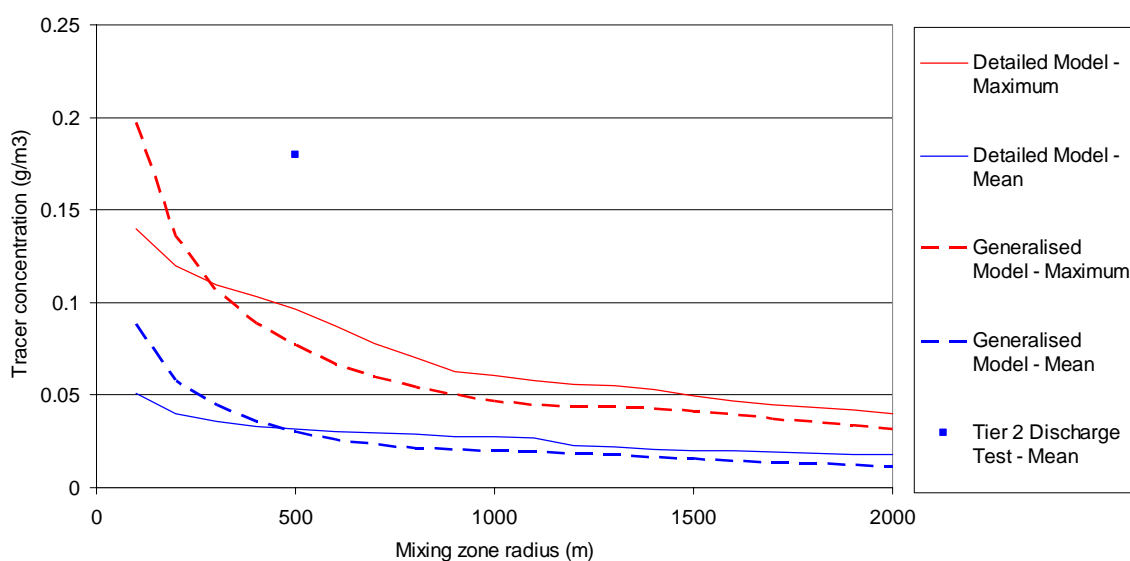


Figure 5.6 Relation between the dimensions of the mixing zone (radius in m) and the concentrations at the edge of the mixing zone of a conservative tracer (released at a rate of 1 g/s in Izmir Bay). The figure shows maximum and mean concentrations as they are calculated by different modelling approaches.

As a final step in the evaluation of the results, the relation between the m-ELV and the EQS is established, in this case for a mixing zone with a radius of 500 m. Figure 5.7 shows the results. Both models provide almost identical results for the mean concentrations. Figure 5.6 shows that for a mixing zone radius of 500 m the results from both model approaches are indeed identical. This is co-incidental. For the maximum concentrations, both model approaches provide different results. Figure 5.6 illustrates that the detailed model is more conservative for a mixing zone radius of 500 m.

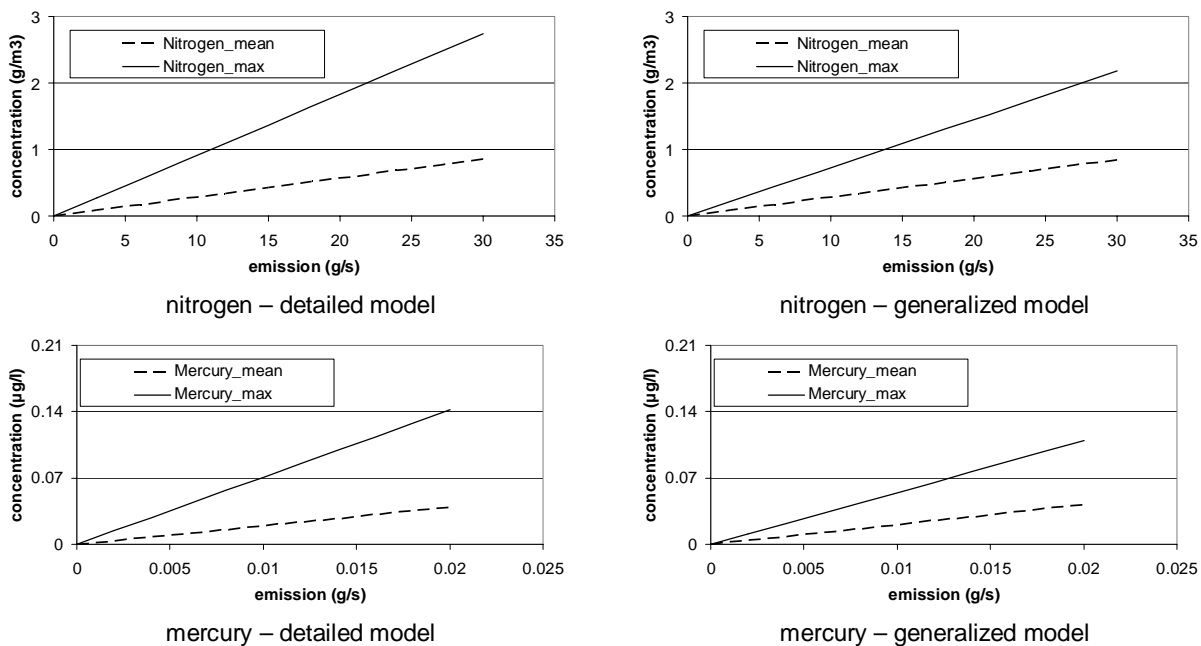


Figure 5.7 Relation between the emission and the concentration at the edge of the mixing zone for a discharge of nitrogen and mercury in Inner Izmir Bay, for a mixing zone with a radius of 500 m.

From Figure 5.7, the m-ELV for nitrogen can be derived for a given EQS. Note that in this example, a background concentration of zero is used. An EQS for the mean concentration of nitrogen of 0.4 mg/l, would allow a discharge of 14 g/s. In this case, both model approaches provide the same result.

For mercury, Figure 5.7 allows the derivation of the m-ELV from the Water Framework Directive Maximum Allowable Concentration (MAC-EQS) of 0.07 µg/l and the Annually Averaged concentration (AA-EQS) of 0.05 µg/l, for a mixing zone with a radius of 500 m. Again, a background concentration of zero is used. In this case, the MAC-EQS is the most critical, and leads to an ELV of 9.9 mg/s (detailed model) or 13 mg/s (generalised model). The generalised model provides a 31% higher ELV than the detailed model.

The assessment of mixing zones is used to ensure that water systems can meet the assigned water quality and ecological objectives, represented by the relevant EQSs. An approach with certain simplifications, such as the generalised Tier 3 model presented here (as compared to the detailed 3D model), should therefore produce conservative results, to ascertain that the adopted simplifications will not lead to overestimation of the ELV. The results presented above demonstrate that the generalised Tier 3 model does not always provide conservative results: in some cases it provides a higher ELV than the detailed 3D model. For this reason, the use of a safety factor is recommended. Our initial proposal for such a safety factor is 2.0.

Application of this safety factor brings the m-ELV for nitrogen to 7.1 g/s and the m-ELV for mercury at 6.4 mg/s.

The Tier 2 Discharge Test² provides an approach that is intended to be conservative. One could argue that it is overly conservative in cases where the tidal motion is small, as in the Mediterranean, because it superimposes the jet dispersion pattern on the far field concentration increase due to the discharge (Kleissen, 2011). For reference, we also derived the Tier 2 Discharge Test result for the nitrogen ELV, considering the jet dispersion pattern only, and neglecting the specific behaviour of nitrogen. Figure 5.6 shows the calculated concentration for a discharge of 1 g/s for a conservative tracer. This translates to an m-ELV for nitrogen of 2.2 g/s.

For mercury, the Tier 2 Discharge Test neglects the partitioning and the fact that the EQSs are defined for the dissolved fraction only. For this reason, we do not compare the present results with the Tier 2 Discharge Test results. We note that the Tier 2 Discharge Test uses a 40x smaller mixing zone for the assessment of a MAC-EQS than for the AA-EQS. In this case, the MAC-EQS-MZ amounts to 12.5 m (500 m divided by 40). On such scales, we consider the near field behaviour of the plume decisive for the MAC-EQS assessment. In this case, the near field dilution is estimated as 5 (Table 4.1). If we would base our assessment on the requirement that after the near field dilution the concentration in the jet should be smaller than the MAC-EQS, we can derive the associated m-ELV as follows:

$$c - ELV \cdot f_d = S \cdot MAC\ EQS \quad so \quad m - ELV = \frac{Q_e \cdot S \cdot MAC\ EQS}{f_d}$$

with S the near field dilution factor (-) and f_d the freely dissolved fraction of mercury (-). The resulting m-ELV is 0.88 mg/s.

The ELVs discussed above, derived by different methods under different assumptions are compiled in Table 5.2.

Table 5.2 Overview of calculated ELVs for the Inner Izmir Bay discharge

Substance	Detailed 3D model	Generalised Tier 3 model, safety factor 2	Near field method only	Tier 2 Discharge Test
Nitrogen m-ELV (g/s), based on AA-EQS, MZ = 500	14	7.1	-	2.2
Mercury m-ELV (mg/s), based on AA-EQS, MZ = 500	25	12	-	-
Mercury m-ELV (mg/s), based on MAC-EQS, MZ = 500	9.9	6.4	-	-
Mercury m-ELV (mg/s), based on MAC-EQS, MZ << 500	-	-	0.88	-

2. Discharge test, in support of Tier 1 and Tier 2 of the Technical Guidelines for the identification of mixing zones pursuant to Art. 4(4) of the Directive 2008/105/EC, <http://dgs-as2.geodelft.nl/eitoets/>

5.4 Gulf of Lions detailed 3D model

A water quality simulation has been carried out with the Gulf of Lions detailed 3D model for a period of 30 days. The discharge of all 3 simulated pollutants, a conservative tracer, total nitrogen and total mercury, equals 1 g/s.

Figure 5.8 shows snap shots from the simulation results for the conservative tracer. These results show that the transport patterns of the released tracer are to a large extent determined by local circulation patterns. These circulations cause most of the released material to move rapidly towards the south if the wind is from a northwestern direction and move north if the wind is from a southeastern direction. The circulation patterns are clearly the result of the variable wind in combination with the coastline and bathymetry.

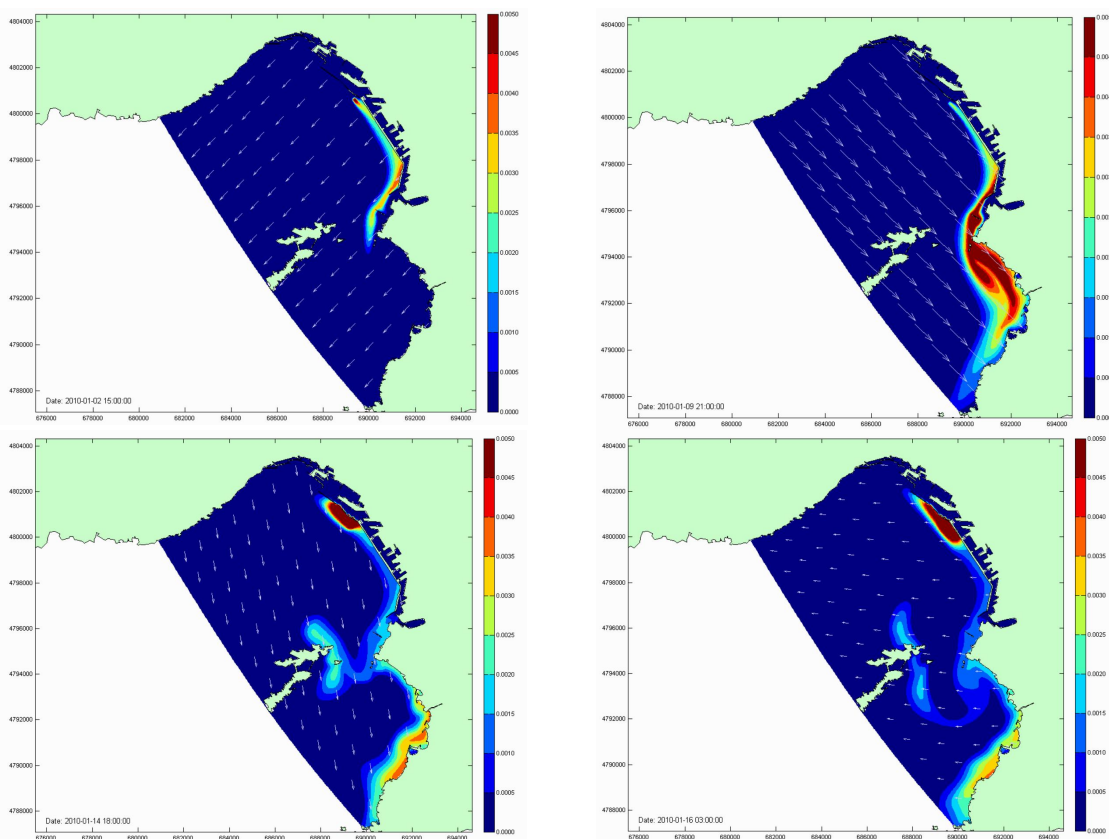


Figure 5.8 Snap shots from the Gulf of Lions simulation. Colours represent the concentrations of a conservative tracer released near the Harbour. The arrows represent the wind direction.

The temporal changes of the transport patterns are best observed from the Gulf of Lions animation provided with this report. The statistical properties of this time behaviour are best expressed by the mean concentration and the maximum concentration observed at any grid point. Figure 5.9 shows the maximum and mean concentrations for a conservative tracer. Figure 5.10 shows the mean and maximum concentrations for total nitrogen and dissolved mercury. For these substances, the concentrations are lower than for the conservative tracer, due to the removal and partitioning processes in the simulations.

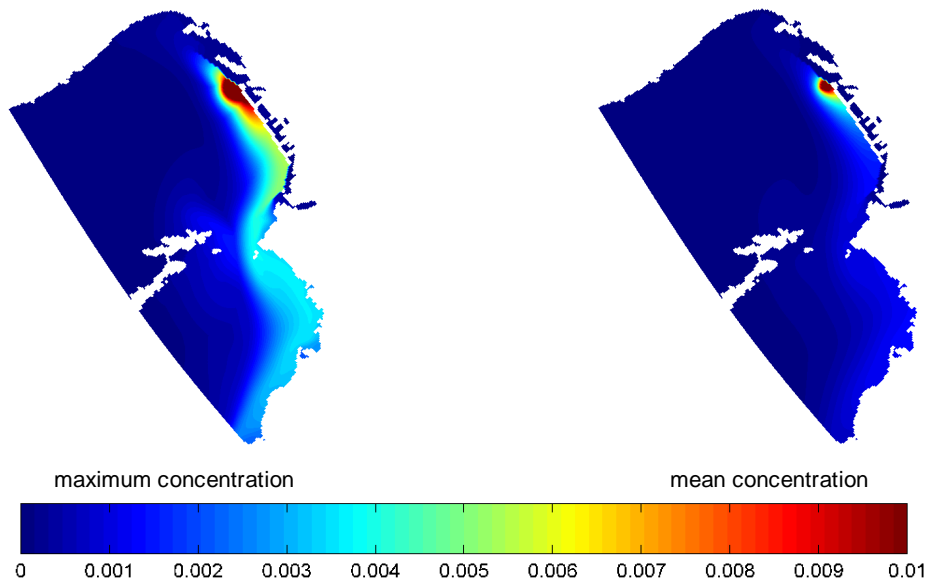


Figure 5.9 Maximum (left) and mean (right) simulated concentrations of a conservative substance released in Marseille Bay (Gulf of Lions) at a rate of 1 g/s (detailed model).

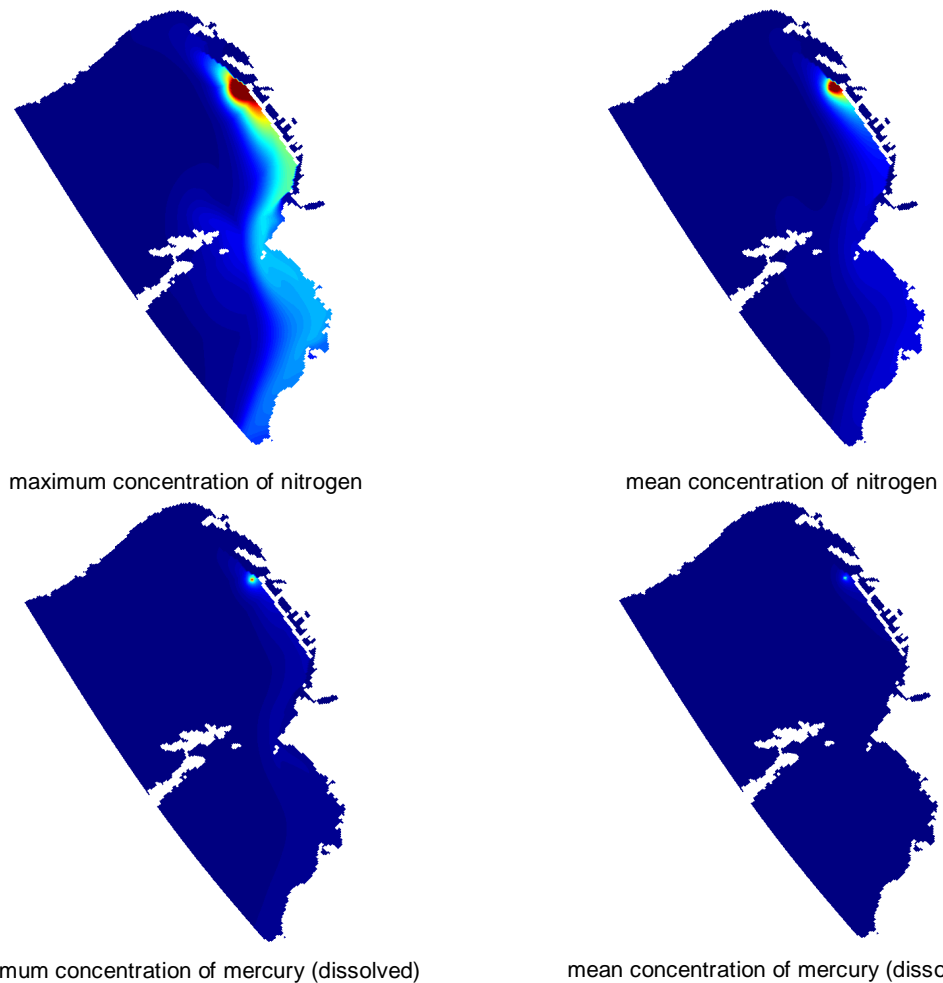


Figure 5.10 Maximum and mean simulated concentrations of total nitrogen and dissolved mercury, released in Marseille Bay (Gulf of Lions) at a rate of 1 g/s (detailed model).

5.5 Gulf of Lions generalised Tier 3 model

Four water quality simulations have been carried out with the Gulf of Lions generalised Tier 3 model, each of them coinciding with one particular set of environmental conditions, in particular the wind direction and strength. The input data for the simulations are summarised in Table 4.2.

Figure 5.11 shows the overall statistical properties of the results from the generalised model for a conservative tracer. Figure 5.12 shows these results for nitrogen and dissolved mercury. Again, the concentrations of these substances are lower than the conservative tracer, due to the removal and partitioning processes in the simulations.

We note that the colour scales used are the same as in Figure 5.9 and Figure 5.10, to allow easy comparison with the detailed model results. Though the generalised model lacks detail both in the geometry and in the details of the concentration patterns, the concentrations obtained from both models to some extent comparable. The generalised model shows a more pronounced transport of pollutants towards the northwest, under southeast wind conditions. This will be further elaborated below for the relationships between the ELVs and the EQSs from both models.

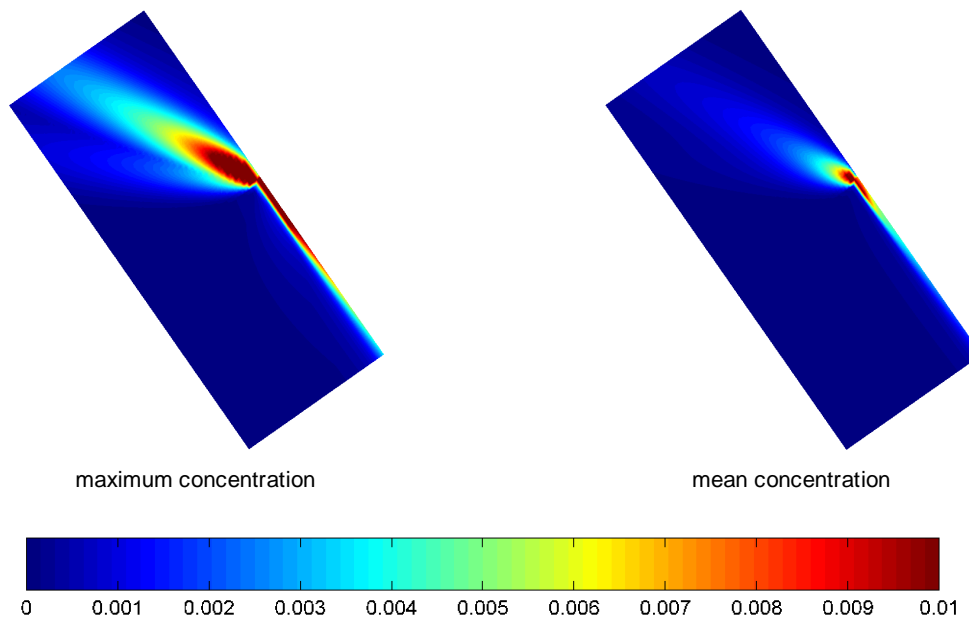


Figure 5.11 Maximum (left) and mean (right) simulated concentrations of a conservative substance released in Marseille Bay (Gulf of Lions) at a rate of 1 g/s (generalised model).

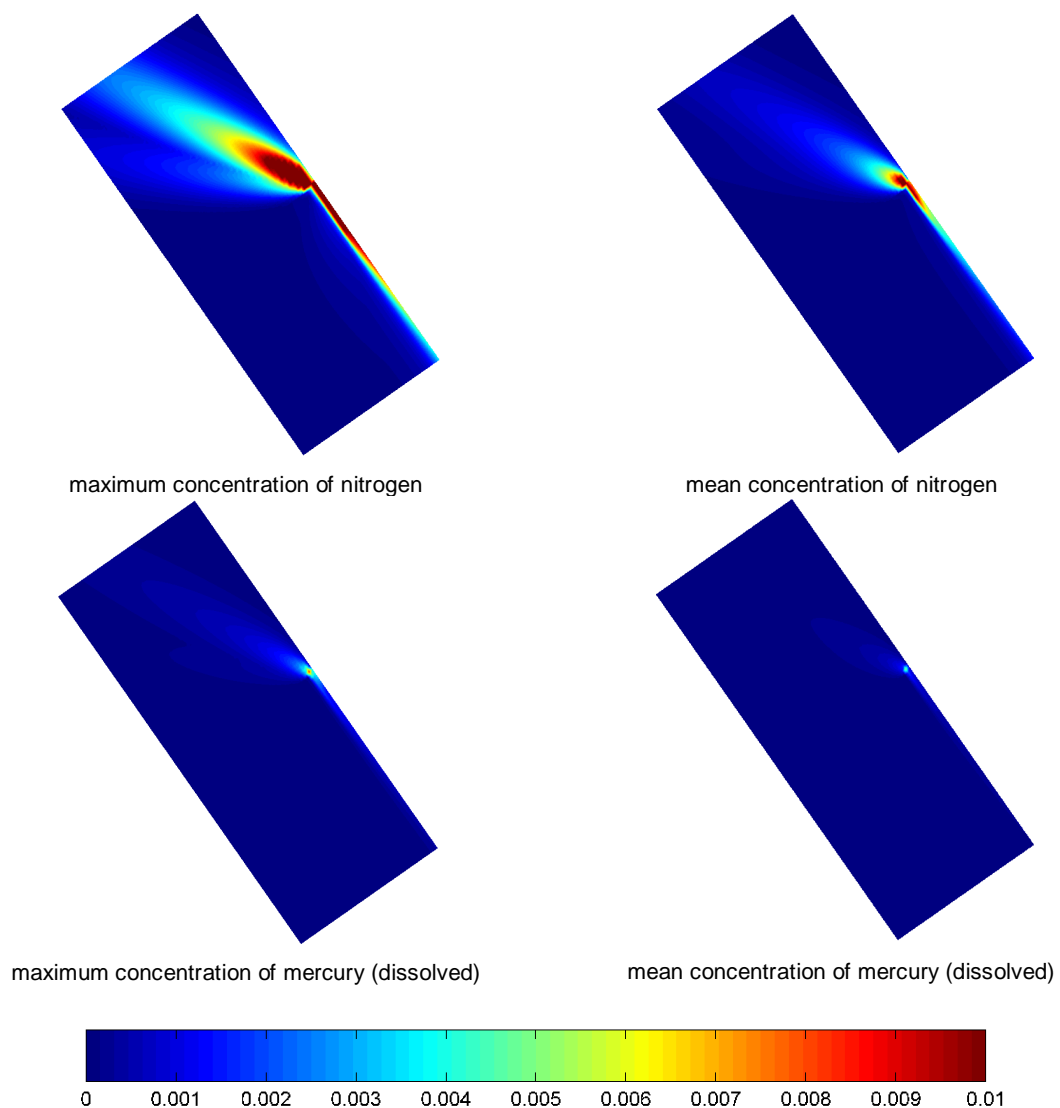


Figure 5.12 Maximum and mean simulated concentrations of total nitrogen and dissolved mercury, released in Marseille Bay (Gulf of Lions) at a rate of 1 g/s (generalised model).

5.6 Relation between ELVs and EQSs for Gulf of Lions

Based on the results from the detailed 3D model and the generalised Tier 3 model, we derive the concentrations of the simulated pollutants at the edge of the mixing zone, as a function of the mixing zone dimension. We consider the mixing zone to be circular, with the discharge point at the centre of the circle. Table 5.3 shows the results.

These results are affected by processes specific for nitrogen and mercury. The differences between both model approaches are best illustrated by similar results for a conservative tracer. These are shown graphically in Figure 5.13. This figure illustrates that the results from both modelling approaches are comparable but not equal. In this case, the generalised model calculates lower concentrations than the detailed model for small mixing zones, while for larger mixing zones the results are about equal.

Table 5.3 Simulated concentrations at the edge of the mixing zone (Gulf of Lions, all discharges are 1 g/s)

mixing zone radius (m)	detailed model				generalized Tier 3 model			
	Nitrogen (total)	Nitrogen (total)	Mercury (dissolved)	Mercury (dissolved)	Nitrogen (total)	Nitrogen (total)	Mercury (dissolved)	Mercury (dissolved)
	max	mean	max	mean	max	mean	max	mean
100	0.0414	0.0195	0.00423	0.00199	0.0331	0.0144	0.00340	0.00148
200	0.0273	0.0117	0.00279	0.00120	0.0218	0.0102	0.00223	0.00105
300	0.0215	0.0095	0.00219	0.00097	0.0180	0.0080	0.00185	0.00082
400	0.0191	0.0086	0.00195	0.00088	0.0151	0.0065	0.00155	0.00067
500	0.0126	0.0063	0.00128	0.00065	0.0128	0.0054	0.00131	0.00056
600	0.0111	0.0055	0.00113	0.00056	0.0110	0.0048	0.00113	0.00049
700	0.0101	0.0049	0.00103	0.00050	0.0108	0.0046	0.00110	0.00047
800	0.0094	0.0044	0.00095	0.00045	0.0104	0.0044	0.00107	0.00045
900	0.0088	0.0041	0.00089	0.00041	0.0099	0.0041	0.00102	0.00043
1000	0.0083	0.0037	0.00084	0.00038	0.0095	0.0039	0.00097	0.00040
1100	0.0081	0.0036	0.00081	0.00037	0.0089	0.0037	0.00092	0.00038
1200	0.0078	0.0035	0.00079	0.00035	0.0084	0.0035	0.00086	0.00036
1300	0.0072	0.0031	0.00072	0.00031	0.0079	0.0033	0.00081	0.00034
1400	0.0068	0.0029	0.00069	0.00029	0.0075	0.0031	0.00077	0.00032
1500	0.0065	0.0027	0.00065	0.00028	0.0071	0.0029	0.00072	0.00030
1600	0.0061	0.0026	0.00062	0.00026	0.0067	0.0027	0.00068	0.00028
1700	0.0059	0.0025	0.00059	0.00025	0.0063	0.0026	0.00064	0.00026
1800	0.0058	0.0024	0.00058	0.00024	0.0059	0.0024	0.00060	0.00025
1900	0.0055	0.0022	0.00055	0.00022	0.0055	0.0023	0.00057	0.00023
2000	0.0054	0.0021	0.00055	0.00021	0.0052	0.0021	0.00053	0.00022

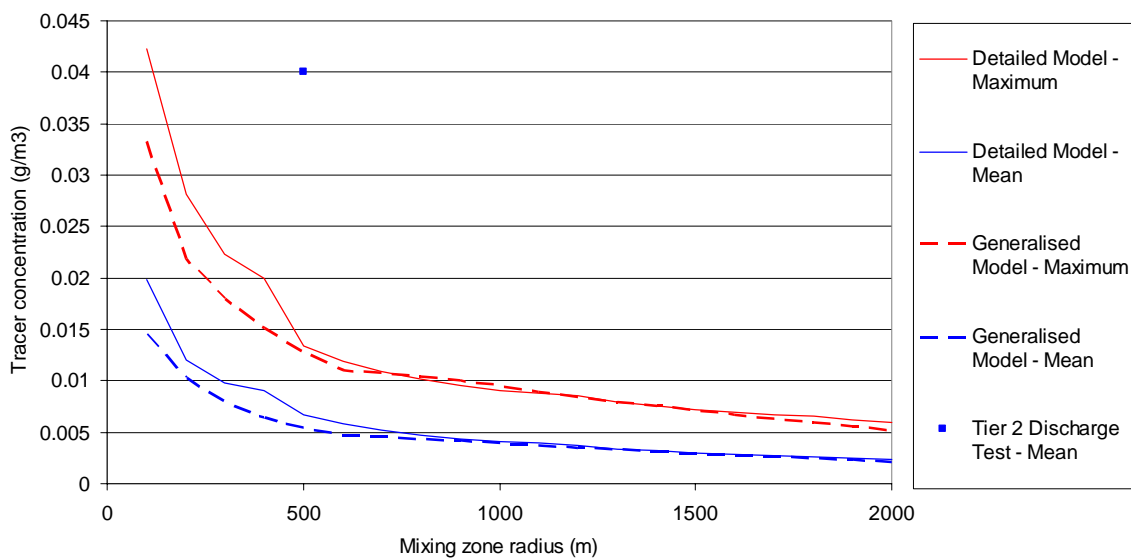


Figure 5.13 Relation between the dimensions of the mixing zone (radius in m) and the concentrations at the edge of the mixing zone of a conservative tracer (released at a rate of 1 g/s in the Gulf of Lions). The figure shows maximum and mean concentrations as they are calculated by different modelling approaches.

As a final step in the evaluation of the results, the relation between the m-ELV and the EQS is established, in this case for a mixing zone with a radius of 500 m. Figure 5.14 shows the results. Both models provide very comparable results. Figure 5.13 shows that the results from both models show larger differences only for a mixing zone radius smaller than 500 m.

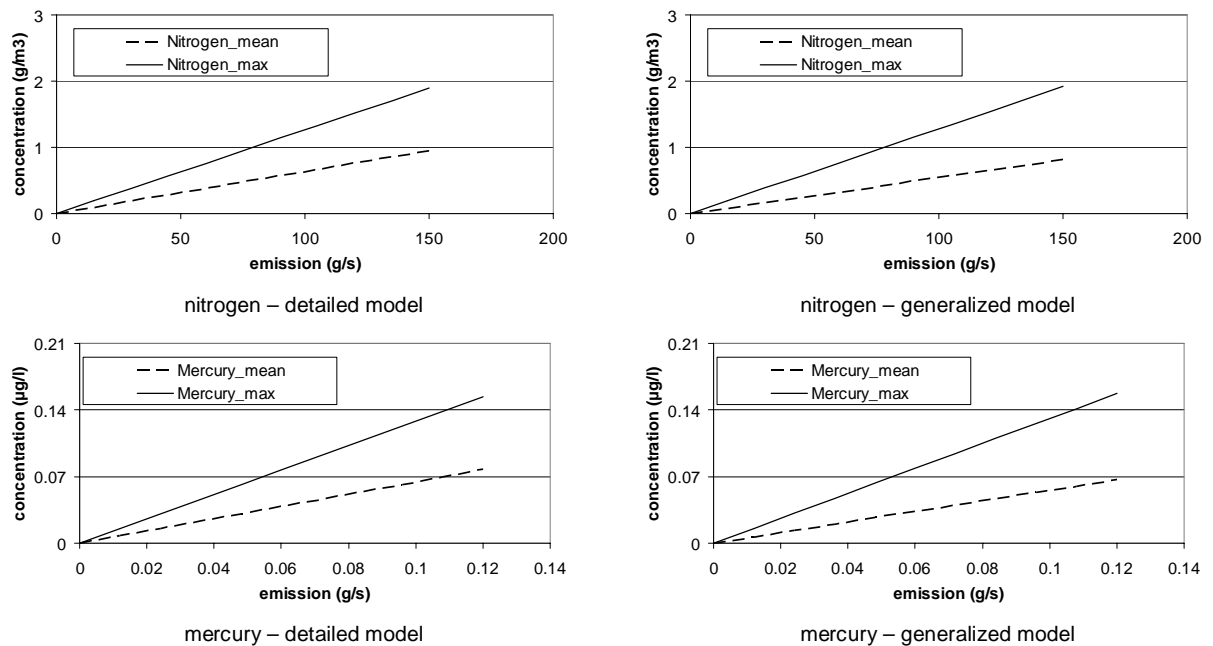


Figure 5.14 Relation between the emission and the concentration at the edge of the mixing zone for a discharge of nitrogen and mercury in Marseille Bay (Gulf of Lions), for a mixing zone with a radius of 500 m.

From Figure 5.14, the m-ELV for nitrogen can be derived for a given EQS. Note that in this example, a background concentration of zero is used. An EQS for the mean concentration of nitrogen of 0.4 mg/l, would allow a discharge of 63 g/s (detailed model) or 74 g/s (generalized model). The generalised model provides a 17% higher ELV than the detailed model.

For mercury, Figure 5.14 allows the derivation of the m-ELV from the Water Framework Directive Maximum Allowable Concentration (MAC-EQS) of 0.07 µg/l and the Annually Averaged concentration (AA-EQS) of 0.05 µg/l. Again, a background concentration of zero is used. In this case, the MAC-EQS is the most critical, and leads to an ELV of 55 mg/s (detailed model) or 53 mg/s (generalized model). The generalised model provides a 2% lower ELV than the detailed model.

For reasons explained in Section 5.3, we propose the use of a safety factor in the generalised Tier 3 model. The initially proposed value of 2.0 for Izmir Bay is sufficient to ensure that the generalised Tier 3 model produces conservative results. Application of this safety factor brings the m-ELV for nitrogen to 37 g/s and the m-ELV for mercury at 27 mg/s.

For reference, we also derived the Tier 2 Discharge Test result for the nitrogen ELV, considering the jet dispersion pattern only, and neglecting the specific behaviour of nitrogen. Figure 5.13 shows the calculated concentration for a discharge of 1 g/s for a conservative tracer. This translates to an m-ELV for nitrogen of 10 g/s.

Just as for Izmir Bay, we used a near field assessment to evaluate the ELV for mercury if the MAC-EQS mixing zone is chosen to be much smaller than the AA-EQS mixing zone (see Section 5.3). The resulting m-ELV is 8.8 mg/s.

The ELVs discussed above, derived by different methods under different assumptions are compiled in Table 5.4.

Table 5.4 Overview of calculated ELVs for the Marseille Bay discharge (Gulf of Lions)

Substance	Detailed 3D model	Generalised Tier 3 model, safety factor 2	Near field method only	Tier 2 Discharge Test
Nitrogen m-ELV (g/s), based on AA-EQS, MZ = 500	63	37	-	10
Mercury m-ELV (mg/s), based on AA-EQS, MZ = 500	77	45	-	-
Mercury m-ELV (mg/s), based on MAC-EQS, MZ = 500	55	27	-	-
Mercury m-ELV (mg/s), based on MAC-EQS, MZ << 500	-	-	8.8	-

6 Conclusions and recommendations

6.1 Conclusions

This report discussed a methodology to provide a bridge between the ecosystem approach and the MEDPOL Land Based Sources Protocol. As such, it establishes a relation between environmental quality standards (EQS) and emission limit values (ELV) following a combined, precautionary approach. In this study, we used the concept of a mixing zone as defined in the related EC Guidance Document (EC, 2010). A mixing zone is an area around a discharge point where the concentration of a substance may locally exceed the EQS. This implicitly determines the highest acceptable emission or the ELV: if the EQS is given, the ELV follows from the requirement that the EQS is satisfied at the edge of the designated mixing zone.

The quantitative assessment of the relation between the EQS and the ELV depends on the characteristics of the discharge, on the characteristics of the substance of concern and on the characteristics of the receiving water body. Mathematical water quality modelling is an accepted and often applied way of quantifying the relation between the EQS and the ELV, taking into account all these factors.

Within the Water Framework Directive community, a simple web-based tool (the “Tier 2 Discharge Test”) has been developed that evaluates the acceptability of a certain discharge, given the EQS and a defined mixing zone. This tool implicitly establishes the relation between the EQS and the ELV, but it discards the substance characteristics and most of the (variability of the) characteristics of the receiving water body.

In this study we used two 3D modelling approaches. The “detailed 3D modelling” approach takes into account in detail the characteristics of the receiving water body and the substance characteristics. This approach however, requires a high level of skill from its user, is very site specific and requires detailed input data. The effort required for the detailed 3D modelling approach is so large that the application to all hot spots would be very costly, and would not lead to coherent and harmonised results.

This report also discusses a “generalised Tier 3” method, which is based on the “Screening Model for Coastal Pollution Control in the Mediterranean”, developed in 1989 for the Ministry of the Environment of Greece. This method takes into account in detail the substance characteristics, but uses a simplified representation of the characteristics of the receiving water body. This obviously leads to a loss of accuracy, but it allows for easy application and offers a generic, coherent and harmonized approach. The method includes sufficient site-specific information to allow application to the variety of coastal environments encountered in the Mediterranean.

The objective of using both approaches simultaneously is to explore the possibilities to have credible and site-specific results from the generalised Tier 3 method, which can much easier be applied to a large amount of sites than the detailed 3D modelling approach.

In water quality modelling, experts distinguish the “near field” where the fate of a pollutant discharge depends primarily on the properties of the discharge, and the “far field” where the fate of the pollutants depends primarily on the properties of the receiving water body and the substance properties. A water quality model that deals with both the near field and the far field in a detailed and fully integrated way is not yet available for routine application. The Tier

2 Discharge Test mentioned above focuses on the near field, whereas the 3D models used in this study focus on the far field.

In view of the commonly applied range of mixing zones (500-1000 m) for the assessment of EQSs for the annually averaged concentration (AA-EQS), the spatial scale of the analysis of an individual discharge is in the order of 5 km. At this spatial scale and close to the shore where we typically find coastal discharges, the fate of a pollution discharge under Mediterranean conditions needs to be analysed taking into account the far field. Transport patterns are typically dominated by wind induced horizontal and vertical circulation patterns. The detailed 3D model can definitely simulate such patterns, but it will need input from field data to establish that the simulated current patterns are indeed correct. The generalized Tier 3 model lacks this ability: it simply uses field data directly as input.

The spatial scale of the mixing zone for an evaluation of EQSs for the maximum allowable concentration (MAC-EQS) may be much smaller. In some countries, mixing zones of 10-25 m are used to evaluate the MAC-EQS. At these small spatial scales, the evaluation results are dominated by the near field stage, and both the detailed 3D modelling and generalised Tier 3 modelling methods lose their relevance. At such occasions, a dedicated near-field model is more appropriate. In this report we provided two alternative approaches: (a) for larger MAC-EQS mixing zones, we applied the detailed 3D modelling and generalised Tier 3 modelling methods, and (b) for small MAC-EQS mixing zones, we demonstrate the near field based approach.

Our case studies demonstrate that the far field is essential at the spatial scale that we are interested in for the evaluation of AA-EQS. The near field is typically much smaller (10-50 m). This suggests that more detail about the characteristics of the receiving water body is required than included in the Tier 2 Discharge Test.

The results from our ELV assessments for nitrogen and mercury for discharges in Izmir Bay and the Gulf of Lions (near Marseille) are compiled in Table 5.2 and Table 5.4.

Our results indicate that while using the same EQSs, the ELVs for the study site in the Gulf of Lions (near Marseille) are about 5 times higher than those for the study site in the Inner Izmir Bay. This can be attributed to the differences between those water bodies: the Izmir Bay is shallower and more enclosed than the bay near Marseille.

Our case studies for nitrogen and mercury also demonstrate that it is vital to include the substance characteristics in the assessment. This is particularly relevant for mercury, because the WFD-EQS applies to the dissolved concentration only. In our case studies, this concentration was about 10% of the total concentration.

Our case studies demonstrated that the generalized Tier 3 model provides results that are in the same range as the detailed 3D model, though not equal. An approach with certain simplifications, such as the generalised Tier 3 model presented here, should produce conservative results, to ascertain that the adopted simplifications will not lead to overestimation of the ELV. The results presented in this report demonstrate that the generalised Tier 3 model does not always provide conservative results: in some cases it provides a higher ELV than the detailed 3D model. For this reason, we recommend the use of a safety factor. Our initial proposal for such a safety factor is 2.0 (based on the currently available applications to Izmir Bay and the Gulf of Lions).

Our case studies for nitrogen indicate that the Tier 2 Discharge Test produces significantly more conservative results than the generalized Tier 3 model and the detailed 3D model. For mercury, this tool could not be applied.

Our case studies indicate that the size of the mixing zone for the evaluation of the MAC-EQS is decisive for the ELVs for mercury. If the mixing zone is the same as for the AA-EQS, the ELVs found are an order of magnitude higher than if the mixing zone is in the order of 10-50 m.

Table 6.1 provides an overview of the strengths and weaknesses of the tools and methods applied in this report. This table demonstrates how an increasing effort, an increasing level of required skill and increasing data needs result in more advanced assessments with a higher accuracy, a lower uncertainty and higher ELVs.

Table 6.1 Overview of strengths and weaknesses of methods discussed in this report

	Tier 2 Discharge Test	Generalized Tier 3 model	Detailed 3D model
High level of skill required	No	A little more than the Tier 2 Discharge Test	Yes
Large amount of data needed	No, about 20 numbers to characterise the load and the environment	A little more than the Tier 2 Discharge Test, see Table 4.1 and Table 4.2	Yes
Large effort needed	No	No	Yes
Representation of discharge characteristics / near field	Good	Medium	Medium
Representation of substance characteristics	No	Yes	Yes
Representation of receiving water body / far field	Poor	Medium	Good
Accuracy in Case Studies carried out	Conservative (ELVs 6-7 times lower than detailed 3D model)	Conservative due to use of a safety factor (ELVs ≈ 2 times lower than detailed 3D model)	Presumably the best

6.2 Recommendations

In view of the large amount of hot spots around the Mediterranean and the diversity of these sites, in terms of their natural environment and the socio-economic conditions, we recommend that an easily applicable method will be made available to water managers and policy makers. This method should offer a clear framework, and allow for a generic, coherent and harmonized approach, which ensures a “level playing field” for the permitting policy around the Mediterranean. The successful implementation of such a method probably requires a Guidance Document and a supporting software tool. Examples of similar methods are available or under development for the permitting of anti-fouling paints and ballast water treatment systems (OECD, 2005; van Hattum et al, 2006; Zipperle et al., 2011).

We recommend a method which combines the strong points of the Tier 2 Discharge Test and the generalized Tier 3 model discussed in this report (see Table 6.1). In particular, the generalised Tier 3 model requires some improvements with respect to the representation of discharge characteristics and the near field modelling, for example like it has been implemented in the Tier 2 Discharge Test. The input required for this recommended method would comprise about 30 items as indicated in Table 6.2.

Table 6.2 List of input required for the recommended model

Substance / Discharge	Receiving Environment
EQS of substance (optionally MAC- and AA-EQS)	Type of environment (Case I or II, Figure 3.9)
Position of discharge	Orientation of study area relative to North
Discharge flow rate and concentration	Depth of thermocline and/or halocline
Discharge density	Salinity above and below halocline
Discharge pipe opening diameter	Temperature above and below thermocline
Substance partition coefficient	Water depth near-shore
Substance decay rate	Bottom slope
Mixing zone for evaluation AA-EQS	Wind speed and direction (optionally several typical conditions with associated probability)
Mixing zone for evaluation MAC-EQS	Current speed (optionally several typical conditions with associated probability)
	Suspended solids concentration
	Settling velocity of particles

The recommended method is not yet available in a way that allows easy application at the regional level and at the national level. The effort to make it available via the internet is fairly limited based on the results of the present study and on the existing web-based Tier 2 Discharge Test. If this effort will be made, the use of the model will require very limited training for the future user. The available experience with the existing web-based Tier 2 Discharge Test indicates that a 1-day training workshop is more than sufficient.

We quantified the reduced accuracy of the generalized Tier 3 model discussed in this report, as compared to a detailed 3D modelling study, for two study sites and two substances. This leads to the recommendation to apply a safety factor of 2 to the results obtained. It is recommended that UNEP discusses with the stakeholders whether or not the present study provides a sufficient picture of the uncertainties connected to this method. If not, then additional substances and/or additional sites should be studied in a similar way as it has been done in this report.

A final recommendation is that UNEP-MAP discusses the size of the mixing zone to be used for the evaluation of MAC-EQs. Should this mixing zone be in the same order as the mixing zone for the evaluation of AA-EQs? Or should it be much smaller, as it is in some European countries?

7 References

- Alpar B., S. Burak, C. Gazioglu, 1997. Effect of weather system on the regime of sea level variations in Izmir Bay. *Turkish J. Mar. Sci.* 3(2): 83-92 (1997).
- Amante, C. and B. W. Eakins, ETOPO1 1 Arc-Minute Global Relief Model: Procedures, Data Sources and Analysis. NOAA Technical Memorandum NESDIS NGDC-24, 19 pp, March 2009.
- Becker, J. J., D. T. Sandwell, W. H. F. Smith, J. Braud, B. Binder, J. Depner, D. Fabre, J. Factor, S. Ingalls, S-H. Kim, R. Ladner, K. Marks, S. Nelson, A. Pharaoh, R. Trimmer, J. Von Rosenberg, G. Wallace, and P. Weatherall., 2009. Global Bathymetry and Elevation Data at 30 Arc Seconds Resolution: SRTM30_PLUS. *Marine Geodesy* 32(4), 355-371.
- Benitez-Nelson, C., 2000. The biogeochemical cycling of phosphorus in marine systems. *Earth-Science Reviews*, 51, 109-135.
- Berné, S., Carré, D., Loubrieu, B., Mazé, J. P., Normand, A., 2004. Le Golfe du Lion. Carte morpho-bathymétrique du Golfe du Lion. Échelle 1/250 000. Ifremer-Région Languedoc-Roussillon, Brest.
- Béthoux, J.P., 1989. Oxygen consumption, new production, vertical advection and environmental evolution in the Mediterranean Sea. *Deep Sea Research I*, 36, 769-781.
- Biszel N. and O. Uslu, 2000. Phosphate, nitrogen and iron enrichment in the polluted Izmir Bay, Aegean Sea. *Marine Environmental Research* 49 (2000) 101-122.
- Boris J.P. & D.L. Book, 1973. Flux corrected transport I. SHASTA, a fluid transport algorithm that works. *Journal of Computational Physics* 1973; 11:38–69.
- Bourrin, F. and X. Durrieu de Madron, 2006. Contribution to the study of coastal rivers and associated prodeltas to sediment supply in Gulf of Lions (N-W Mediterranean Sea), *Vie & Milieu - Life & Environment*, 56 (4), 1-8.
- Berné S. and C. Gorini, 2005. The Gulf of Lions: An overview of recent studies within the French 'Margins' Programme. *Marine And Petroleum Geology*, August 2005; 22(6-7): 691-693.
- Caumette, P., Castel, J. & Herbert, R.A., 1996. Coastal Lagoon Eutrophication and Anaerobic Processes (CLEAN), Kluwer Academic Publishers, Dordrecht.
- Chapra SC. *Surface Water Quality Modelling*. McGraw-Hill: New York, 1997.
- Cossa D. and M. Conquery, 2005. The Mediterranean mercury anomaly, a geochemical or a biological issue. In: *The Handbook of Environmental Chemistry*, volume 5K, 121-130, DOI: 10.1007/b107147

- Cossa D., and J.-M. Martin. 1991. Mercury in the Rhone delta and adjacent marine areas. *Marine Chemistry* 36, 291-302.
- Crank, J., 1975. *The Mathematics of Diffusion*. Oxford University Press, 1975.
- Delft Hydraulics, 1989. A water quality screening model for coastal pollution control in the Mediterranean; User's Guide. Report prepared for the Water Section of the Environmental Planning Division of the Ministry of Environment, Physical Planning and Public Works of Greece. T417, Delft, The Netherlands, November 1989.
- Devol, A.H., 1991. Direct measurement of nitrogen gas fluxes from continental shelf sediments. *Nature*, 349, 319-321.
- Diaz, F., Raimbault, B., Boudjellal, B., Garcia, N. and T. Moutin, 2001. Early spring phosphorus limitation of primary productivity in a NW Mediterranean coastal zone (Gulf of Lions). *Marine Ecology Progress Series*, 211, 51-62.
- Dufois F., P. Garreau, P. Le Hir and P. Forget, 2008. Wave- and current-induced bottom shear stress distribution in the Gulf of Lions. *Continental Shelf Research* 28 (2008) 1920– 1934.
- Dugdale, R.C. & Goering, J.J., 1967. Uptake of new and regenerated forms of nitrogen in primary productivity. *Limnology and oceanography*, 12, 196-206.
- Duman M., M. Avci, S. Duman, E. Demirkurt and M.K. Duzbastilar, 2004. Surficial sediment distribution and net sediment transport pattern in Izmir Bay, western Turkey. *Continental Shelf Research* 24 (2004) 965–981.
- Durrieu de Madron, X., Abassi, A., Heussner, S., Monaco, A., Aloisi, J.-C., Radakovitch, O., Giresse, P., Buscail, R., and P. Kerherve, 2000. Particulate matter and organic carbon budgets for the Gulf of Lions (NW Mediterranean). *Oceanologica Acta*, 23, 717–730.
- EC, 2010. Technical Guidelines For The Identification Of Mixing Zones, pursuant to Art. 4(4) of the Directive 2008/105/EC (December, 2010).
- EC, 2008. Daughter Directive 2008/105/EC of 16 December 2008, on environmental quality standards in the field of water policy.
- EPA, 1985. Rates, constants and kinetics formulations in surface water quality modeling (2nd edition). Report EPA/600/3-85/040, EPA, Athens, Georgia, June 1985.
- Herut, B. & Collier, R., 2002. The role of dust in supplying nitrogen and phosphorus to the Southeast Mediterranean. *Limnology and Oceanography*, 47, 870-878.
- Kernkamp HWJ, Petit HAH, Gerritsen H, De Goede ED (2005) A unified formulation for the three-dimensional shallow water equations using orthogonal coordinates: theory and application, *Ocean Dynamics*, 55, pp. 351-369.

- Kleissen, F.M., 2011. Discharge Test for surface waters; functional design and technical documentation. Deltares report 1203331, Delft, The Netherlands, April 2011 (in Dutch).
- Kontas A., F. Kucuksezgin, O. Altay, E. Uluturhan, 2004. Monitoring of eutrophication and nutrient limitation in the Izmir Bay (Turkey) before and after Wastewater Treatment Plant, *Environment International* 29 (2004), 1057-1062.
- Kontas, A., 2006. Mercury in the Izmir Bay: An assessment of contamination, *J. Mar. Sys.* 61, 67–78.
- Krom, M.D., Groom, S. & Zohary, T., 2003. The eastern Mediterranean. In K. Black & G. B. Shimmield (Eds). *Biogeochemistry of marine systems*. Blackwell Publishing, pp. 91-126.
- Kucuksezgin F., A. Kontas, O. Altay, E. Uluturhan, E. Darilmaz, 2006. Assessment of marine pollution in Izmir Bay: nutrient heavy metal and total hydrocarbon concentrations, *Environment International* 32 (2006), 41-51.
- Lamy, A., C. Millot, and J.M. Molines, 1981. Bottom pressure and sea level measurements in the Gulf of Lions. *J. Phys. Oceanogr.*, 11, 394–410.
- Lax P.D., B. Wendroff, 1960. Systems of conservation laws. *Commun. Pure Appl Math.* 13: 217–237.
- Lesser GR, Roelvink JA, Van Kester JATHM, Stelling GS (2004) Development and validation of a three-dimensional morphological model, *Coastal Engineering* 51, pp. 883-915.
- Leveau, M. & Coste, B., 1987. Impact des apports rhodaniens sur les milieux pélagiques du Golfe du Lion. *Bulletin d'Écologie*, 18, pp.119-122.
- Lochet, F. & Leveau, M., 1990. Transfers between a eutrophic ecosystem, the river Rhône, and an oligotrophic ecosystem, the north-western Mediterranean Sea. *Hydrobiologia*, 207, 95-103.
- Ludwig, W. & Meybeck, M., 2003. Riverine transport of water, sediments and pollutants to the Mediterranean Sea. United Nations Environment Programme Mediterranean Action Plan, 121 pp.
- Ludwig, W., Dumont, E., Meybeck, M. and S. Heussner, 2009. River discharges of water and nutrients to the Mediterranean and Black Sea: Major drivers for ecosystem changes during past and future decades? *Progress In Oceanography*, 80, 199-217.
- Millot, C., 1987. The circulation of the Levantine intermediate water in the Algerian Basin, *Journal of Geophysical Research*, 92, 8265-8276.
- Millot, C., 1990. The Gulf of Lions' hydrodynamics. *Continental Shelf Research*, 10, 885–894.
- Monaco, A., Durrieu de Madron, X., Radakovitch, O., Heussner, S. and J. Carbonne, J., 1999. Origin and variability of downward biogeochemical fluxes on the Rhône continental margin (NW mediterranean). *Deep-Sea Research I*, 46, 1483–1511.

- Monperrus M., Tessier E., Amouroux D., Leynaert A., Huonnic P., Donard O.F.X. (2007), Mercury methylation, demethylation and reduction rates in coastal and marine surface waters of the Mediterranean Sea. *Marine Chemistry* 107, 49-6.
- Morel, A., Bricaud, A., André, J.-M., and J. Pelaez-Hudle, 1990. Spatial-temporal evolution of the Rhône River plume as seen by CZCS imagery: consequences upon primary productions in the Gulf of Lions. In J. M. Martin & H. Barth (Eds). *Water Pollution Research Reports 20. EROS-2000*, Nerc, Plymouth, UK, pp. 45-62.
- Moutin, T., P. Raimbault, H.L. Golterman and B. Coste, 1998. The input of nutrients by the Rhone river into the Mediterranean Sea: recent observations and comparisons with earlier data, *Hydrobiologia*, 373–374, 237–246.
- OECD, 2005. Emission Scenario Document on Antifouling Products. OECD Series on Emission Scenario Documents No. 13. ENV/JM/MONO(2005)8.
- Pairaud, I. L., Gatti, J., Bensoussan, N., Verney, R. and P. Garreau, 2011. Hydrology and circulation in a coastal area off Marseille: Validation of a nested 3D model with observations. *Journal of Marine Systems*, 88, 20-33.
- Pinazo, C., Marsaleix, P., Millet, B., Estournel, C. and R. Véhil, 1996. Spatial and temporal variability of phytoplankton biomass in upwelling areas of the Northwestern Mediterranean: a coupled physical and biogeochemical modelling approach. *Journal of Marine Systems*, 7, 161-191.
- Postma, L. and Hervouet, J.-M., 2006. Compatibility between finite volumes and finite elements using solutions of shallow water equations for substance transport. *Internat. J. Numer. Methods Fluids*. 53: 1495-1507.
- Sandwell, D.T., and Smith, W.H.F., 2009. Global marine gravity from retracked Geosat and ERS-1 altimetry: Ridge Segmentation versus spreading rate. *J. Geophys. Res.* 114, B01411, doi:10.1029/2008JB006008.
- Sayin, E., 2003. Physical features of the Izmir Bay. *Continental Shelf Research* 23 (2003) 957–970.
- Seitzinger, S.P., Harrison, J.A., Dumont, E., Beusen, A.H.W. and A.F. Bouwman, 2005. Sources and delivery of carbon, nitrogen, and phosphorus to the coastal zone: An overview of Global Nutrient Export from Watersheds (NEWS) models and their application. *Global Biogeochemical Cycles*, 19, 1-11.
- Seitzinger, S.P. & Giblin, A.E., 1996. Estimating denitrification in North Atlantic continental shelf sediments. *Biogeochemistry*, 35, 235-260.
- Rajar R, Matjaž Č, Horvat M, Žagar D (2007), Mass balance of mercury in the Mediterranean Sea, *Marine Chemistry* 107, 89-102.
- SIO, 2011. SRTM30_PLUS V7.0 dataset, by the Scripps Institution of Oceanography. Available online at http://topex.ucsd.edu/WWW_html/srtm30_plus.html.

- Thomann R.V. & J.A. Müller, 1987. Principles of water quality modelling and control. New York, USA, Harper & Row, , 644 pp.
- Twigt D.J., E.D. De Goede, F. Zijl, D. Schwanenberg, E.W.K. Au, W.P. Yu, A.Y.W. Chiu, 2009. Coupled 1D-3D hydrodynamic modelling, with application to the Pearl River Delta. Ocean Dynamics, DOI 10.1007/s10236-009-0229-y.
- van Hattum B, Baart AC, Boon JG (2006) Emission estimation and chemical fate modelling of antifoulants. In: Konstantinou, I.K. (ed.). Antifouling Paint Biocides. Handbook of Environmental Chemistry Vol. 5/O. Springer Verlag, Berlin (Germany). pp. 101-120.
- Vousdoulas M.I., R. Verney, F. Dufois, C. Pinazo, D. Sauzade, S. Meule, P. Cann, and T.A. Plomaritis (2011) Sediment Dynamics in the Bay of Marseille, Gulf of Lions (France): Hydrodynamic Forcing vs. Bed Erodibility. Journal of Coastal Research: Volume 27, Issue 5: pp. 942 – 958.
- Žagar D., Petkovšek G., Rajar R., Sirnik N., Horvat M., Voudouri A., Kallos G., Četina M., (2007) Modeling of mercury transport and transformations in the water compartment of the Mediterranean Sea, Marine Chemistry 107, 64-88.
- Zipperle A., J. van Gils, B. van Hattum, S. Heise, 2011. Guidance For A Harmonized Emission Scenario Document On Ballast Water Discharge. Final Report on behalf of the German Federal Environment Agency issued by Beratungszentrum für integriertes Sedimentmanagement, Hamburg, Germany.

A Vertical velocity profiles

Logarithmic profile for bottom shear

The logarithmic profile for bottom shear is given by:

$$v_z = C \ln \left(\frac{H - Z}{Z_0} + 1 \right) \times v \quad (6.14)$$

where C is:

$$C = \left[\left(1 + \frac{Z_0}{H} \right) \ln \left(\frac{H}{Z_0} + 1 \right) - 1 \right]^{-1} \quad (6.15)$$

with:

v_z	vertical profile of the horizontal velocity
Z	depth co-ordinate (from 0 (surface) to H (bottom))
H	water depth
Z_0	roughness length
v	depth-average velocity

The roughness length is of the order 2 cm. The depth-averaged velocity is obtained from a

Parabolic profile for wind

The parabolic profile for wind is given by:

$$v_z = \alpha \left(3 \left(1 - \frac{Z}{H} \right) - 2 \right) \left(1 - \frac{Z}{H} \right) W \quad (6.16)$$

with:

W	wind speed at 10 m above sea level
α	wind drag coefficient

The wind-drag coefficient is typically in the order of 0.03. The integral over depth is zero and is superimposed on the normal velocity profile which already includes the gross average influence of the wind. This gross wind effect on the velocity field must have been incorporated in the 2DH-hydrodynamic velocity field.